Susana Cristina Dias Ramos Ferreira

Licenciatura em Ciências da Engenharia Química e Bioquímica

Application of OSN in membrane cascade for purification of the API Amoxicillin

Dissertação para obtenção do Grau de Mestre em
Engenharia Química e Bioquímica

Orientadores: Professor Andrew G. Livingston (IC)
Doutora Ludmila Peeva (IC)

Co-orientador: Professora Isabel Coelhoso (FCT-UNL)

Júri:

Presidente: Prof. Doutora Ana Maria Martelo Ramos
Arguente: Prof. Doutor João Paulo Serejo Goulão Crespo
Vogal: Prof. Doutora Isabel Maria Rola Coelhoso

FACULDADE DE CIÊNCIAS E TECNOLOGIA
UNIVERSIDADE NOVA DE LISBOA

Outubro de 2013

Susana Cristina Dias Ramos Ferreira

Licenciatura em Ciências da Engenharia Química e Bioquímica

Application of OSN in membrane cascade for purification of the API Amoxicillin

Dissertação para obtenção do Grau de Mestre em
Engenharia Química e Bioquímica

Orientadores: Professor Andrew G. Livingston (IC)
Doutora Ludmila Peeva (IC)

Co-orientador: Professora Isabel Coelhoso (FCT-UNL)

IMPERIAL COLLEGE LONDON
Faculty of Engineering
Department of Chemical Engineering and Chemical Technology
UNIVERSIDADE NOVA DE LISBOA
Faculdade de Ciências e tecnologia
Departamento de Química

Outubro 2013

ACKNOWLEDGMENTS

First of all, I would like to thank to Professor Andrew Livingston for receiving me in his research group and provide me this amazing experience.

To my coordinator Ludmila Peeva for the guidance, support, help, attention and availability. I appreciate the comfort she gave me with any questions and uncertainties.

I am deeply grateful to João Burgal, my daily supervisor, who helped me through the whole project, including writing this thesis. Thank you for all the caring, support, joy, good mood and friendship with which you received me every day.

To my colleagues/friends Carlos Gomes, Irina Valtcheva, James Campbell, Shanta Kumar, Ana Gil, Pedro Bastos, Jeong Kim and Joana Guedes that supported me in every step of the way and made my days much brighter and fun inside and out of the university.

I would also like to thank all the other members of the Separation Engineering and Technology research group for their support during my stay at Imperial College.

To Professor Isabel Coelhoso for being always available to help with any questions and showing interest in my work.

To my parents and sister that made this amazing journey possible and were always there to support, encourage, understand and help me when I most needed.

I would like to thank to Karta, Fateh, Denise and Lockram that received me with open arms and made me feel at home.

I also would like to thank all my friends for their emotional support, encouragement and friendship even being far away from them.

Last but not least, I have to thank to my boyfriend André Lourenço that came with me in this adventure and without him my seven mouths in London would not have been the same for sure. Thank you for all the care, patience, understanding, courage and love.

ABSTRACT

The present work developed at Imperial College London (ICL) in collaboration with the Massachusetts Institute of Technology (MIT) had the objective of purifying the API amoxicillin containing an initial concentration of 30ppm of the compound 4-hydroxy-l-phenylglycine (impurity) using an OSN membrane cascade.

Project proposal:

- Solubility and stability studies of the API in different solvents.
- Solvent choice for the separation process.
- Dissociation study of the API and impurity to exploit a promising optimization of the process.
- Membrane screening using dead-end and m-CSTR upside-down measurements.
- Process modeling and simulation of different configurations

Amoxicillin showed to be a sensitive compound to work with having a low solubility and a fast decomposition in the studied solvents. The solvents tested in detail were water, acetone, ethanol and methanol, being water the one choose to performed the purification.

From the dissociation study it was possible to understand the possible exploitation of the pH parameter in the optimization of the separation process.

In the membrane screening the effect of pressure and pH were studied in six types of membranes. It could be conclude that the main obstacle for the purification process was the membrane performance itself, with insufficient separation between the compounds (difference of 10 p.p. in rejection). The most promising results were obtained using the TFNF-DL membrane, with an API rejection of 99.12% and an impurity rejection of 87.80%.

The process modelling was performed in a semi-batch mode with one and two stages, respectively, and in continuous mode with two-stages and two different configurations. An increase from two to three stages was also analyzed for the continuous configuration II. A maximum purity of 99.65% with a yield of 97.86% was obtained with the semi-batch two-stage cascade system. From the continuous three stage cascade system, a purity of 98.65% and a yield of 98.54% were achieved.

Keywords: Amoxicillin; Purification; Organic solvent nanofiltration (OSN); Active pharmaceutical ingredients (API); Membrane cascade

RESUMO

O presente projecto desenvolvido na Universidade Imperial de Londres (ICL) em colaboração com Instituto de Tecnologia de Massachussets (MIT) tinha como objectivo a purificação do API amoxicilina partindo de uma concentração inicial do composto 4-hydroxy-l-phenylglycine (impureza) de 30 ppm recorrendo a nanofiltração com solventes orgânicos numa cascada de membrana.

Proposta de trabalho:

- Estudos de solubilidade e estabilidade do API em diferentes solventes.
- Escolha do solvente mais conveniente para à purificação.
- Estudo da dissociação de ambos os compostos para explorar uma possível optimização do processo.
- Testes de diafiltrações a diferentes membranas utilizando dead-end e m-CSTR.
- Modelação e simulação do processo considerando diferentes configurações.

A amoxicilina demonstrou ser um composto de difícil solubilidade e fácil decomposição. Os solventes testados em detalhe foram água, acetona, etanol e metanol, sendo água o solvente escolhido para proceder à purificação.

O estudo da dissociação iónica dos compostos demostrou a possível optimização do processo de separação através da exploração do parâmetro pH.

Na realização dos testes de diafiltração, o efeito da pressão e do pH foram estudados em seis tipos de membranas. Conclui-se que o principal obstáculo do processo de purificação seria o desempenho da própria membrana, pelo facto de nao efectuar uma separaracao eficiente entre os dois compostos (diferença de 10 p.p. entre rejeições). O resultado mais promissor foi obtido com a membrana TFNF-DL, tendo uma rejeição do API de 99.12% e uma rejeição da impureza de 87.80%.

A modelação do processo foi realizada a um sistema semi-continuo contendo uma única e duas etapas de separação; e ainda a duas configurações diferentes de um sistema em continuo com duas etapas de separação. Um aumento do número de duas para três etapas foi também analisado para a configuração II em contínuo. Uma pureza de 99.65% com um rendimento de 97.86% foi obtida usando o sistema semi-continuo com duas etapas de separação. Através do sistema de três etapas em contínuo, foi possível alcançar uma pureza de 98.65% com um rendimento de 98.54%.

Palavras-Chave: Amoxicilina; Purificação; Nanofiltração com solventes orgânicos; Ingredientes farmacêuticos activos; Cascatas de membrana

TABLE OF CONTENTS

LIST OF FIGURES……XIII
LIST OF TABLES……XVII
ABREVIATIONS……..IXX
NOMENCLATURE……..XXI

CHAPTER I - LITERATURE REVIEW 1
1.1 Membrane Technology 3
1.1.1 Membrane types 3
1.1.2 Membrane Processes 4
1.1.3 Membrane Characterization 5
1.1.4 Transport in membranes 6
1.1.5 Strengths and drawbacks in membrane processes 7
1.1.5.1 Concentration Polarization 8
1.1.5.2 Membrane fouling 9
1.1.5.3 Insufficient separation 9
1.1.5.4 Membrane compaction……10
1.1.5.5 Membrane stability and lifetime 10
1.2 Membrane technology in the pharmaceutical industry 11
1.2.1 Drug production and purification 11
1.2.2 OSN process for API separation or purification 12
1.2.3 Application of membrane cascade for API separation or purification 14
1.2.3.1 Membrane configurations and modes of operation 15
1.2.3.2 Membrane cascade applications 17

CHAPTER II – OBJECTIVES AND RESEARCH MOTIVATION 19
2.1 Amoxicillin purification via OSN 21
2.1.1 Amoxicillin manufacturing and purification routes 22

CHAPTER III – MATERIALS AND METHODS 25
3.1 Experimental 27
3.1.1 Model Mixture 27
3.1.1.1 Chemicals…… 27
3.1.2 Amoxicillin characterization (solvent choice) 28
3.1.2.1 Solubility study 28
3.1.2.2 Stability study 28
3.1.2.3 Isoelectric point determination 28
3.1.2.3.1 Dissociation study 28
3.1.3. Membranes 29
3.1.3.1 Polybenzimidazole membranes 29

3.1.3.2 Membrane performance 30
3.1.4 Experimental set-ups 30
3.1.4.1 Dead-end measurements 30
3.1.4.2 m-CSTR upside down measurements 31
3.1.4.2.1 Precipitated powder analysis 32
3.1.4.2.2 Mass transfer coefficient of amoxicillin 32
3.1.4.2.3 Concentration polarization analysis 33
3.1.5 Analytical Methods 34
3.2 Process modelling 35
3.2.1 Semi-Batch mode 35
3.2.2 Continuous mode 37
3.2.2.1 Configuration I 37
3.2.2.2 Configuration II 38

CHAPTER IV – RESULTS AND DISCUSSION 41
4.1 Solvent choice 43
4.1.1 Amoxicillin solubility and stability study 43
4.2 Isoelectric point determination 46
4.3 Membrane screening 48
4.3.1 Dead-end measurements 48
4.3.1.1 Pressure effect 49
4.3.1.2 Separation optimization based on solution pH effect 52
4.3.2 m-CSTR upside down measurements 53
4.3.2.1 PBI22 screening results 54
4.3.2.2 TFNF-DL screening results 56
4.3.2.2.1 Precipitated powder analysis 57
4.3.3 Membrane screening conclusion 60
4.4 Process modelling 61
4.4.1 Semi-Batch mode 62
4.4.1.1 One stage system 62
4.4.1.2 Two stage system 63
4.4.2 Continuous mode 65
4.4.2.1 Configuration I 65
4.4.2.2 Configuration II 70
4.4.3 Process modelling conclusion 76

CHAPTER V – CONCLUSION REMARKS AND FUTURE WORK 77
CHAPTER VI - REFERENCES 81
CHAPTER VII - APPENDIX 89

LIST OF FIGURES

Figure 1.1 – Schematic diagrams of the principal types of membranes (Adapted from Baker, 2004)…….3

Figure 1.2 – Typical rejection curves for membranes with a sharp cut-off and a diffuse cut-off (Adapted from Mulder, 1996)……6

Figure 1.3 – Schematic representation of the two transport mechanisms through membranes: (A) the pore-flow model and (B) the solution-diffusion model (Adapted from Baker, 2004)..……6

Figure 1.4 – Concentration polarization: concentration profile under steady-state conditions (Adapted from Baker, 2004)……..8

Figure 1.5 – Effect of fouling and concentration polarization on flux (Adapted from Mulder, 1996)…….9

Figure 1.6 – Typical pharmaceutical batch operation (Adapted from Dunn, Wells and Williams, 2010)……..11

Figure 1.7 – Schematic representation of membrane filtration system design: a) dead-end, b) cross-flow mode (Adapted from Arunima Saxena, 2009)…….14

Figure 1.8 – General representation of the modules and units in a membrane cascade: P- permeate; R- retentate; y – number of stages; n, p and z -number of membrane units in the first, second and y stage, respectively (Adapted from Siew et all, 2013)……...15

Figure 1.9 – Modes of cascade operation: A) simple symmetric cascade; B) symmetric countercurrent recycle cascade (Adapted from Siew et all, 2013)……..16

Figure 2.1 – Molecular representation of the studied compounds: A) Amoxicillin; B) 4-hydroxy-L-phenylglycine…….21

Figure 2.2 - Kinetically controlled synthesis of amoxicillin using penicillin G acylase as catalyst. (Adapted from Alemzadeh, 2010)……..22

Figure 3.1 - Schematic of experimental pressure cell used for membrane screening. (Adapted from Scarpello & Livingston, 2002)…….....30

Figure 3.2 – Layout of the membrane separator cell (m-CSTR). Legend: 1 – Inlet/outlet ports; 2 – Feed/retentate chamber; 3 – Inner o-ring; 4 – Membrane; 5 –Sintered plate; 6 – Outer o-ring; 7 – Cover. (Adapted from Peeva & Livingston , 2013)……...31

Figure 3.3 - Process diagram of the single membrane system (PI: Pressure gauge; TI: Temperature indicator)…….32

Figure 3.4 - Scheme of the two-stage cascade with the main equipment and streams highlighted. Legend: $Feed_{cell}$ – Feed flow-rate to the first stage; F_{R1} – Retentate flow-rate from stage 1; F_{P1} – Permeate flow-rate from stage 1; F_{P2} – Permeate flow-rate from stage 2; F_{R2} – Retentate flow-rate from stage 2……36

Figure 3.5 - Scheme of the continuous two-stage cascade with the main equipment and streams highlighted. Legend: $Feed_{in}$ – Feed flow-rate in (to be purified); $Feed_{out}$ – Feed flow-rate out (purified); $Feed_{cell}$ – Feed flow-rate to the first stage; F_{R1} – Retentate flow-rate from stage 1; F_{P1} – Permeate flow-rate from stage 1; F_{P2} – Permeate flow-rate from stage 2; F_{R2} – Retentate flow-rate from stage 2…….37

Figure 3.6 - Scheme of the continuous two-stage cascade with the main equipment and streams highlighted. Legend: $Feed_{in}$ – Feed flow-rate in (to be purified); $Feed_{out}$ – Feed flow-rate out (purified); $Feed_{cell}$ – Feed flow-rate to the first stage; F_{R1} – Retentate flow-rate from stage 1; F_{P1} – Permeate flow-rate from stage 1; F_{P2} – Permeate flow-rate from stage 2; F_{R2} – Retentate flow-rate from stage 2……..38

Figure 3.7 - Scheme of the continuous two-stage cascade with the main equipment and streams highlighted. Legend: $Feed_{in}$ – Feed flow-rate in (to be purified); $Feed_{out}$ – Feed flow-rate out (purified); $Feed_{cell}$ – Feed flow-rate to the first stage; F_{R1} – Retentate flow-rate from stage 1; F_{P1} – Permeate flow-rate from stage 1; F_{P2} – Permeate flow-rate from stage 2; F_{R2} – Retentate flow-rate from stage 2; F_{P3} – Permeate flow-rate from stage 3; F_{R3} – Retentate flow-rate from stage 3……39

Figure 4.1 – UV signal, from the HPLC analysis, of the samples taken over time for each solution. Solutions prepared with 1g.L^{-1} of amoxicillin in the different solvents……..44

Figure 4.2 - Concentration of amoxicillin over time in the different solvents. Solutions prepared with 1 g.L^{-1} of amoxicillin. These results represent an average of two experiments and the error bars are the standard deviation of the mean……45

Figure 4.3 – Isoelectric point determination: A) Titration curve of amoxicillin a T=20ºC. Experimental conditions: C_{API}= 1.32 mmol.L^{-1}; C_{NaOH}= 49.65 mmol.L^{-1}; $V_{iniz.}$ = 10 mL; B) Titration curve of 4-hydroxy-L-phenylglycine a T=20ºC. Experimental conditions: C_{API}= 1.43 mmol.L^{-1}; C_{NaOH}= 49.65 mmol.L^{-1}; $V_{iniz.}$ = 10 mL; C) Molecular structure and ionizable groups from amoxicillin; D) Molecular structure of 4-hydroxy-L-phenylglycine…….46

Figure 4.4 - Dissociation profiles of the amoxicillin and 4-hydroxy-L-phenylglycine, considering 100% molar percentage in the beginning (see appendix III for calculations)……..47

Figure 4.5 - Process diagram of the single membrane system (PI: Pressure gauge; TI: Temperature indicator)…….53

Figure 4.6 – HPLC UV signal from the mixture compounds in 1 g.L^{-1} aqueous solution: A) amoxicillin (90.0% pure); B) 4-hidroxy-L-phenylglycine (99.0% pure). The red points indicate the different peak areas and the label values the retention times of those peaks……..57

Figure 4.7 - HPLC UV signal results from the powder analysis. A) powder from TFNF-DL- C membrane trial at 0.7 g.L^{-1}; B) powder from TFNF-DL- D membrane trial at 0.9 g.L^{-1}; C) powder from TFNF-DL- E membrane trial at 1 g.L^{-1}. The red points indicate the different peak areas and the label values the retention times of those peaks. The peaks without red points are the ones with dispersible areas (≤ 2)…….58

Figure 4.8 – Concentration profile for the API in the membrane interface, C_{im}, as a function of the mass transfer coefficient. Profiles for the experimental trial using the TFNF-DL – E for both pH conditions considering a retentate API concentration of 2.74 mol.m^{-3} (1 g.L^{-1}) and a solvent rejection of 1%.....59

Figure 4.9 – Single-stage semi-batch system: A) Mass profiles over filtration time for both compounds in the retentate stream; B) Yield and purity profiles for the API, amoxicillin……..62

Figure 5.1 – Two-stage semi-batch system considering an effective pressure in the second stage of 25 bar and a Rc = 0.17: A) Total normalized mass profiles over filtration time for both compounds in the retentate stream; B) Yield and purity profiles for the API, amoxicillin, , and the correspondent zoom……..63

Figure 5.2 – Modeled effect of recycle ratio, Rc, on the API yield and purity of amoxicillin in a two-stage cascade after 35 h (25 vols) obtained by MATLAB®……..64

Figure 5.3 – Concentration profile of the API in the purified outlet stream ($Feed_{out}$) obtained using MATLAB®, considering a ΔP1 of 30 bar and varying the feed flow rate ($Feed_{in}$) and the effective pressure of the second stage (ΔP2) parameters. A permeability of 2.14 $L.m^{-2}.h^{-1}.bar$, an API rejection of 99.12% and an impurity rejection of 87.80% were used based on the TNFN-DL-E membrane trials.……65

Figure 5.4 – Purity and yield profiles of the API in the purified outlet stream ($Feed_{out}$) obtained by MATLAB®, considering a ΔP1 of 30 bar and varying the feed flow rate ($Feed_{in}$) and the effective pressure of the second stage (ΔP2) parameters. A permeability of 2.14 $L.m^{-2}.h^{-1}.bar$, an API rejection of 99.12% and an impurity rejection of 87.80% were used based on the TNFN-DL-E membrane trials……..66

Figure 5.5 – Purity (figure A) and yield (figure B) profiles of the API in the purified outlet stream (Feedout) obtained using MATLAB®, considering a ΔP1 of 30 bar and varying the feed flow rate (Feedin) and the effective pressure of the second stage (ΔP2) parameters. A permeability of 2.14 $L.m^{-2}.h^{-1}.bar$, an API rejection of 99.12% and an impurity rejection of 87.80% were used based on the TNFN-DL-E membrane trials.……67

Figure 5.6 – Concentrations in the purified stream over time (h) obtained using MATLAB®: A) API profile; B) Impurity profile Parameters considered: ΔP1= 30 bar; ΔP2= 25 bar; $Feed_{in}$ = 0.343 $L.m^{-2}.h^{-1}$ and a permeability of 2.14 $L.m^{-2}.h^{-1}.bar$. The recycle ratio and the feed utilization of the systems are respectively Rc= 0.17 and FU= 7.90 (vide Table 5.1)…….68

Figure 5.7 – Profiles of the API purity and yield obtained using MATLAB®. Parameters considered: ΔP1= 30 bar; ΔP2= 25bar; $Feed_{in}$ = 0.343 $L.m^{-2}.h^{-1}$ and a permeability of 2.14 $L.m^{-2}.h^{-1}.bar$. The recycle ratio and the feed utilization of the systems are respectively Rc= 0.17 and FU= 7.90 (vide Table 4.9)…..……..69

Figure 5.8 – Concentration profile of the API in the $Feed_{out}$ obtained using MATLAB®, considering a ΔP1 of 30 bar and varying the $Feed_{in}$ and ΔP2 parameters. A permeability of 2.14 $L.m^{-2}.h^{-1}.bar$, an API rejection of 99.12% and an impurity rejection of 87.80% were considered.……70

Figure 5.9 – Purity (figure A) and yield (figure B) profiles of the API in the purified out stream (Feedout) obtained using MATLAB®, considering a ΔP1 of 30 bar and varying the feed flow rate (Feedin) and the effective pressure of the second stage (ΔP2) parameters. A permeability of 2.14 $L.m^{-2}.h^{-1}.bar$, an API rejection of 99.12% and an impurity rejection of 87.80% were used based on the TNFN-DL-E membrane trials.……71

Figure 6.1 – Behavior of the feed utilization (FU) and recycle ratio (Rc) with the difference of effective pressure between the two stages (ΔP1-ΔP2) obtained using MATLAB®. A ΔP1 of 30 bar, permeability of 2.14 $L.m^{-2}.h^{-1}.bar$, an API rejection of 99.12% and an impurity rejection of 87.80% were considered.…….....72

Figure 6.2 – Concentrations in the purified stream over time (h) obtained using MATLAB®: A) API profile; B) Impurity profile. Parameters considered: ΔP1= 30 bar; ΔP2= 5 bar; $Feed_{in}$ = 0.343 $L.m^{-2}.h^{-1}$ and a permeability of 2.14 $L.m^{-2}.h^{-1}.bar$. The recycle ratio and the feed utilization of the systems are respectively Rc= 0.17 and FU= 7.90 (vide Table 5.2)……..73

Figure 6.3 – Profiles of the API purity and yield obtained using MATLAB®. Parameters considered: ΔP1= 30 bar; ΔP2= 5 bar; $Feed_{in}$ = 0.343 $L.m^{-2}.h^{-1}$ and a permeability of 2.14 $L.m^{-2}.h^{-1}.bar$. The recycle ratio and the feed utilization of the systems are respectively Rc= 0.17 and FU= 7.90 (vide *Table 4.9*)……..……..……..74

LIST OF TABLES

Table 1.1 – Classification of membrane processes according to their driving forces (Adapted from Mulder, 1996)……4

Table 1.2 – Comparison of various pressure driven membrane processes. (Adapted from Coulston Vol.2, 2002)……5

Table 3.1 - Amoxicillin and 4-hydroxy-l-phenylglycine relevant properties. (Data obtain from Sigma-Aldrich safety data sheets; Foulstone, 1982; O'Neil, 2001; VSDB and the chemical book via online)……...27

Table 3.2 – Summary of the membrane tested in this work……..29

Table 4.1 – Results summary of the solvents tested in the laboratory previously……43

Table 4.2. - Comparison of the results obtained for the amoxicillin solubility. Solutions prepared with 10g.L^{-1} of amoxicillin in the different solvents……..43

Table 4.3 - Summary of the screening results conducted using water as solvent with a pressure of 10 bar and a temperature of 22ºC……49

Table 4.4 - Summary of the screening results conducted using water as solvent with a pressure of 20 bar and a temperature of 22ºC……50

Table 4.5 - Summary of the screening results conducted using water as solvent with a pressure of 30 bar and a temperature of 22ºC……51

Table 4.6 - Summary of the screening results conducted using water as solvent at 22º……52

Table 4.7 - Summary of the screening results conducted using water as solvent at 20 bar at 22ºC. Pure solvent average flux is 52.5± 2.5 L.m^{-2}.h^{-1}……...54

Table 4.8 - Summary of the screening results conducted using water as solvent at 20 and 30 bar at 22ºC. Pure solvent average flux is 160.7± 0.1 L.m^{-2}.h^{-1} at 20bar and 225.0± 15.2 L.m^{-2}.h^{-1} at 30 bar……56

Table 4.9 - Summary of the parameters considerations based on the semi-batch experimental trial using the TFNF-DL-E membrane……...61

Table 5.1 - Values for independent and dependent variables, obtained with MATLAB®, in order to optimize contions (considering a permeability of 2.14 L.m^{-2}.h^{-1}.bar, an API rejection of 99.12% and an impurity rejection of 87.80%). Boundary condition established: API maximum concentration = 8 g.L^{-1}……68

Table 5.2 - Values for independent and dependent variables, obtained with MATLAB®, in order to optimize conditions (considering a permeability of 2.14 L.m^{-2}.h^{-1}.bar, an API rejection of 99.12% and an impurity rejection of 87.80%). Boundary condition established: API maximum concentration = 8 g.L^{-1}……73

Table 5.3 - Values for independent and dependent variables, obtained with MS Excel Solver™, in order to optimize contions (considering a permeability of 2.14 L.m^{-2}.h^{-1}.bar, an API rejection of 99.12% and an impurity rejection of 87.80%). Boundary condition established: API maximum concentration = 8 g.L^{-1}……75

Table 5.4 - Comparison between the performances of the different systems configurations described previously. A permeability of 2.14 L.m^{-2}.h^{-1}.bar, an API rejection of 99.12% and an impurity rejection of 87.80% were considered……76

ABREVIATIONS

API	Active pharmaceutical ingredient
CP	Concentration polarization
DCM	Dichloromethane
DBB	Dibromobutane
DBX	Dibroxylene
DMAc	N,N-dimetylacetamide
FU	Feed utilization ratio
GTI	Genotoxin impurity
HPLC	High pressure liquid chromatography
HPGM	P-hydroxyphenylglycine methyl ester
HVNC	High value natural compounds
IPA	Isopropanol
ISA	Integrally skinned asymmetric membranes
m-CSTR	Continuous single stirred tank reactor/membrane separator
MeCN	Acetonitrile
MEK	Methyl ethyl ketone
MF	Microfiltration
MeOH	Methanol
MW	Molecular weight ($g.mol^{-1}$)
MWCO	Molecular weight cut-off
NF	Nanofiltration
NRe	Reynolds number
Nsh	Sherwoods number
NSc	Schmidts number
PEEK	Poly(ether ether ketone)
PEG 400	Polyethylene glycol
PFR	Flow reactor
PGA	Enzyme penicillin G acylase
PI	Polyimide
PP	Polypropylene
Rc	Rcycle ratio
RO	Reverse osmosis
TFC	Thin-film composite membranes
THF	Tetrahydrofuran
UF	Ultrafiltration
UV	Ultraviolet
6-APA	6-aminopenicillanic acid

NOMENCLATURE

J	Membrane flux ($L.m^{-2}.h^{-1}$)
R	Rejection of the solute (%)
B	Membrane permeability ($L.m^{-2}.h^{-1}.bar$)
C	Concentration ($g.L^{-1}$)
$C_{s,0}$	Solute concentration in the feed side ($mol.m^{-3}$)
$C_{s,p}$	Solute concentration in the permeate side ($mol.m^{-3}$)
A	Membrane area (m^2)
r_P	Pore size
ε	surface porosity (dimensionless)
Ƭ	Pore tortuosity (dimensionless)
η	Solvent viscosity ($kg.m^{-1}.s^{-1}$)
l	Membrane thikness
K^L	Solvent sorption
$K_S{}^L$	Solute distribution
D	Fick's law diffusion coefficient ($m^2.s^{-1}$)
R	Gas constant ($8.341\ J.mol^{-1}.K^{-1}$)
k'	Mass transfer coefficient ($m.s^{-1}$)
d	Diameter (m)
D	Diffusion coefficient ($m^2.s^{-1}$)
w	Radial speed of the stir ($rad.s^{-1}$)
ρ	Density ($kg.m^{-3}$)
μ	Viscosity (Pa.s)
V_{API}	API molal volume ($cm^3.mol^{-1}$)
υ	Molar volume of the compound ($m^3.mol^{-1}$)
F	Flow rate ($L.h^{-1}$)
$Feed_{cell}$	Feed into the first stage
$Feed_{in}$	Fresh feed into the feed tank
$Feed_{out}$	Purified feed out of the feed tank
Rc	Recycle ratio
FU	Feed utilization
t	Time (h)
T	Temperature (°C / K)
V	Volume (L)
P	Pressure (bar/Pa)

SUBSCRIPTS

i	Solute
R	Retentate stream
P	Permeate stream
FM	Feed side liquid phase at the membrane liquid interface
b	Bulk
m	Membrane surface
v	Volume
∞	Limiting

CHAPTER I

LITERATURE REVIEW

1.1 Membrane Technology

Membranes have gained an important place in chemical technology and are used in a broad range of applications. This emerging technology has the potential to be applied in diversified industries such as the medical, pharmaceutical, wastewater, petrochemical and food.

A membrane is defined as a selective barrier between two phases which restricts the transport of some substances and allows the transport of others from one phase to another (Mulder, 1996). This transport trough the membrane takes place as a result of a driving force, i.e. by pressure, temperature, concentration or electrical potential difference, acting on the components in the feed. In addition to steric exclusion membrane-solvent interactions, pressure, feed concentration, temperature and charge can influence the membrane performance and such factors can hence be used to fine tune the separation (Mulder, 1996; Screewathanawut et al., 2010; Baker 2004).

1.1.1 Membrane types

A membrane can be homogeneous or heterogeneous, symmetric or asymmetric in structure, solid or liquid in terms of state and can be charged or neutral.

Membranes can generally be classified into biological membranes, or synthetic membranes which can be either organic (polymeric or liquid) or inorganic (ceramic, metal or zeolite) (Mulder, 1996). Synthetic polymeric membranes are commonly classified according to their structure as symmetric or asymmetric. These two classes can be subdivided as shown in *Figure 1.1*.

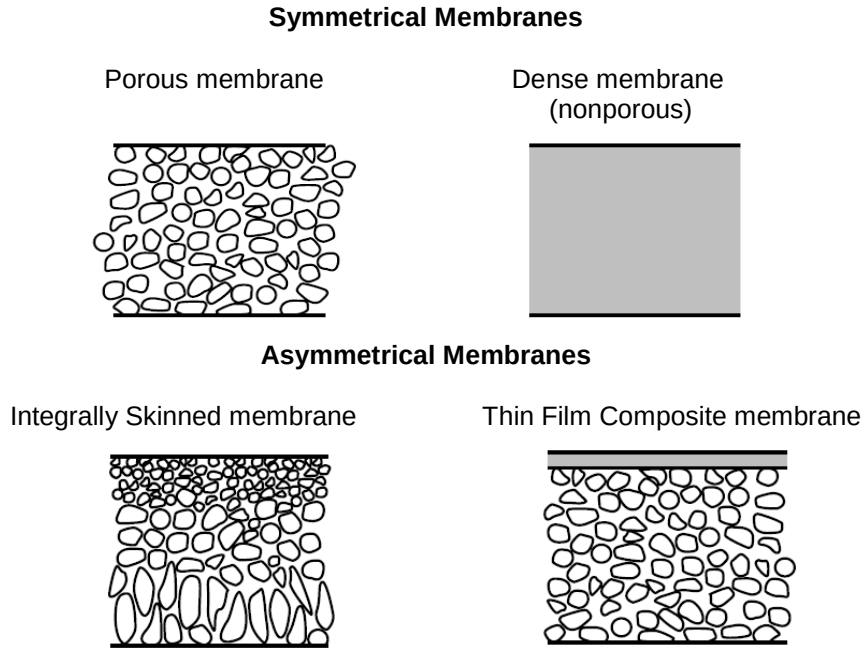

Figure 1.1 – Schematic diagrams of the principal types of membranes (Adapted from Baker, 2004).

The porous membranes are usually used in filtration processes, where separation is made by particle size. Nonporous membranes are frequently used in pervaporation and gas separation processes where the separation occurs according to the difference in solubility and diffusivity of the molecules in the membrane material. When these membranes are charged, they mostly separate by exclusion of ions of the same charge as the fixed ions of the membrane structure

Asymmetric membranes were a major breakthrough in the last decades. These membranes consist of an extremely thin surface layer supported on a much thicker porous structure, being the first layer the one that determinates exclusively the separation properties and permeation rates of the membrane whereas the porous sublayer functions, in conjunction with the backing material (such as polypropylene or polyester), as a mechanical support. With this technology it is possible to achieve,

unlike symmetric membranes, high selectivity with high transport rates, which brings a great economical advantage (Mulder, 1996; Screewathanawut et al., 2010).

The toplayer and its porous sublayer may be formed in a single operation, with the formation of integrally skinned asymmetric membranes (ISA), or separately, with the formation of thin-film composite (TFC) membranes. In TFC membranes the skin-layer and the porous sublayer can be made of different materials, which mean that the active layer and porous sublayer can be independently optimized to maximize the overall membrane performance. Nevertheless, the skinned asymmetric membranes have considerably lower manufacturing costs comparing to the TFC membranes (Mulder, 1996; Screewathanawut et al., 2010).

The interest in membranes formed from less conventional materials has increased. Ceramic membranes for example are being applied in microfiltration and ultrafiltration fields do to their superior performance in terms of chemical and thermal stability relative to polymeric membranes. This main class of inorganic membranes do not deform under pressure nor do they swell and are easier to clean, (cleaning agents such as strong acids and alkali, can be used). Furthermore, they have a greater lifetime than that of organic polymeric membranes. However, they tend to be more expensive and brittle than polymeric membranes and are also less versatile in applications. In addition, their large-scale synthesis and module construction is not as easy as for polymeric membranes (Vandezande, Givers and Vankelecom, 2008). That is why the majority of membranes used commercially are still polymer-based (Mulder, 1996; Screewathanawut et al., 2010; Vandezande, Givers and Vankelecom, 2008)

1.1.2 Membrane Processes

Membrane processes can be classified according to their driving forces.

Table 1.1 – Classification of membrane processes according to their driving forces (Adapted from Mulder, 1996).

Pressure difference	Concentration difference	Temperature difference	Electrical potential difference
Microfiltration	Pervaporation	Thermo-osmosis	Electrodialysis
Ultrafiltration	Gas separation	Membrane distillation	Electro-osmosis
Nanofiltration	Vapour permeation	-	Membrane electrolysis
Reverse Osmosis	Dialysis	-	-
Piezodialysis	Difusion dialysis	-	-
	Carrier-mediated transport	-	-

The most important pressure driven membrane processes are microfiltration (MF), ultrafiltration (UF), nanofiltration (NF) and reverse osmosis (RO). All of them are used to concentrate or purify a dilute (aqueous or non-aqueous) solution. What differs between them is basically the size of the solutes to be separated. By changing the separation process from microfiltration to ultrafiltration, nanofiltration and reverse osmosis, the size (or molecular weight) of the particles or molecules separated diminishes and consequently the pore size in the membrane become smaller. This also implies that the resistance of the membranes to mass transfer increases and this is the reason why higher pressures are applied when changing the operation from microfiltration to reverse osmosis (Mulder, 1996). A comparison of the various pressure driven processes is given in *Table 1.2*.

Table 1.2 – Comparison of various pressure driven membrane processes. (Adapted from Coulston Vol.2, 2002)

Microfiltration	Ultrafiltration	Nanofiltration and Reverse Osmosis
Particle separation	Macromolecules separation (bacteria, yeast)	Separation of low MW solutes (salts, glucose, lactose, micropollutents)
Pore sizes ≈ 0,05-10 μm	Pore sizes ≈ 1-100 nm	Pore sizes < 2nm
Low pressure applied (< 2 bar)	Medium pressure applied (1-10 bar)	High pressure applied (≈ 10-60 bar)
Separation based on the particle size	Separation based on the particle size	Separation based on differences in solubility and diffusivity

1.1.3 Membrane Characterization

Membranes can be characterized in terms of their performance and morphology. In terms of performance the most important parameters are flux, permeance, rejection, diffusion coefficients and separation factors. Morphological parameters include both physical (e.g. pore shape, pore size, pore distribution, membrane/top layer thickness, etc) and chemical parameters (e.g. charge, hydrophobicity, etc).

Performance parameters are dependent on morphological parameters, for instance pore size, shape and distribution have a big influence on the membrane flux. Depending on the pore size and shape the molecules will permeate easily or not (bigger pore sizes correspond to a better permeation and a higher flux) and if the pore distribution is uniform or not, membrane flux can be compromised due to fouling formation and pore blocking (non uniform pore distribution results in areas with higher flux than others promoting fouling in the less permeated areas). However, and despite the importance of characterizing and better understanding physical-chemical parameters, it is the functional parameters that from a practical perspective, determine the usefulness of the membrane (Mulherkar and Van Reis, 2004; Cuperus and Smolders, 1991).

The permeability rate, also denominated by flux, J ($L.m^{-2}.h^{-1}$), is defined as the volume of liquid permeating through the membrane (V_p) per unit of area (A) and time (t).

$$J = \frac{V_P}{A.t}$$

Equation I.1

Many parameters like temperature, pressure and solute concentration affect the flux of membranes. The permeate rate tend to increase with increasing temperature, because of reduction in solvent viscosity and increased polymer chain mobility (Van der Bruggen, Geens and Vandecasteele, 2002). An increase in pressure also led to an increase in flux. Solute concentration has an adverse effect on flux because of osmotic pressure and concentration polarization.

Membrane selectivity can be expressed using the rejection coefficient, R_i. This coefficient is defined as the ability of the membrane to separate a solute i from the feed solution and it is usually given by,

$$R_i = \left(\frac{C_{R,i} - C_{P,i}}{C_{R,i}}\right) \times 100 = \left(1 - \frac{C_{P,i}}{C_{R,i}}\right) \times 100$$

Equation I.2

where $C_{R,i}$ and $C_{P,i}$ denotes the concentration of solute i at the retentate and permeate side, respectively. If a component has 100% rejection, none of it goes through the membrane; if a component has 0% rejection, all of it goes through the membrane.

The selectivity can also be described by separation factor, α, when working with gas or organic solvent mixtures, being defined as the ratio between the coefficient of the concentrations of components A and B in the permeate, y_A and y_B, and the concentrations of the components in the retentate, x_A and x_B (Mulder, 1996).

Another important concept in the characterization of a membrane is the 'molecular weight cut-off' (MWCO), which represents the minimum molecular weight (MW) that is 90 % rejected by a membrane. This parameter, despite being useful as a starting point when screening for suitable membranes for a specific mixture separation, can be a poor estimation of the membrane performance. Pore size distribution, solvent environment, molecular shape, charge, functional groups, occurrence of polarization phenomena, temperature and the applied pressure are all factors that also affect the membrane rejection. (Mulder, 1996; Vandezande, Gevers and Vankelecom, 2008; See Toh et al., 2007; Yang et al., 2001).

NF and OSN membranes are characterized by a sigmoidal rejection curve, as the ones depicted in *Figure 1.2*, and they can discriminate molecules with molecular weight in the range of 200 to 2000 Da (Mulder, 1996; Vandezande, Gevers and Vankelecom, 2008).

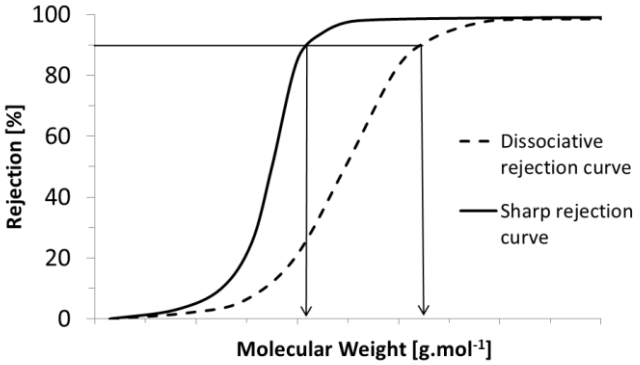

Figure 1.2 – Typical rejection curves for membranes with a sharp cut-off and a diffuse cut-off (Adapted from Mulder, 1996).

1.1.4 Transport in membranes

In order to understand and possibly predict fluxes and rejections for a certain membrane, the transport mechanism of solutes and solvents through porous or dense films of different membranes should be thoroughly understood.

Three groups of mathematical models are used to describe the transport through membranes: irreversible thermodynamics models, pore-flow model and solution-diffusion model. The most reliable and commonly used transport models are the pore-flow and the solution-diffusion models. They describe, respectively, the transport through porous (e.g. micro and ultrafiltration membranes) and dense membranes (e.g. reverse osmosis, gas separation and pervaporation membranes).

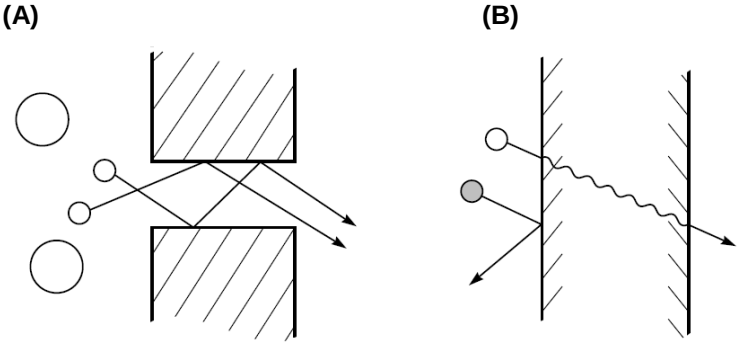

Figure 1.3 – Schematic representation of the two transport mechanisms through membranes: (A) the pore-flow model and (B) the solution-diffusion model (Adapted from Baker, 2004).

Pore-flow model

The pore-flow model assumes that different permeants are separated through tiny pores in the membrane by size-exclusion. This separation is accomplished by a pressure gradient across the membrane transporting the permeants through the pores. It is supposed that there are no concentration gradients, i.e. the solute and solvent concentration are constant over the membrane. Thus, the transport through porous membranes can be described based on hydrodynamic analysis by Darcy's law (*Equation I.3*) in which k is the permeability coefficient, that contains membrane structural factors as membrane pore size (r_p), surface porosity (ε), pore tortuosity (τ), solvent viscosity (η) and dP/dX is the pressure gradient over the membrane.

$$J = k.\frac{dP}{dX} = \frac{\varepsilon.r_p}{8.\eta.\tau}\frac{dP}{dX}$$

Equation I.3

Solution-diffusion model

The solution-diffusion was initially used to explain transport of gases across polymeric film and nowadays it became the most widely accepted explanation of membrane transport. This model assumes that permeants dissolve in the membrane material and then dissolve through the membrane due to a concentration gradient, while the pressure within the membrane is constant at the highest level. The separation between different permeants occurs due to differences in their solubilities and diffusivities (Baker, 2004). Following the assumptions made, two simple equations could be derived for volume and solute flux:

$$J_V = \frac{D.K^L.C.v}{l.R.T}(\Delta P - \Delta\pi) = B_a(\Delta P - \Delta\pi)$$

Equation I.4

$$J_S = \frac{Ds.Ks^L}{l}(C_{s,0} - C_{s,p}) = B_s(C_{s,0} - C_{s,p})$$

Equation I.5

where D and D_S are the Fick's law diffusion coefficients, K^L and $K_S{}^L$ are the solvent sorption and the solute distribution, respectively, C is the solvent concentration, v is the solvent molar flux, l is the membrane thickness, $C_{s,0}$ is the solute concentration in the feed side and $C_{s,p}$ is the solute concentration in the permeate side; the constants B_a and B_s are known as the solvent and solute permeability, respectively (Baker, 2004).

OSN membranes are intermediate between truly porous and truly solution-diffusion membranes, and so they are best described by transient mechanisms that take into account the changing contributions of the diffusive and convective mechanisms, like the irreversible thermodynamics and the pore-flow models presented, or the solution-diffusion with imperfections model (Bhanushali et al., 2002), that accounts for the occurrence of convective flow and for the partial flux coupling effect. Plus, and since OSN membranes are applied to non-aqueous systems, special considerations regarding the various interactions between the system components and membrane swelling are also needed (Bhanushali et al., 2002; Boam and Nozari, 2006; Dijkstra Bach and Ebert., 2006; Robinson et al., 2004).

1.1.5 Strengths and drawbacks in membrane processes

Compared with traditional separation processes as distillation or crystallization, membranes are an easy-to-operate and low-maintenance process. They can be easily installed as continuous processes and readily combined with existing processes into a hybrid process. The latter fact can be attributed to their modular set-up, which also renders upscaling relatively simple (Vandezande, Gevers and Vankelecom, 2008). These systems usually non-thermal and have low capital cost, compact size and power consumption, which reduce the production cost. Membrane technology also has a trend in being more energy efficient than the conventional techniques as well as being cleaner, therefore more environmentally friendly. Membrane processes are also extremely versatile, as membranes can be tailored to fit the most diverse applications like water purification, carbon capture and even organic solvent exchange.

Membrane processes still have some limitations, that particularly slow down large-scale applications (Baker, 2004; Vandezande, Gevers and Vankelecom, 2008). The most relevant limitations are discussed in the following sub-sections. A special attention was given to problems related to pressure driven membrane processes, like NF and OSN.

1.1.5.1 Concentration Polarization

Concentration polarization (CP) is the accumulation of solutes at the membrane active layer surface as a result of a permeate flow through the membrane. It creates a higher solute concentration at the membrane surface compared with bulk. This phenomenon has greater effects in pressure-driven processes due to high pressures used. In such processes CP leads to flux reduction due to increased pressure, that must be overcome, but also an increase in the driving force for the solute(s), reducing membrane selectivity. The increase in solute concentration at the membrane surface can also lead to a diffusive back flow towards the bulk of the feed, resulting in a concentration gradient between the bulk ($C_{s,b}$) and the membrane surface (C_m), creating a boundary layer which increases the resistance to mass transfer (Mulder, 1996).

In the boundary layer:

$$J_V.C_S + D_S\frac{dC_S}{dx} = J_V.C_{S,p}$$

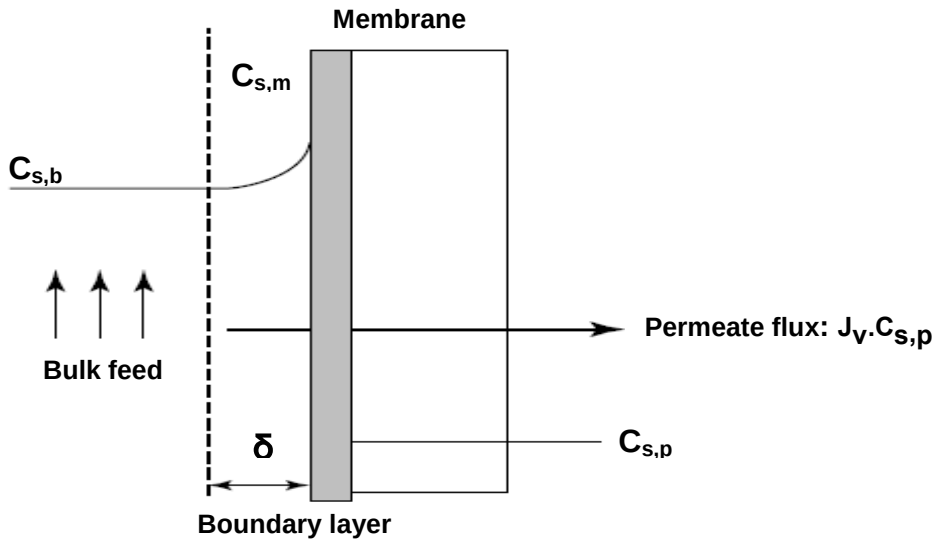

Figure 1.4 – Concentration polarization: concentration profile under steady-state conditions (Adapted from Baker, 2004).

It is possible to minimize the concentration polarization effect by decreasing the boundary layer thickness. This can be achieved by increasing the fluid flow velocity past the membrane surface, by using membrane spacers, or by using pulsating flow, as all these options increase turbulent mixing at the membrane surface (Mulder, 1996; Baker, 2004).

It is known that concentration polarization increases exponentially with the volume flux, J_v. That is why after a certain pressure, the flux does not increase further on increasing the pressure and the so called limiting flux, J_∞, is achieved. Thus, there is no point in having super-high-flux membranes, since the maximum flux will always be limited by osmotic pressure and concentration polarization. The only advantage of these membranes would be a reduction in energy costs, since they would allow for the same flux at lower applied pressure, minimize the overall processing time and limit the required membrane area (Mulder, 1996).

1.1.5.2 Membrane fouling

Concentration polarization can result in membrane fouling, which is the deposition of retained solutes in the membrane, by adsorption, pore blocking, precipitation or cake formation. The type of separation problem and the type of membrane used in MF and UF make these processes the most susceptible to concentration polarization and fouling of all pressure driven membrane processes (Mulder, 1996). Fouling problems are, however, much more complex for NF processes, since the interactions leading to fouling take place at nanoscale, and are therefore difficult to understand (Van der Bruggen Mänttäri & Nyström., 2008).

One of the main consequences of membrane fouling is the decrease of flux. This has a negative impact on the operational costs of the process since the permeate production gets lower and/or higher trans-membrane pressures are required (Mulder, 1996).

Classical solutions to fouling are the pre-treatment of the feed and cleaning of membranes. Membrane design and process conditions can also be optimized to minimize fouling phenomena. Nevertheless, membrane modification is potentially the most sustainable solution, as it would allow to virtually avoid the problem (Mulder, 1996; Van der Bruggen Mänttäri & Nyström., 2008).

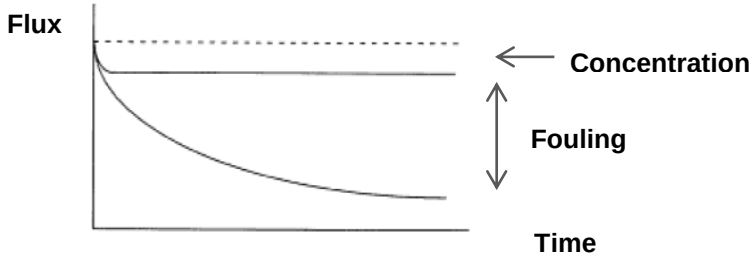

Figure 1.5 – Effect of fouling and concentration polarization on flux (Adapted from Mulder, 1996).

1.1.5.3 Insufficient separation

The incomplete separation is a major impediment for a wide application of membrane processes, including NF (Van der Bruggen Mänttäri & Nyström, 2008).

As mentioned before, membranes are characterized by a sigmoidal rejection curve which never is completely sharp. This will be translated in an insufficient separation between the different compounds on the basis of molecular size. A separation is dependent on other physical and chemical properties of the compounds and of the membrane, like charge (Bellona and Drewes, 2005), and since the pores of NF membranes follow a distribution of sizes (Richard Bowen and Doneva, 2000), the permeate usually contains molecules with variable sizes, both below and above the claimed average pore size of the membrane. The separation can be even more challenging for OSN processes, since solvents can change membrane characteristics, like pore size and hydrophobicity, and even solute characteristics, like solute effective diameter (Van der Bruggen Mänttäri & Nyström., 2008; Geens et al., 2005). Therefore, a single membrane separation is often insufficient to obtain the desired separation (Van der Bruggen Mänttäri & Nyström., 2008).

There are different process strategies to overcome this problem, like multiple membrane passages, diafiltration or membrane cascades. As will be seen forward, membrane cascades offer further benefits, and begin to be considered for NF and OSN processes.

1.1.5.4 Membrane compaction

Compaction is the mechanical deformation of a polymeric membrane matrix, due to the sealing and collapse of the pores at elevated pressures. Thus, this is a phenomenon which occurs specially with porous membranes used in pressure driven membrane operations, where the applied pressures are relatively high, like NF and RO (Mulder, 1996; See Toh et al., 2008). However, dense membranes tend also to suffer some compaction when exposed to swelling conditions (Vankelecom et al., 2004). This is never a problem for ceramic membranes due to their superior mechanical stability.

During compaction the flux declines until the membrane reaches a steady state in which no further permeate flux reduction occur. On the other hand, the rejection tends to increase, eventually stabilizes after a critical volume of solvent permeates through the membranes. After relaxation, the flux and rejection can return or not to its original value, depending on the reversibility of the membrane deformation (Mulder, 1996; Whu, Baltzis and Sirkar., 2000). In order to avoid this time dependent behavior, polymeric membranes should be pre-conditioned with pure solvent until a steady flux is obtained (Gibbins et al., 2002).

1.1.5.5 Membrane stability and lifetime

Membranes for industrial application require reproducibility performance as well as long-term stability and cleanability.

Lifetime and chemical resistance of nanofiltration membranes is related with the occurrence of fouling (therefore the need for cleaning) and the application of the membranes in demanding circumstances, such as the ones created by organic solvents (Van der Bruggen Mänttäri & Nyström., 2008).

The cleaning regularity of the membranes is critical in aqueous applications. Even the mildest agents used in the cleaning process damaged the membrane to some extend and accelerate the deterioration process (Van der Bruggen Mänttäri & Nyström., 2008).

Compatibility of polymeric membranes with a wide range of organic solvents for solvent resistant nanofiltration is a new and even more challenging issue in discussions about membrane lifetime. Membranes can be made more stable by, e.g., increasing the degree of crosslinking of the polymeric top layer, by using alternative membrane materials. Ceramic membranes, as mention before, can be a solution to the swelling, changes in performance, and limited lifetime problems.

1.2 Membrane technology in the pharmaceutical industry

1.2.1 Drug production and purification

The manufacturing of a drug product involves two phases: the production of the API and the formulation process, in which the API is combined with one or more excipients to produce the final product.

A scheme of the different steps involved in a typical API synthesis process, including solvent waste streams generated in each step is shown on *Figure 1.6*.

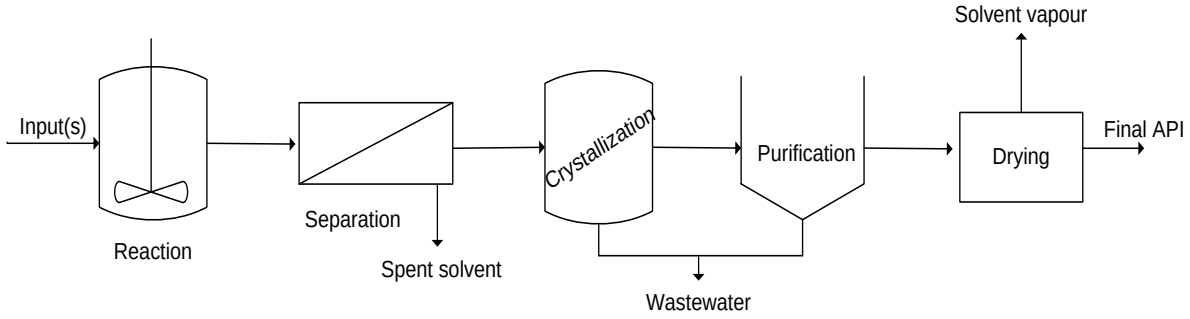

Figure 1.6 – Typical pharmaceutical batch operation (Adapted from Dunn, Wells and Williams, 2010).

Most APIs are produced using liquid phase organic reactions which often require large quantities of different solvents. Since pharmaceutical legislation is very tight in relation to the impurity levels of the active compound, procedures of separation/purification have to be conducted. Between each reaction step, there are a series of operations required to separate, purify and isolate APIs intermediates (work-up phase). These steps frequently require more solvents and/or generate solvent waste. Because of the considerable number of steps and the large amount of solvents required per each step, solvent use can account for as much as 80-90% of the total mass in an API production process (Elin and Rundquist, 2012).

Crystallization and chromatography are the techniques of choice to isolate or purify materials such as API's or HVNC's (high value natural compounds). Precipitation and adsorption can also be used.

Crystallization is widely used for manufacturing specific, active ingredients during final and intermediate stages of purification and separation, and this process determines chemical purity and physical properties of active ingredients, such as crystal morphology, size distribution, and crystal structure (Myerson, 2002). These properties of crystalline solids can have important effects on their fluidity, filterability, tableting behavior, bioavailability, and stability (Myerson, 2002). Crystallization processes are regulated by both thermodynamic properties and crystallization kinetics, and understanding the crystallization processes is fundamental in better controlling and optimizing existing processes and designing new processes (Mullin, 2001). Nevertheless, during crystallization some concerns such as the scale-up, controllability of the process and the production of solute rich waste (mother liquors – impurities removed in the operation and API dissolved to the saturation limit) are observed.

In the case of chromatography, high consumptions of solvents and block issues in the stationary phase can be found (Screewathanawut et al., 2010; Elin and Rundquist, 2012; Justin Chun-Te Lin, 2007). Many new green solvents or alternative reaction medium have been suggested for organic synthesis. Although their potential environmental and health risks are still unclear, they contribute as an alternative approach to decrease solvent consumption and reduce consequential pollution during organic synthesis processes.

Distillation is conventionally used in solvent exchange and in solvent recovery (approximately 95% of all solvent separation processes) (Dunn, Wells and Williams, 2010), but it may not be ideal for API's as many of them are thermally labile materials; also this operation consumes significant amounts of energy, generates significant quantities of intermediate solvent mixtures when used for solvent exchange (especially in a large scale) and inadequate condensing of distillate products (Justin Chun-Te Lin, 2007)

Pharmaceutical industry is known to be relatively solvent intensive with high energy consumption. (Screewathanawut et al., 2010; Elin and Rundquist, 2012). It is essential that pharmaceutical companies reduce the overall environmental footprint, design even more efficient and robust processes, minimize solvent utilization, energy consumption and waste generation (Dunn, Wells and Williams, 2010). Membrane processes can be easily installed as a continuous process, and due to its modular set up, they can be combined readily with existing processes into hybrid processes. All these factors make membrane technology an attractive alternative (Vandezande, Givers and Vankelecom, 2008).

1.2.2 OSN process for API separation or purification

OSN has attracted a great deal of attention as an alternative process for purification of APIs as of HVNCs and also for recycle of solvents (Screewathanawut et al., 2010; Elin and Rundquist, 2012; Justin Chun-Te Lin, 2007; Stewart Slater, 2010).With recent introduction of stricter environment legislation, the expected price increase of the pure solvent and pressure from the regulatory agencies gives a chance to this technique (Stewart Slater, 2010; Siew et al., 2012).

Although OSN is still a relatively novel technology, it offers unique advantages over conventional separation methods. One of the benefits it is that the separation can be performed at near ambient or sub-ambient temperatures. This is a considerable advantage for thermolabile compounds, such as APIs and HVNCs that are susceptible to thermal degradation, minimizing the loss of activity, nutritive value and unwanted side-reactions. Other benefits associated are the energy-efficiency, recovery of organic solvents with a purity suitable for re-use in API, reduced purchase of solvents, less storage and waste costs, increased compliance with environmental legislation and even reduced emissions of greenhouse gases (Screewathanawut et al., 2010; Elin and Rundquist, 2012).

In the field of purification and concentration of antibiotics and pharmaceutical intermediates, M. Kyburz, et all (2005) and X. Cao et all (2001) (Vandezande, Givers and Vankelecom, 2008) developed a post-synthesis recovery of 6-aminopenicillanic acid (6-Apa, 216 Da), an intermediate in the enzymatic manufacturing of synthetic penicillin, from its bioconversion solution with a Koch® membrane (commercial membrane MPS) (KOCH Membrane Systems Inc., 2013). With a recovery of 90-95%, product loss was restricted to a minimum, leading to a pay-back time of less than one year.

A cross-flow microfiltration (MF) using Koch Membrane Systems (KMS) spiral wound elements has also been effectively employed as a replacement for traditional clarification methods to provide high product recovery with gentle processing conditions. For instance, in amino acid production older clarification technologies such as centrifugation and rotary vacuum filtration were substitute by KMS and with this system were possible to achieve yields as high as 98%. With KMS the improved and consistent filtrate quality will also simplify the downstream processing steps (KOCH Membrane Systems Inc., 2013).

Another example is the production of the antibiotic Spiramycin® normally extracted from bacterial broths with butyl acetate, which is traditionally recovered via evaporation, (has a negative influence on the quality of the final product). D. Shi et all (2006) (Vandezande, Givers and Vankelecom, 2008) developed a polyamide membrane for the concentration of this antibiotic, forming a mixture of three compounds with molecular weights between 830 and 800 Da. Rejections around 99% and a much better product quality were achieved.

Recently a comparative study of flash chromatography and recrystallization, both conventional API purification technologies, versus OSN was performed by G. Székely et all (2012) in order to evaluate the feasibility and sustainability of OSN as a potential API purification technology. Eleven GTIs and nine APIs of industrial interest were used as model compounds and various diafiltration studies were carried out. OSN was proven to be competitive and hence various solvent resistant nanofiltration membranes were screened in tetrahydrofuran (THF), methyl ethyl ketone (MEK) and dichloromethane (DCM). Using OSN technology, studies of the degenotoxification in the presence of various APIs of different chemical classes were also developed with success.

OSN has been also applied to other innumerous processes such, continuous solvent exchange, solvent recycling and catalyst recycling.

Important applications in solvent exchange and recovery for pharmaceutical processes were also developed. Sereewatthanawut et al. (2010) proposed the utilization of a dual OSN membrane process for the recovery of THF during the diafiltration of an organic synthesis solution containing an API intermediate from Janssen Pharmaceutical, its isomer, and a series of oligomeric impurities based on the API intermediate (i.e., dimers, trimers, tetramers and pentamers). Using this process they were able to recover 99.2% of the product while reducing the overall content of impurities from 6.8 wt% to 2.4 wt%, which is below the allowed limit of 3 wt % oligomeric impurities. They also claim that the integration of the solvent recovery stage allowed the reduction of the fresh solvent requirement by up to 90%. With the previous configuration, they proved that membrane technology can contribute towards a solvent-efficient process; such configuration does not generate large volumes of waste and/or does not provide a dilute product solution that would require further processing.

Rundquist, Pink and Livingston (2012) investigated the feasibility of using OSN as an alternative to distillation for solvent recovery from crystallization mother liquors. They observed that despite less solvent is recovered by OSN, this technique is capable of recovering organic solvent with suitable purity for re-use in subsequent API crystallizations and it uses 25 times less energy per liter of recovered solvent when compared to distillation. They also demonstrated that equivalent recovery volumes can be obtained by using an OSN hybrid process with the energy consumption remaining 9 times lower than when distillation is used alone.

OSN has also been applied in the recycle of homogeneous catalysts. Nair et al (2001), permeated the post-reaction mixture through a polyimide OSN membrane achieving an overall 90% catalyst retention after four catalyst recycles (five reaction–filtration sequences) and a total catalyst turnover number (TON, moles of product synthesized per mol of catalyst added) of 1200.

Aerts et al. (2006) used silicon-based OSN membranes to recycle the Co-Jacobsen catalyst four times in diethylether (Et2O), achieving 98.5% retention and a minor decrease in the conversion from one cycle to another.

Recently, Peeva, Burgal and Livingston (2013) presented a continuous Heck coupling reaction combined with OSN separation of the catalyst in situ, using polymeric membranes (poly(ether ether ketone), PEEK) at high temperature (80ºC) and high concentration of base (>0.9 mol L^{-1}). Two reactor configurations were investigated: a continuous single stirred tank reactor/membrane separator (m-CSTR) and a plug flow reactor (PFR) followed by m-CSTR (PFR–m-CSTR). The combined PFR–m-CSTR configuration was found to be the most promising, achieving conversions above 98% and high catalyst turnover numbers (TONs) of 20,000. In addition, low contamination of the product stream (27 mg palladium per kg of product) makes this process configuration attractive for the pharmaceutical industry.

The application of OSN is still limited, despite a wide range of potential opportunities in the pharmaceutical and natural products industries. One of the main reasons for the slow technology breakthrough of the OSN membranes is the lack of robustness of commercially available membranes. Another issue is the mutual interactions between solute and solvent, solvent and membrane, as well as between solute and membrane that play a key role in addition to molecular pore size. This makes this process less accessible for the non-specialist, and renders selection of a suitable membrane type for a given separation relatively difficult. Adding to this, economical reasons and the long time that takes to update rules and considerations followed by the industries, slows the progression of these processes (Screewathanawut et al., 2010; Elin and Rundquist, 2012; Vandezande et al., 2007).

1.2.3 Application of membrane cascade for API separation or purification

OSN membranes have made significant advance in terms of performance, but when working within the range of concentrations for APIs, it is unable to achieve total rejection (Screewathanawut et al., 2010; Elin and Rundquist, 2012). Insufficient discrimination between quite similar species is another obstacle that severely limits the industrial application of OSN when product purity is of high importance. In order to compete with conventional separation methods, such as chromatography, adsorption and crystallization, membranes must offer much better separation performance.

To improve the separation performance one might develop better membranes with superior performance, but an alternative is to modify the process configuration, for instance by using a membrane cascade.

The concept of membrane cascade dates back to the 1940s when it was first applied for uranium-235 (235U) enrichment using porous membranes (Mulder, 1996). A cascade consists in a series of separation units arranged in parallel (a stage/module). The simplest membrane process design is one in which a single module is used. However, the single-module design does not often result in the desired separation, since membranes are not always sufficiently selective (Van der Bruggen Mänttäri & Nyström., 2008).

There are two basic module configurations which are flat and tubular. The choice of the configuration should be based both on economic considerations and on the type of application (Mulder, 1996). Both configurations can be arranged either in parallel or in series in a cascade, according to the scale and the purpose of each application. The applications can be obtained by two filtration modes: the dead-end filtration mode in which the feed is forced through the membrane by a perpendicular pressure on the membrane surface; or the cross-flow filtration mode where the feed flows parallel to the membrane surface.

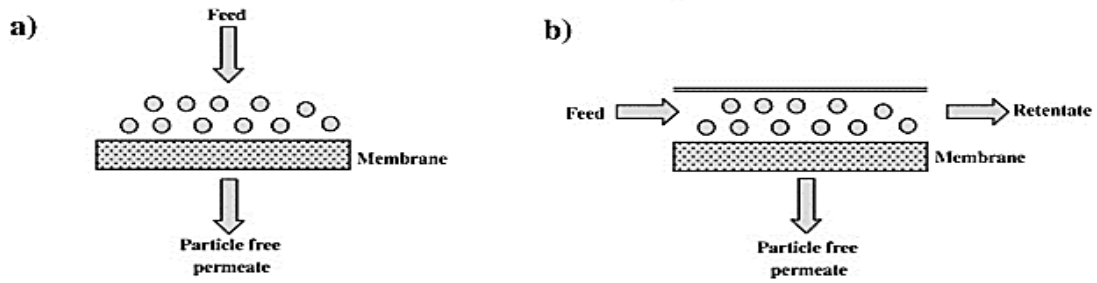

Figure 1.7 – Schematic representation of membrane filtration system design: a) dead-end, b) cross-flow mode (Adapted from Arunima Saxena, 2009).

The main disadvantage of a dead end filtration is the extensive membrane fouling and concentration polarization. The tangential flow devices are less susceptible to fouling due to the sweeping effects and high shear rates of the passing flow.

There are other cross-flow operation modes where the feed and the permeate streams are parallel to each other, namely the concurrent and counter-current operation modes. It can be demonstrated by process calculations that the counter-flow gives the best separation results (higher driving force), followed by the cross-flow and co-current flow, respectively (Mulder, 1996).

Ultimately the module configuration in which the membrane is packed has a profound influence on its performance. The cascade system performance is determined by the separative capability inherent to the system and the properties of the feed and waste and in many cases the configuration has to be adapted to the requirements and limitations of the work system.

1.2.3.1 Membrane configurations and modes of operation

Hwang laid the foundations of cascade theory in 1965 by applying the McCabe-Thiele method, originally developed for distillation, to the design of a membrane cascade for the separation of binary gas mixtures. This work showed the potential and the advantages of a well-designed membrane cascade system, with the ability to achieve any desired solute fractionation. Since then different schemes have been proposed by many authors.

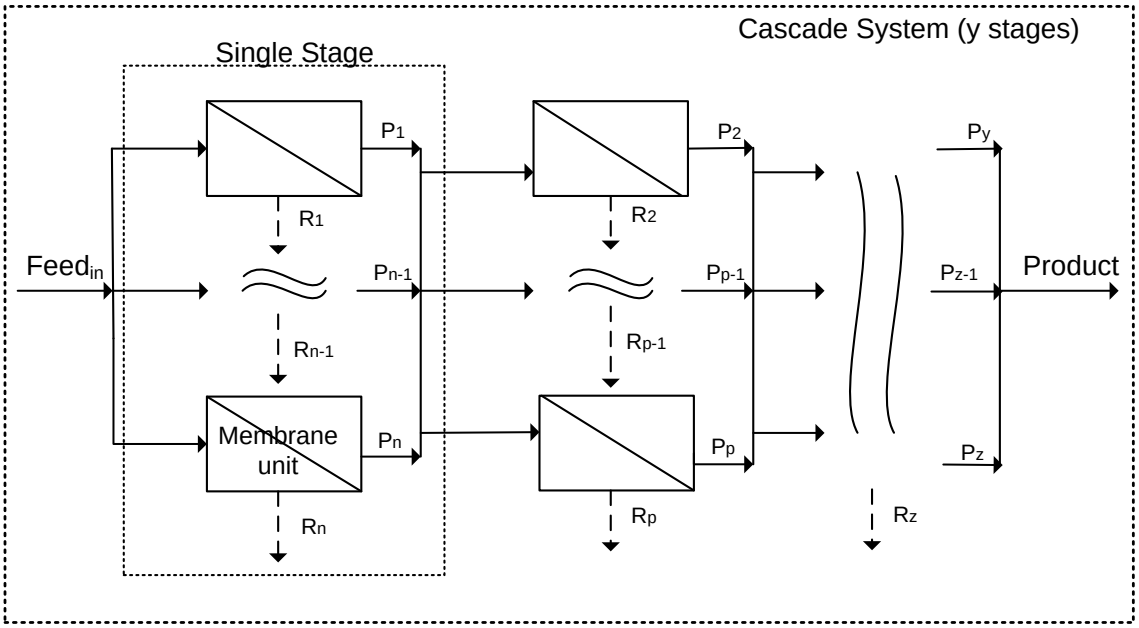

Figure 1.8 – General representation of the modules and units in a membrane cascade: P- permeate; R- retentate; y – number of stages; n, p and z -number of membrane units in the first, second and y stage, respectively (Adapted from Siew et al., 2013).

Above is represented a configuration of stages and membrane units in a general multistage membrane process. In each stage the membrane units disposed in parallel have the same feed stream and similar permeate streams. On the other hand, the various stages are connected to each other in series, that is, each stage receives input from the previous one and passes its output on to the next stage. The number of units in each stage varies but when units have low capacity, it is necessary to use many units in parallel so large amounts of material can be processed (Krass, 1983; Benedict, Pigford and Levi, 1981; Villani and Becker, 1979).

In simple cascades, the stream that follows to the next cell is always a fraction of the feed. Consequently the final product stream amount decrease as the number of cells in the cascade increase. To overcome this problem one can use either cells of different size or a tapered-cascade arrangement (number of separating units decreases with each stage). A disadvantage of simple schemes is that these ones involve the discharge and no utilization of considerable material in discarded streams, so one should use such schemes only when relatively few stages are involved and if the disposed components are not fairly valuable (Villani and Becker, 1979; Hwang and Kammermeyer, 1975). However, the discarded streams can be recycled and passed back down as input to a preceding stage in a recycle cascade.

A recycling cascade has two sections: the enriching section, consisting of the stages above the point at which the feed enters the cascade and the stripping section below the feed point. The stripping section increases the recovery of the material, whereas the enriching section produces material of increased concentration. A simple cascade has only an enriching section.

In a symmetric cascade, the waste stream from each stage is recycled back to the immediately preceding stage. In an asymmetric cascade, the waste is recycled more than one stage back. A common asymmetric cascade feeds the product stream into the next stage and sends the tails stream back two stages back. This is called a two-up, one-down cascade (Olander, 1981).

A very effective and common cascade design used is the symmetric countercurrent recycle cascade, which in some ways is very similar to a continuous distillation column (Benedict, Pigford and Levi, 1981). In the case of the countercurrent recycle cascade, the permeate of a stage feeds the next upper stage, while its retentate stream is recycled back to the immediately preceding stage (Villani and Becker, 1979).

A)

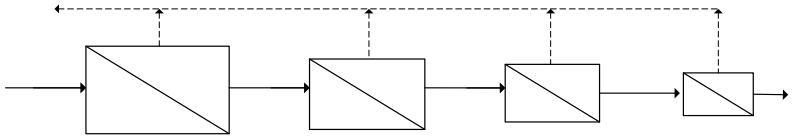

B)

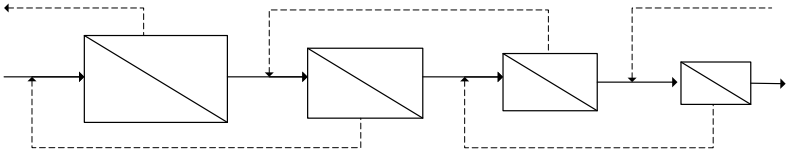

Figure 1.9 – Modes of cascade operation: A) simple symmetric cascade; B) symmetric countercurrent recycle cascade (Adapted from Siew et al., 2013).

The ideal cascade proposed by Hwang, assumes that the compositions of permeate and retentate streams that make up the feed to interior stages are kept constant, which means that there is no mixing of streams of different compositions between stages, and so there are no losses of separative work. To meet the no-mix criteria the flow rate between stages and the size of each stage must vary, which means that each stage has to be of different size. In addition, the feed is introduced within the cascade where the retentate composition is the same as the feed (Hwang and Kammermeyer, 1965).

In spite of the fact that ideal cascades minimize the energy consumptions and the global size of the plant, its assembling is complicated in terms of design, fabrication, operation and maintenance (McCandless, 1990; McCandless and Herbst, 1990). The solution to this problem in practical terms of cascade design is to approximate the ideal cascade by a small number of squared cascade segments connected in series, in what is called a squared-off cascade. With this configuration, all of the stages can be made identical and so a large reduction in the cost of separative units can be achieved (McCandless and Herbst, 1990).

It was suggested by Lightfoot (2008), and verified by Siew et al. (2012), that the biggest challenge in cascade implementation is the delicate control of interacting flows. Inadequate control results in reduced separation efficiency, and can even lead to worse performance than a single-stage system. In addition, with an increasing number of membrane units, extra buffer tanks and pumps are usually required, complicating the process and increasing the initial capital cost. Thus, the theoretical advantages of membrane cascade diminish rapidly with an increasing number of units (Vanneste et al., 2012) Therefore, for a membrane cascade system to be practical, the number of cascade units must be minimized, the control of the system should be simple, and the system design should be easy to reconfigure for multiple operations. Simplicity and flexibility in process design should not be understated, as the versatility of equipment is considered vital to reducing capital expenditure in the pharmaceutical industry (Roberge et al., 2005; Székely et al., 2011).

1.2.3.2 Membrane cascade applications

After the huge advance in membrane cascade theory during the 1940s (Mulder, 1996; Hwang and Kammermeyer, 1975; Halle and Shacter, 2000), a lot of authors started proposing different cascade schemes, derived from the countercurrent recycle cascade, for the separation of binary systems (McCandless and Herbst, 1990; Agrawal and Xu, 1996; Yan and Kao, 1989; McCandless, 1985; Keureties et al., 1992).

Cascade design has been widely used not only for gas separation but also for liquid separation (McCandless, 1985) and solid fractionation (Vanneste et al., 2011)

Most of the studies on membrane cascades for the purification of liquid solutions are related to wastewater treatment. Several authors like Evangelista (1987) and Maskan et al. (2000) developed design methodologies to optimize RO network configurations and operating conditions.

Peng and Tremblay (2008) designed and tested a pilot scale membrane cascade system using MF, UF and NF membranes to remove oil and grease from bilge water accumulated in ships. The authors concluded that it is possible to reduce the oil and grease content of water to the allowable discharge limit through the proper design of the membrane system, selection of appropriate membranes, determination of optimal operating parameters, and assessment membrane performance.

The increasing need for a continuous, high-throughput, economical and easily scalable separation process for downstream processing of biological substrates, like proteins, carbohydrates, plasmids, viruses, organelles, and even whole cells, led Lightfoot (2005) to propose membrane countercurrent cascades as an alternative for chromatography and simulated moving bed chromatography. He and his co-workers also proposed (2008) an extended version of the binary ideal cascade theory for modeling diafiltration membrane cascades for fractionation of binary systems of two solutes in a single solvent. Each stage of a diafiltration membrane cascade consists of a UF module combined with a RO module to remove excess solvent from the permeate stream.

Lin, Peeva and Livingston (2006) were the first to propose membrane cascades for solute separation in an organic solvent environment. In their study they compared the performance of a three-stage OSN membrane cascade with recycle with the performance of a single OSN membrane module operating in diafiltration mode for API purification. Two dyes, Martius Yellow and Brilliant Blue R, were used as API product and color impurity, respectively. Both systems allowed to control the impurity level in the final product. However, the single-stage configuration showed better performance in terms of product productivity than the three-stage cascade (5.25 $g \cdot h^{-1} \cdot m^{-2}$ and 3.45 $g \cdot h^{-1} \cdot m^{-2}$ at the 40th minute, respectively).

CHAPTER II

OBJECTIVES AND RESEARCH MOTIVATION

2.1 Amoxicillin purification via OSN

The present dissertation will focus on the separation of the API Amoxicillin (MW=365.40 Da) and the compound 4-hydroxy-L-phenylglycine (MW=167.16 Da), which is a sub-product of amoxicillin enzymatic synthesis, using an OSN membrane cascade,

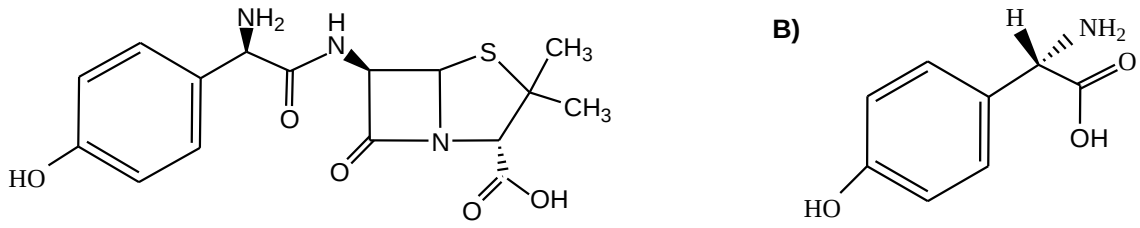

Figure 2.1 – Molecular representation of the studied compounds: A) Amoxicillin; B) 4-hydroxy-L-phenylglycine.

Amoxicillin was one of several semisynthetic derivatives of 6-aminopenicillanic acid (6-APA) developed at Beecham company in the 1960s. It became available in 1972, and was the second aminopenicillin to reach the market (after ampicillin in 1961) (Raviña, 2011; Bruggink, 2001).

This moderate-spectrum, bacteriolytic, beta-lactam antibiotic is used to treat bacterial infections caused by susceptible microorganisms, such as ear infections, bladder infections, pneumonia, gonorrhea, and *E. coli* or *salmonella* infection. Can also be administrated to animals .This antibiotic is available in form of capsules, chewable and dispersible tablets, syrup and pediatric suspension for oral use and can even be found as a sodium salt for intravenous administration.

In spite of the availability of many new generation antibiotics, amoxicillin is still a popular drug in our days being one of the top drugs prescribed worldwide. It is one of the most prescribed antibiotics for children (Dave Mihalovic, 2012; Daniel DeNoon, 2012; IMS Health, 2012; Magalhães et al., 2012; Hiral Khoda, 2011; Fiona Aberdeen, 2012; Infobanc, 2009; Lai, 2009; Chandon, et al., 2007).

In the year of 2012 were count around 53 million dispensed prescriptions of different brands of amoxicillin in the US [1] and 2.9 million in retail pharmacies in Canada (IMS Health, 2012) [2]; and in Brazil were sold more than 6 billion pharmaceutical units (pills) of amoxicillin, with sales of USD 780 million, in the past 5 years (2007-2011). The growth in the mentioned period was about 10-20% per year (Magalhães et al., 2012).

In Europe, amoxicillin is one of the most used antibiotics in hospitals (Hiral Khoda, 2011); for example in France it accounts for 52% of the total percentage of antibiotics used in hospitals (considering the different formulations) (Fiona Aberdeen, 2012).

In India, between the years 2008-09, amoxicillin was estimated to have a market of 118 million USD, being the main exportations to South Africa, Nigeria, Myanmar, Sri Lanka and Netherlands. The growth in the mentioned period was in average 5% per year (Infobanc, 2009).

Since the patent from Beecham industry for the production of the API (by the name of Clamoxyl®) expired in 1980 (Lai, 2009; Chandon, et al., 2007), amoxicillin is marketed under many trade names, including Amoxil® (GlaxoSmithKline, UK), DisperMox® (Ranbaxy Laboratories, Inc., India), Moxatag® (Shionogi inc., China), Novamoxin® (TEVA., Canada), Trimox® (Sandoz - generic pharmaceuticals division of Novartis, Switzerland) and many others.

The future and need for beta-lactam antibiotics remains important; major pharmaceutical companies continue to have research and development efforts for new and improved beta-lactam biotechnology and chemistry. It is accurate to say that this antibiotic is very relevant in the pharmaceutical industry and that it has a solid and stable market and gives good signs of a continuous grow over the years.

[1] Total market of 4 billion (dispensed prescriptions)
Includes all prescriptions dispensed through retail pharmacies - including independent and chain drug stores, food store pharmacies and mail order as well as long-term care facilities. Prescription counts are not adjusted for length of therapy. 90-day and 30-day prescriptions are both counted as one prescription.

[2] Estimated prescriptions dispensed in retail pharmacies (excludes hospitals includes new and refills)

2.1.1 Amoxicillin manufacturing and purification routes

Amoxicillin is mostly produced by chemical synthesis by adding an amino beta-lactam such as 6-aminopenicillanic acid (6-APA), usually having its carboxyl group protected, with an activated side-chain derivative followed by the removal of the protecting group by hydrolysis.

In spite of the high yields that this process has achieved, it has been criticized for several disadvantages. These reactions typically involve costly steps, such as low temperatures (less than -30ºC), and toxic organic solvents, such as methylene chloride and silylation reagents. In addition, high volumes of waste and byproducts have made this process undesirable (Alemzadeh, 2010; Falciani, 1979; Grossman et al., 1975; Zang et al., 2010).

Due to the above mentioned disadvantages, the enzymatic synthesis of amoxicillin has become more interesting due to the increasingly tight environmental regulations. Enzymatic synthesis of beta-lactam antibiotics can be achieved by condensation of nucleophile and acyl donor through kinetic or thermodynamic controlled synthesis (Falciani, 1979). One of the most used, is the kinetically controlled synthesis of amoxicillin from P-hydroxyphenylglycine methyl ester (HPGM) and 6-amino penicillanic acid (6-APA), catalyzed by the enzyme penicillin G acylase (PGA). The use of enzymes, such as PGA, could be of great interest due to its high selectivity, specificity, and activity in mild reaction conditions (aqueous medium, neutral pH, and moderate temperatures) (Mitesh Shah, 2010; Grossman et al., 1975).

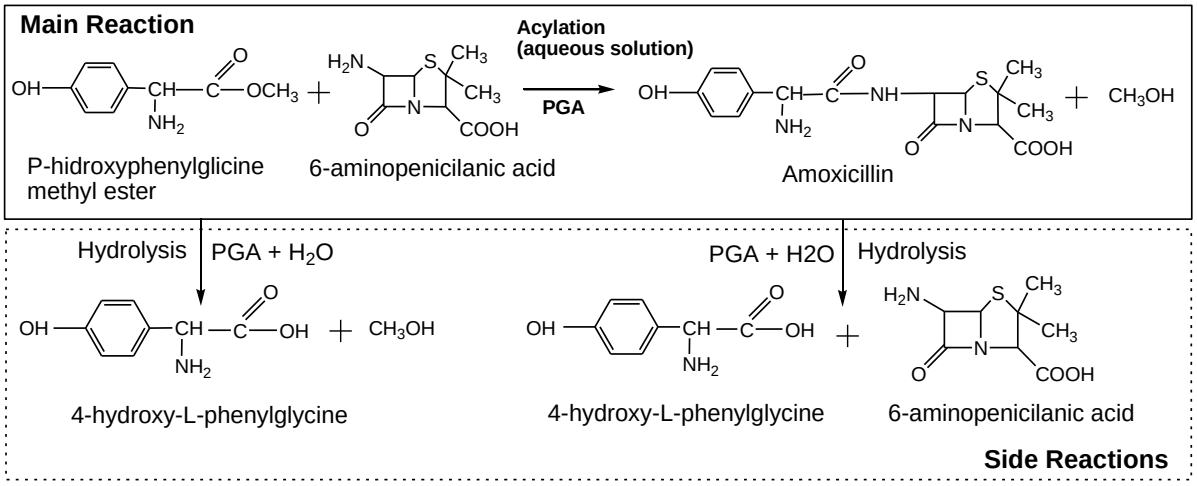

Figure 2.2 - Kinetically controlled synthesis of amoxicillin using penicillin G acylase as catalyst. (Adapted from Alemzadeh, 2010).

Figure 2.2 shows the kinetically controlled synthesis of amoxicillin from HPGM and 6-APA, which is conducted in an aqueous solution. Two side reactions, also catalyzed by PGA, compete with the synthesis of amoxicillin. Both side reactions lead to 4-hydroxy-l-phenylglycine, being the impurity present in our reaction mixture. Combining reactants and enzyme concentrations with pH and temperature conditions, it is possible to prioritize the main reaction, which is the production of amoxicillin. The optimized conditions for this reaction are: T= 35ºC, pH= 6.3, 20 mM 6-APA and 60 mM HPGM (Mitesh Shah, 2010). It is possible to develop this enzymatic synthesis in other ways (Mitesh Shah, 2010; Shaohua Feng, 2006; Alemzadeh, 2010), but these will not be discussed in this study.

In the final formulation, normally is incorporated a beta-lactamase inhibitor, such as clavulanic acid, to avoid the antibiotic deactivation when in contact with gram-negative bacteria (Lai, 2009).

Since pharmaceutical legislation is very tight in relation to the impurity levels of the active compound, procedures of separation and/or purification have to be conducted carefully.

Our objective is purifying a solution of amoxicillin containing 30ppm of 4-hydroxy-l-phenylglycine using an OSN membrane cascade to achieve a concentration of our main impurity to a value equal or less than 3ppm.

The separation and purification of this API consists in a series of steps, being crystallization one of most important steps in API purifications; in fact it is responsible for chemical purity and physical properties such as crystal morphology, size distribution, and crystal structure (Myerson, 2002; Mullin, 2001; Cai Shan-Ying, 2003).

This API is crystallized from aqueous solutions by the pH controlled crystallization method, and a recent patent claims that the bulk density, particle size distribution, and dissolution rate of crystalline amoxicillin powder can be improved by optimizing the crystallization conditions (Shaohua Feng, 2006)

It is easy to hydrolyze and degrade amoxicillin in acid and alkali solutions, and many degradation products are formed, including penicilloic acids and the dimer and trimer of amoxicillin (Chandon, et al., 2007). The existence of these degradation products not only reduces the yield of the synthesis but also affects downstream purification and separation processes. It was reported that impurities have a clearly negative influence on the nucleation and growth-rate kinetics of the crystallization of ampicillin (Shaohua Feng, 2006), which has a structure similar to that of amoxicillin. Besides these decomposition products, impurities derived directly from the amoxicillin synthesis, such as 4-hydroxy-L-phenylglycine that has similar structure and active groups, have to be considered and minimized to avoid this effect in the final purity

In view of the massive production of amoxicillin around the world and the marked influence of impurities on crystallization, cost-effective crystallization techniques to separate amoxicillin from degradation products are potentially of significant importance (Shaohua Feng, 2006; Kessels, 1993).

Another possibility could be a complementary step in the separation and/or purification process. Such step could an OSN system before crystallization, with the purpose of decreasing the concentration of impurities. In this study is the concentration of 4-hydroxy-L-phenylglycine that has to decrease in order to improving the feed stream for the crystallization process. As mention before, this membrane process works at ambient temperatures, is energy efficient and in theory is easy to scale-up and operate with. Is mostly probable to be necessary the use of a membrane cascade system, derivative of the common problems of using an OSN process in API purifications already described. This can imply more equipment and controllability concerns, but may also enable an organic solvent recovery step, turning the all process more cost-efficient and environmental friendly.

Therefore, this dissertation will study the viability of this incorporation, focusing only in the elimination of a specific impurity, 4-hydroxy-L-phenylglycine, considering an initial solution purity of 97.09% (initial solution concentrations used: $1 g.L^{-1}$ for amoxicillin and 30 ppm for the impurity) and a final purity of at least 99.70% (represents an impurity concentration of 3ppm or less).

The initial solution concentrations established and the choice of the specific impurity to integrate in the solution are representative of an actual production challenge referenced by one of the study collaborators Massachusetts Institute of Technology (MIT).

CHAPTER III

MATERIALS AND METHODS

3.1 Experimental

3.1.1 Model Mixture

All experimental nanofiltrations trials were performed using an aqueous solution containing the API Amoxicillin (MW=365.40 Da) in a concentration of 1g.L^{-1} and the impurity 4-hydroxy-L-phenylglycine (sub-product of Amoxicillin enzymatic synthesis) (MW= 167.16 Da) in a concentration of 0.03g.L^{-1} (30 ppm).

Two different volumes of the initial solution were used depending on the system: 50 mL when filtrating in a dead-end cell; and 200 mL when filtrating in an upside down membrane cell (membrane CSTR, m-CSTR).

3.1.1.1 Chemicals

Amoxicillin non try-hydrate powder (with 90.0% purity) and the 4-hydroxy-L-phenylglycine powder (with 99.0% purity) were purchased from Sigma-Aldrich. The Amoxicillin powder was stored at 4ºC and the 4-hydroxy-L-phenylglycine powder was stored at room temperature. All chemicals were used as received without further purification.

Table 3.1 - Amoxicillin and 4-hydroxy-l-phenylglycine relevant properties. (Data obtain from Sigma-Aldrich safety data sheets; Foulstone, 1982; O'Neil, 2001; VSDB and the chemical book via online)

PROPERTIES	AMOXICILLIN	IMPURITY
CAS Number	26787-78-0	32462-30-9
Molecular formula	$C_{16}H_{19}N_3O_5S$	$C_8H_9NO_3$
Molecular weight	365.40 g.mol^{-1}	167.16 g.mol^{-1}
Appearance	Powder /white crystalline solid	White solid
pH	4.4–4.9 (0.25% w/v solution)	No literature data available
Density (g.cm^{-3})	No literature data available Experimental data: 6.126 [1]	Literature data: 1.396 Experimental data: 0.928 [1]
Melting point (ºC)	194	240
Water solubility at 20ºC (for tri-hydrate amoxicillin)	3430 mg.L^{-1} Polar, Hydrophilic	No literature data available
Solubility in organic solvents at 20ºC (for tri-hydrate amoxicillin)	Methanol: 7500 mg.L^{-1} Ethanol: 3400 mg.L^{-1} Soluble in: ether, dilute acids, alkalihydroxides solutions	No literature data available
Other solubility	Lipid insoluble Low lipophilicity.	Water (likely at low pH) Alcohol's (methanol, ethanol)
Stability/Reactivity	Stable in gastric acid	No literature data available
Hazards identification	Health issues - Reproduction / development effects	Harmful by ingestion; irritant
Material to avoid/ incompatible	Oxidizing agents	Strong oxidizing agents
Storage Information	Recommended storage temperature: 2 - 8 °C. Keep container tightly closed in a dry and well-ventilated place	Keep container tightly closed in a dry and well-ventilated place.

[1] Procedure followed: a quantity of powder was placed into a graduated cylinder (2 cm^3) and weighed with 0.01% accuracy. The powder was gently compacted and flattened. The volume occupied by the powder in the cylinder was recorded. Dividing the mass of powder by the volume that occupies was possible to calculate de proximal density of the compound.

3.1.2 Amoxicillin characterization (solvent choice)

3.1.2.1 Solubility study

Solutions with 10 $g.L^{-1}$ of amoxicillin were prepared in water, acetone, ethanol and methanol, separately. These solutions were maintained for 24 h with constant stirring and temperature set to 20 ºC in a carrousel. Samples of 1 mL were taken, centrifuged, air dried at 20ºC, diluted in 1 mL of water and then analyzed by high pressure liquid chromatography (HPLC) (calibration curve presented in the appendix I).

3.1.2.2 Stability study

Solutions with 1$g.L^{-1}$ of amoxicillin were prepared in water, acetone, ethanol and methanol, separately. These solutions were left to stir with the temperature set at 20ºC and were taken samples two times each day for two weeks. The first sample was taken after 15 min. of stirring to ensure the proper dilution of the powder in the solution. From the water and methanol mixtures, the samples were air dried at 20ºC and then diluted in 1 mL of water. The samples of the ethanol solution was first centrifuged, due to the presence of substantial quantity of non-dissolved powder in the bottom of the flask and then air dried and diluted in water. The procedure for the acetone solution was the same as for the ethanol solutions with an additional step of filtration, due to the appearance of powder floating in the solution after less than 24h. All the samples were then analyzed by HPLC (calibration curve presented in the appendix I). This experience was conducted twice using the same conditions.

3.1.2.3 Isoelectric point determination

A simple titration of both compounds (amoxicillin and 4-hydroxy-l-phenylglycine) was preceded at 20ºC. The 10 mL aqueous solutions of amoxicillin, with a concentration of 1.32 $mmol.L^{-1}$, and 4-hydroxy-l-phenylglycine, with a concentration of 1.43 $mmol.L^{-1}$, were first neutralized with a 10 $mmol.L^{-1}$ acid chloride solution (acid purchased from VWR at 37%) and then titrated using a 49.65 $mmol.L^{-1}$ sodium hydroxide solution (base purchased from VWR). These titrations were repeated twice being the results presented from the second trial.

3.1.2.3.1 Dissociation study

Ferreira F. C. A. in 2004 deducted an equation that permits to calculate the concentration of the neutral and ionic species for a given pH and therefore allows the study of the dissociation profiles of the different species in a solution. This author started by defining the general equilibrium of the chemical reaction of a stripping solution as, $A + B \rightleftarrows AB$, being A the neutral organic, B the free ionic reagent (i.e hydroxide for organic acids and hydrogenium for organic bases) and AB the ionic organic product. He defines B concentration in the stirring solution, for an extraction of organic acid or basis, as

$$C_{B,S} = 10^{-pH}$$

Equation III.1

in which K_w is the auto-ionization constant and pK_w the correspondent pH. He also defines the total concentration of the organic in the stripping solution as the sum of the neutal organic concentration and the ionic organic product concentration:

$$C^T_{B,S} = C_{A,S} + C_{AB,S}.$$

Equation III.2

The equilibrium constant (K) can be directly related to the acid or base dissociation constant (K_a and K_b respectively),

$$K = \frac{C_{AB}}{C_A \,.\, C_B} = \frac{1}{K_b} = \frac{K_a}{K_w}$$

Equation III.3

Derived from *Equations III.1, III.2* and *III.3*, the concentration of the neutral organic and the dissociated specie are given by,

$$C_{A,S} = \frac{C^T_{B,S}}{1 + C_{B,S}.K} = \frac{C^T_{B,S}}{1 + \frac{K_a}{10^{-pH}}}$$

Equation III.4

$$C_{AB,S} = 1 - C_{A,S}$$

Equation III.5

With these equations it is possible to study the dissociation profiles of each compound and compared them to see if the pH factor can favor the separation process. The base dissociation constant (K_a) is obtain from the pKa's determinated above for each specie ($K_a = 10^{-pKa}$).

3.1.3. Membranes

Polybenzimidazole (PBI) membranes were prepared for this work using the phase inversion technique. Were also used poly(ether ether ketone) (PEEK) and polyimide (PI) membranes prepared by colleagues in the laboratory as well as some purchased commercial membranes (DuraMem® 200, Thin Film Nanofiltration membrane and M130).

Table 3.2 – Summary of the membrane tested in this work.

Membrane Code	Description	MWCO (Da)
PBI26	Polybenzimidazole, 26wt%, Uncrosslinked	600 [a]
PBI22	Polybenzimidazole, 22wt%, Cross-linked with DBX for 24 hrs	350 [a]
PBI20	Polybenzimidazole, 20wt%, Cross-linked with DBX for 24 hrs	430 [a]
PBI17	Polybenzimidazole, 17wt%, Cross-linked with DBX for 24 hrs	550 [a]
PI(1:4)	Polyimide, 24 wt%, 1:4 (DMF:Dioxane), Uncrosslinked	395 [b]
PI(1:3)	Polyimide, 24 wt%, 1:3 (DMF:Dioxane), Uncrosslinked	395 [b]
PI(1:2)	Polyimide, 24 wt%, 1:2 (DMF:Dioxane), Uncrosslinked	395 [b]
PEEK	Poly(ether ether ketone), 12%, 1:3 (Sulphuric Acid: Methane Sulphonic Acid)	300 [c]
TFNF-DL	Thin Film Nanofiltration membrane DL (GE Osmonics - Sterlitech)	150-300 [d]
M130	Commercial membrane (Evonik)	130 [e]
DM200	DuraMem® 200 (Evonik) – P84® polyimide membrane	200 [e]

a MWCO measured with a polystyrene/acetonitrile solution at 30 bar.
b MWCO measured with a polystyrene /acetone solution at 15 bar.
c MWCO measured with a polystyrene /DMF solution at 30 bar.
d Obtained from Sterlitech Corporation website.
e. Obtained from Evonik Industries website.

3.1.3.1 Polybenzimidazole membranes

Chemicals

Celazole® 26 wt%, a commercially available 26% dope solution of PBI in NN dimethylacetamide (DMAc), was purchased from PBI Performance products inc. DMAc and acetonitrile (MeCN) were purchased from VWR. Dibromobutane (DBB), and dibroxylene (DBX), used for the crosslinking reaction, and isopropanol (IPA) were purchased from Sigma Aldrich. Polyethylene glycol (PEG 400) was purchased from Merck.

Membrane preparation

When required, Celazole® 26 wt% was diluted with DMAc to a different polymer concentration and stirred continuously (IKA RW 20 digital) at room temperature overnight in order to obtain homogeneous dope solutions. The viscosity of the dope solution was measured in a rotary viscometer (MV-2020 Rotary Viscometer Cannon instruments, S16 spindle). Membranes were cast using the prepared dope solutions on a bench top laboratory casting machine with adjustable knife set at 250 µm. The polymer film was applied (Elcometer 4340 Automatic Film Applicator) on non-woven polypropylene (PP), material used for mechanical support. Following this, the membranes were immersed in deionised (DI) precipitation bath at room temperature for approximately 24 h. The obtained membranes were washed with IPA (at least three times) to remove residual solvent and water. To crosslink the polymer the membranes were immersed in a 3 wt% DBX in MeCN solution and the reaction was carried out at 80 °C for 24 h. After the crosslinking reaction the membranes were first washed with IPA (at least three times) to remove residual crosslinking agent and later on immersed in a PEG400/IPA (v/v) bath for 4 h to preserve the pore structure. Finally, the membrane was air dried at 20ºC to remove excess solvent.

3.1.3.2 Membrane performance

Flux, J, and rejection, R_i, were used to evaluate the membrane performance. The flux was obtained by measuring the volume permeated, V_p, per unit area, A, per time unit, t, using the following equation,

$$J = \frac{V_P}{A.t}$$

Equation III.6

The rejection of species, i, was calculated from its concentrations in the permeate, $C_{P,i}$, and retentate, $C_{R,i}$, using the following equation,

$$R_i = \left(1 - \frac{C_{P,i}}{C_{R,i}}\right) \times 100$$

Equation III.7

3.1.4 Experimental set-ups

3.1.4.1 Dead-end measurements

Membrane cell

Membrane screening tests were performed using a system like the one illustrated in *Figure 3.1*. The dead-end cell, made of stainless steel, have a liquid capacity of 100 mL, and hold circular flat sheet membranes with an effective area of 19 cm^2. These cells contain a magnetic stirrer in the feed/retentate chamber.

Membrane system

In all experiments the membrane active layer was placed against the feed solutions and forced through the membrane by an applied pressure (10, 20 and 30 bar) using nitrogen. The test ends when 50% of the feed volume has been collected.

Prior to any diafiltrations the system was washed with water to wash away membrane preservatives and any remaining impurities from the previous filtrations. Samples from feed, retentate and permeate were taken in the beginning and in the end of each experiment. Samples were analyzed by high pressure liquid chromatography (HPLC) (calibration curve presented in the appendix I).

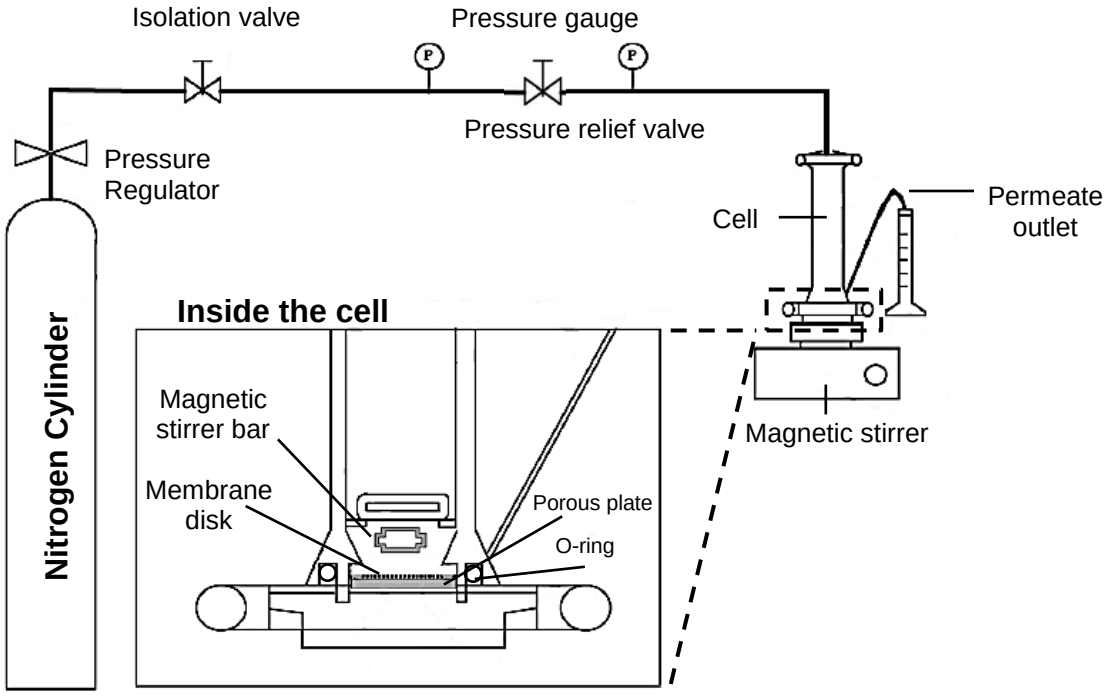

Figure 3.1 - Schematic of experimental pressure cell used for membrane screening. (Adapted from Scarpello and Livingston, 2002).

3.1.4.2 m-CSTR upside down measurements

Membrane cell

The continuous system used in this work was set up using a membrane cell like the one schematized in *Figure 3.2*. The custom made cell (m-CSTR), made of stainless steel, have a liquid capacity of 92 mL, and hold circular flat sheet membranes with an effective area of 51 cm^2. These cells operate in a bottom-to-top permeation mode, and contain a magnetic stirrer in the feed/retentate chamber (see *Figure 3.2-A*). Six ports surround the bottom section of the cells (see *Figure 3.2-B*). These were used as inlet (feed) and outlet (retentate and permeate) ports and to connect a pressure gauge for pressure monitoring and a temperature controller EKT Hein-Con (Heidolph). The retentate port was also connected to a pressure relief valve that allowed to control the pressure within the system. A safety pressure relief valve was also connected to one of the ports. All the ports not in use were maintained tapped.

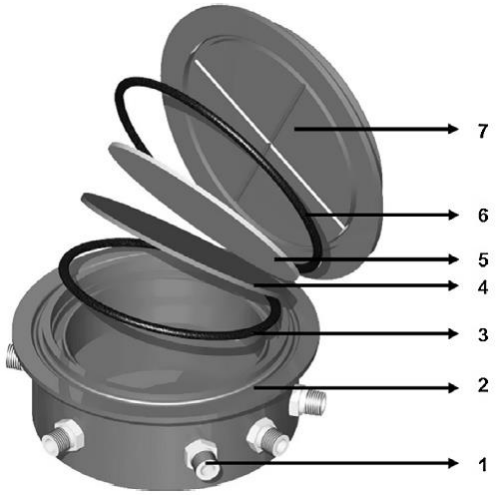

Figure 3.2 – Layout of the membrane separator cell (m-CSTR). Legend: 1 – Inlet/outlet ports; 2 – Feed/retentate chamber; 3 – Inner o-ring; 4 – Membrane; 5 –Sintered plate; 6 – Outer o-ring; 7 – Cover. (Adapted from Peeva and Livingston, 2013).

Single membrane system

Single membrane purifications were performed using a system like the one illustrated in *Figure 3.3*. This system consists of a feed tank and a single membrane cell. It operates in continuous or constant volume diafiltration mode: fresh solvent is added to the feed tank at the same rate as permeate comes out the membrane cell, so the system volume is always constant. Both feed tank and membrane cell are stirred using magnetic stirrers (500 rpm) to maintain homogeneity along the system and avoid osmotic pressure build up and concentration polarization effects in the membrane unit. Circulation is provided by a Gilson 307 HPLC pump able to provide feed flow rates up to 50 $mL.min^{-1}$. To have control over the trans-membrane pressure within a certain range, the pump flow rate must be higher than the permeate flow rate at the maximum pressure of the chosen range.

The feed tank volume was 200 mL, and the volume of the cell plus the associated tubing was approximately 100 mL. All membranes were first washed with at least 1 L of pure solvent at the set pressure (20 or 30 bar) to remove all the conditioning agents and to achieve a steady-state flux. After draining the solvent from the cell, the filtration, using the model solution ($1g.L^{-1}$ of the API and 30 ppm of the impurity in water), was performed for five hours. Permeate and retentate were recirculated back into the feed tank, not requiring the addition of pure solvent to the system. During experiments, samples were taken from feed, retentate and permeate at each hour. Samples were analyzed by HPLC (calibration curve presented in the appendix I). Before each new diafiltration the system was always washed with pure solvent to wash away membrane preservatives and any remaining impurities from the previous filtrations.

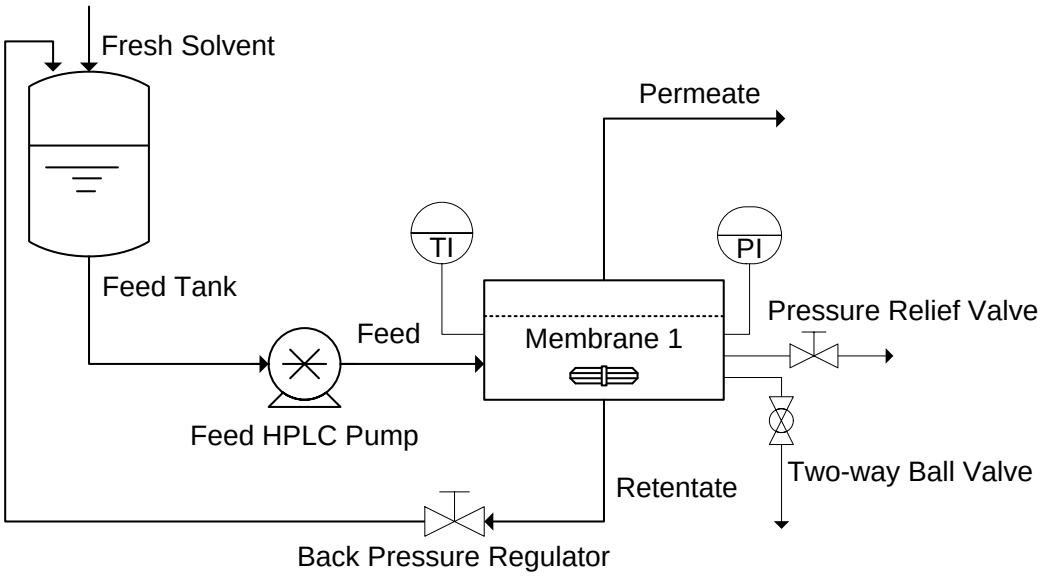

Figure 3.3 - Process diagram of the single membrane system (PI: Pressure gauge; TI: Temperature indicator).

3.1.4.2.1 Precipitated powder analysis

The powder was collected from the edge of the membrane and the inner o-rings, where concentrated, in the end of the complete diafiltration trial to a sample vessel. Formerly was dried in a vacuum system for 3 h at 22ºC and weighted. An aqueous solution of 1g.L^{-1} was prepared and a 1 mL sample was taken and analyzed by HPLC (calibration curve presented in the appendix I).

3.1.4.2.2 Mass transfer coefficient of amoxicillin

Approximating our process to a flat plate membrane in a stirred vessel using water as the solvent was possible to define that,

$$NSh = \frac{k'.\ d_{vessel}}{D} = 0.0443\ .NRe^{0.785}.NSc^{0.33}$$

Equation III.8

in which Nsh is the Sherwoods number, k' the mass transfer coefficient (m.s^{-1}), d_{vessel} is the vessel diameter (0.00844 m) and D the diffusion coefficient (m^2.s^{-1}) (Perry´s, 1999). NRe and NSc are the Reynolds and Schmidts number, respectively, that are defined as,

$$NRe = \frac{w.\ d_{stirrer}^2.\ \rho}{\mu}$$

Equation III.9

$$NSc = \frac{\mu}{\rho.\ D}$$

Equation III.10

in which w is the radial speed of the stir (rad.s^{-1}) having that the stirring speed used was 500rpm , $d_{stirrer}$ the stirrer diameter (0.002 m), ρ and μ are the density (1000 kg.m^{-3}) and viscosity (0.001 Pa.s) of the API, respectively, and were considered to be the same as the water due to the low solute concentration in solution.

The diffusion coefficient of the amoxicillin in water could be calculated using the Wilke and Chang correlation (Perry´s, 1999),

$$D_{API\,/\,H_2O} = 7.4E^{-8}.\ \frac{T.\,(\phi_{H_2O}.MW_{H_2O})^{\frac{1}{2}}}{\mu_{H_2O}.\,V_{API}^{0.6}}$$

Equation III.11

in which T is the work temperature (295.15 K), ϕ_{H_2O} the association parameter that defines the effective molecular weight of the water with respect to the diffusion process (2.6 for water), MW_{H_2O} is the water molecular weight (0.01802 kg.mol^{-1}), μ_{H_2O} the water viscosity (1 cP) and V_{API} is the amoxicillin molal volume (cm^3.mol^{-1}) that was considered to be equal to 500 cm^3.mol^{-1} based on the estimation by the atomic contributions of LeBas (La-Scalea, 2005).

3.1.4.2.3 Concentration polarization analysis

Peeva et al. (2004) studied the effect of concentration polarization on flux in OSN. In the presented work a model based on the copulation of the solution diffusion model for membrane transport and the concentration polarization model for liquid film mass transfer, was proposed for a binary system to describe the membrane transport in a mass transfer limited system (Peeva and Livingston, 2004). The total volumetric flux (m^3.m^{-2}.s^{-1}) for the binary system is defined as,

$$J = J_{solute}.\upsilon_{solute} + J_{solvent}.\upsilon_{solvent}$$

Equation III.12

in which υ is the molar volume of the compound (m^3.mol^{-1}) and the fluxes of the solute and solvent are defined as,

$$\frac{J_{solute}}{k'_{solute}} = \ln\left(\frac{C_{solute,FM} - C_{solute,P}}{C_{solute,b} - C_{solute,P}}\right)$$

Equation III.13

$$\frac{J_{solvent}}{k'_{solvent}} = \ln\left(\frac{C_{solvent,P} - C_{solvent,FM}}{C_{solvent,P} - C_{solvent,b}}\right)$$

Equation III.14

$$J_{solute} = B_{solute}.\left(C_{solute,FM} - \frac{J_{solute}}{J_{solute} + J_{solvent}}.\exp\left(-\frac{\upsilon_{solute}.P}{RT}\right)\right)$$

Equation III.15

$$J_{solvent} = B_{solvent}.\left(C_{solvent,FM} - \frac{J_{solvent}}{J_{solute} + J_{solvent}}.\exp\left(-\frac{\upsilon_{solvent}.P}{RT}\right)\right)$$

Equation III.16

$$R_{solute} = 1 - \frac{J_{solute}}{J.\,C_{solute,b}}$$

Equation III.17

in which $C_{solute,FM}$ and $C_{solvent,FM}$ are the concentrations in the feed side liquid phase at the membrane liquid interface (mol.m^{-3}), $C_{solute,b}$ and $C_{solvent,b}$ are the concentrations in the feed side liquid phase in the bulk (mol.m^{-3}), $C_{solute,P}$ and $C_{solvent,P}$ are the concentrations in the permeate side (mol.m^{-3}),k'_{solute} and $k'_{solvent}$ are the mass transfer coefficient (m.s^{-1}), $B_{solvent}$ and $B_{solvent}$ are the permeabilities in the membrane phase (mol.m^{-2} s^{-1}), P is the system pressure (Pa), R the ideal gas constant (8.3145 m^3.Pa.K^{-1}.mol^{-1}), T the system temperature (K) and R_{solute} the solute rejection. *Equations III.13* and *III.14* describe the diffusion in the liquid film adjacent to the membrane, while *Equations III.15* to *III.16* describe membrane transport and *Equation III.17* defines the rejection.

3.1.5 Analytical Methods

High Pressure Liquid Chromatography (HPLC)

All samples were analyzed by Agilent 1100 Series HPLC system coupled to an UV detector at 280 nm and with an ACE C18 RP column (normal phase column). The pump flow-rate was set at 1 $mL.min^{-1}$, the injection volume was 30 µL, the column temperature was 30ºC, and an ACE C18 RP column was fitted. A mobile phase comprising of 5% MeOH (solvent A) and 95% 0.1 M ammonium acetate aqueous solution (solvent B) was used for 10 minutes. Calibration curves were obtained for each compound from the model mixture using the UV signal.

3.2 Process modelling

In order to understand and predict the separation behavior, using the membrane screening data, a simulation was performed for a semi-batch and continuous system using different configurations.

A simple modulation was performed following the assumptions below:

- The system operates at constant volume.
- The permeability and rejections are constant with time.
- The solute concentration in the solution does not have a considerable influence on rejection.
- Membranes in each stage have the same characteristics of rejection and permeability.

Parameters such as yield and purity were defined as,

$$\text{API Purity } (\%) = \frac{\text{Concentration of API}}{\text{Concentration of API + Concentration of impurity}} \text{ x } 100$$

Equation III.18

$$\text{Yield of specie i } (\%) = \frac{\text{Final concentration of specie i}}{\text{Initial concentration of specie i}} \text{ x } 100$$

Equation III.19

3.2.1 Semi-Batch mode

One stage cascade system

The single-stage diafiltration system, as shown in *Figure 3.3*, can be modeled by writing a mass balance around the system. Assuming that the system operates at a constant volume and it is perfectly mixed,

$$V\frac{dC_{R,i}}{dt} = -F.\ C_{P,i} = J_V.\ A.\ C_{P,i_i}$$

Equation III.20

where V (L) is the entire system volume, F is the permeate flow-rate ($L.h^{-1}$), J_v ($L.m^{-2}.h^{-1}$) is the membrane flux, A (m^2) is the membrane area, and $C_{R,i}$ and $C_{P,i}$ ($g.L^{-1}$) are the concentrations of specie i in the retentate and permeate, respectively.

Substituting *Equation III.7* in *Equation III.20*,

$$\frac{dC_{R,i}}{dt} = \left(\frac{1}{V}\right).\ J_V.\ A.\ C_{R,i}\ .(1 - R_i)$$

Equation III.21

This equation can be solved either numerically or analytically. When integrated analytically with appropriate boundary conditions, the following equation is obtained:

$$\frac{C_{R,i}}{C_{R,i,0}} = \exp\left[- \frac{J_V.\ A.\ t}{V}\ .\ (1 - R_i)\right] = \exp\ [- vols.\ (1 - R_i)\ ]$$

Equation III.22

where *vols* represent the total volume of permeate collected relative to the initial system volume. This useful time-like dimensionless parameter allows different diafiltration systems to be compared.

Two stage cascade system

In this two-stage configuration an assumption is made that the retentate streams from each stage are recycled back to the feed tank and can be solved numerically with MATLAB® using ODE45 function.

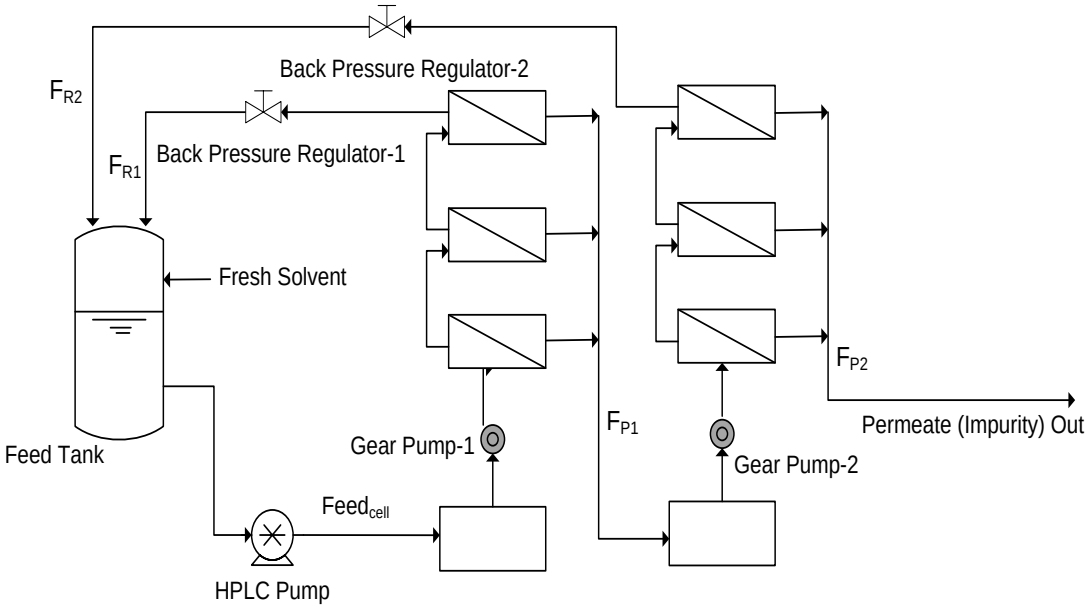

Figure 3.4 - Scheme of the two-stage cascade with the main equipment and streams highlighted. Legend: $Feed_{cell}$ – Feed flow-rate to the first stage; F_{R1} – Retentate flow-rate from stage 1; F_{P1} – Permeate flow-rate from stage 1; F_{P2} – Permeate flow-rate from stage 2; F_{R2} – Retentate flow-rate from stage 2.

The membrane cascade can be modeled by doing a mass balance to the first and second stages of the system:

$$\frac{dC_{R1,i}}{dt} = \left(\frac{1}{V_1}\right).\left[- F_{P1}.C_{R1,i} .(1 - R_{1,i}) + F_{R2}.\ C_{R2,i}\right]$$

Equation III.23

$$\frac{dC_{R2,i}}{dt} = \left(\frac{1}{V_2}\right).\left[F_{P1}.\ C_{R1,i}.(1 - R_{1,i}) - F_{P2}.\ C_{P2,i} - F_{R2}.\ C_{R2,i} \right]$$

Equation III.24

with $C_{P2,i} = C_{R2,i}.(1-R_{2,i})$ and where V_1 is the feed tank plus the first-stage volume, V_2 is the second-stage volume, and F_j (equal to J_v**.** A) represents the flow-rate, being j the correspondent stream as shown in *Figure 3.4*.

An important parameter, the recycle ratio (R_c), is defined as,

$$R_C = \frac{F_{R2}}{F_{P1}} = \frac{(B_1.\ \Delta P_1 - B_2.\ \Delta P_2)}{B_1.\ \Delta P_1}$$

Equation III.25

where ΔP1 and ΔP2 (bar) represent the trans-membrane pressure (TMP) through the first and second stages, respectively, and B_1 and B_2 represent the permeability ($L.m^{-2}.hr^{-1}.bar^{-1}$) of the first and second stage membranes, respectively.

The recycle ratio, R_C, is an independent variable under control because the flow rate through the first and second membranes i.e, the permeate can be controlled using the back-pressure valve at the retentate side of the second stage. Notably, the effect of R_C on the final yield and purity is significant and is discussed in the results section.

3.2.2 Continuous mode

3.2.2.1 Configuration I

Two stage cascade system

In this two-stage continuous configuration an assumption is made that the retentate streams from each stage are recycled back to the feed tank and can be solved numerically with MATLAB® using ODE45 function.

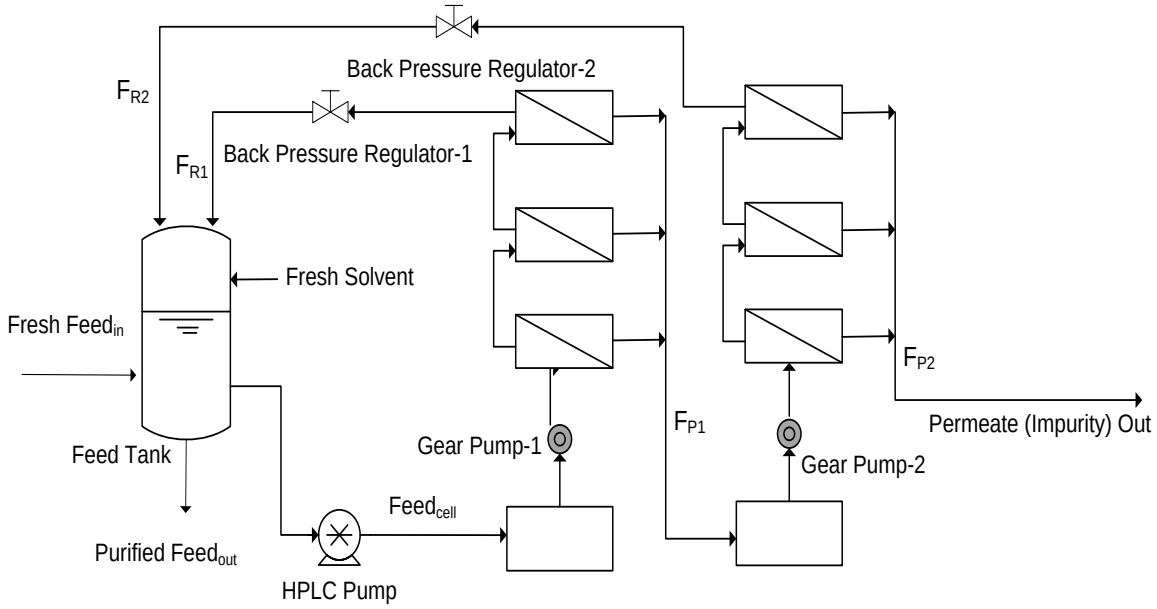

Figure 3.5 - Scheme of the continuous two-stage cascade with the main equipment and streams highlighted. Legend: $Feed_{in}$ – Feed flow-rate in (to be purified); $Feed_{out}$ – Feed flow-rate out (purified); $Feed_{cell}$ – Feed flow-rate to the first stage; F_{R1} – Retentate flow-rate from stage 1; F_{P1} – Permeate flow-rate from stage 1; F_{P2} – Permeate flow-rate from stage 2; F_{R2} – Retentate flow-rate from stage 2.

The membrane cascade can be modeled by doing a mass balance to the first and second stages of the system:

$$\frac{dC_{R1,i}}{dt} = \left(\frac{1}{V_1}\right). [Feed_{in}. C_{i,0} - F_{P1}.C_{R1,i} .(1 - R_{1,i}) + F_{R2} . C_{R2,i} - Feed_{out}. C_{out,i}]$$

Equation III.26

$$\frac{dC_{R2,i}}{dt} = \left(\frac{1}{V_2}\right). [F_{P1}. C_{R1,i} (1 - R_{1,i}) - F_{P2}. C_{P2,i} - F_{R2}. C_{R2,i}]$$

Equation III.27

with $C_{P2,i} = C_{R2,i}.(1-R_{2,i})$ and where V_1 is the feed tank plus the first-stage volume, V_2 is the second-stage volume, and F_j (equal to J_v. A) represents the flow-rate, being j the correspondent stream as shown in *Figure 3.5*.

The results from the equations above can be verified using the mass balance to the feed tank and a global mass balance:

Mass balance to the feed tank:

$$Feed_{in}. C_{i,0} + F_{R1}. C_{R1,i} + F_{R2}. C_{R2,i} = Feed_{out}. C_{out} + F_{Feedcell}. C_{Feedcell,i}$$

Equation III.28

Global mass balance:

$$Feed_{in}.\ C_{i,0} = Feed_{out}.\ C_{out} + F_{P2}.\ C_{R2,i}.(1 - R_{2,i})$$

Equation III.29

The recycle ratio (R_c) is defined as mentioned before, *Equation III.25*, and another important parameter, the feed utilization (FU), is defined as,

$$FU = \frac{Feed_{in}}{Feed_{out}}$$

Equation III.30

Is a parameter that indicates how much of the feed in is going out as purified stream, i.e. it shows the volume reduction in the cascade system.

3.2.2.2 Configuration II

Two stage cascade system

This configuration is similar to the previous one but assumes that the retentate stream from the first stage and the permeate stream from the second stage are recycled back to the feed tank.

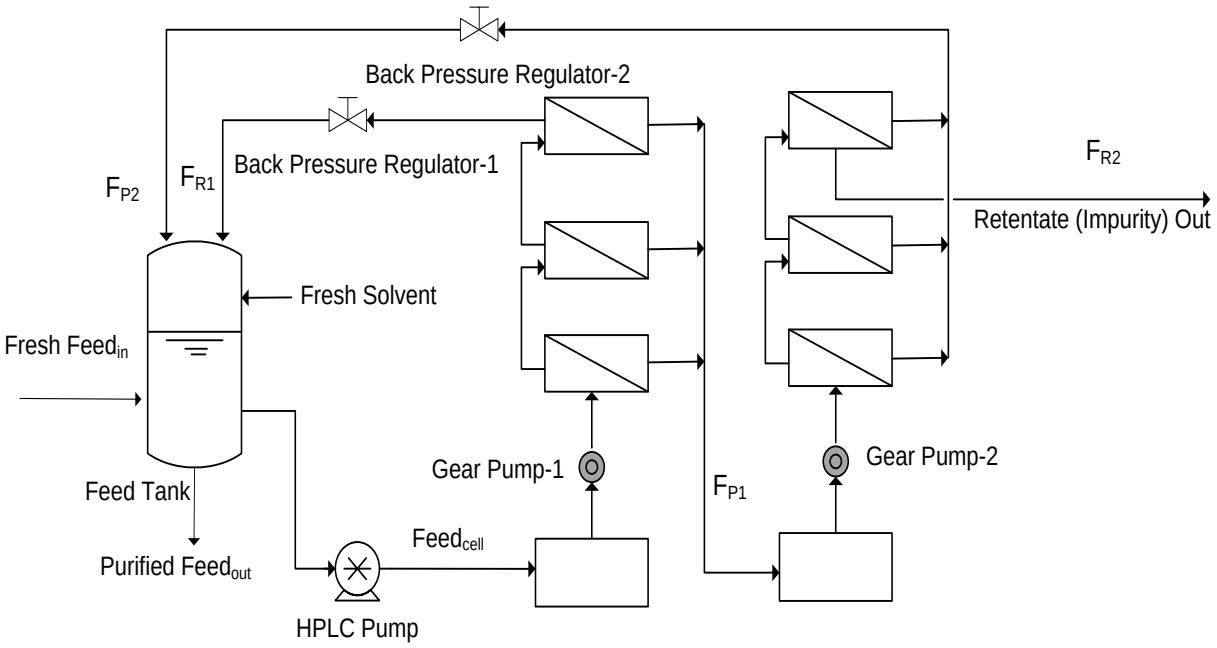

Figure 3.6 - Scheme of the continuous two-stage cascade with the main equipment and streams highlighted. Legend: $Feed_{in}$ – Feed flow-rate in (to be purified); $Feed_{out}$ – Feed flow-rate out (purified); $Feed_{cell}$ – Feed flow-rate to the first stage; F_{R1} – Retentate flow-rate from stage 1; F_{P1} – Permeate flow-rate from stage 1; F_{P2} – Permeate flow-rate from stage 2; F_{R2} – Retentate flow-rate from stage 2.

As mentioned before, the membrane cascade can be modeled by performing a mass balance on stage 1 and 2 and solved numerically with MATLAB® using ODE45 function.

$$\frac{dC_{R1,i}}{dt} = \left(\frac{1}{V_1}\right).\ [Feed_{in}.\ C_{i,0} - F_{P1}.C_{R1,i}\ .(1 - R_{1,i}) + F_{P2}.\ C_{R2,i}.(1 - R_{2,i}) - Feed_{out}.\ C_{out,i}]$$

Equation III.31

$$\frac{dC_{R2,i}}{dt} = \left(\frac{1}{V_2}\right).\ [\ F_{P1}.\ C_{R1,i}.\ (1 - R_{1,i}) - F_{P2}.\ C_{R2,i}.(1 - R_{2,i}) - F_{R2}.\ C_{R2,i}\ ]$$

Equation III.32

where V_1 is the feed tank plus the first-stage volume, V_2 is the second-stage volume, and F_j, represents the flow-rate, being j the correspondent stream as shown in *Figure 3.6*.

The results from the equations above referred can be verified using the mass balance to the feed tank and a global mass balance:

Mass balance to the feed tank:

$$Feed_{in}.\ C_{i,0} + F_{R1}.\ C_{R1,i} + F_{P2}.\ C_{R2,i}.(1 - R_{2,i}) = Feed_{out}.\ C_{out} + F_{Feedcell}.\ C_{Feedcell,i}$$

Equation III.33

Global mass balance:

$$Feed_{in}.\ C_{i,0} = Feed_{out}.\ C_{out} + F_{R2}.\ C_{R2,i}$$

Equation III.34

The feed utilization is defined as before, *Equation III.30,* and the recycle ratio (R_c), is defined as,

$$R_C = \frac{F_{P2}}{F_{P1}} = \frac{B_2.\ \Delta P_2}{B_1.\ \Delta P_1}$$

Equation III.35

Three stage cascade in steady state

A three stage cascade was also studied using the configuration in *Figure 3.7*.

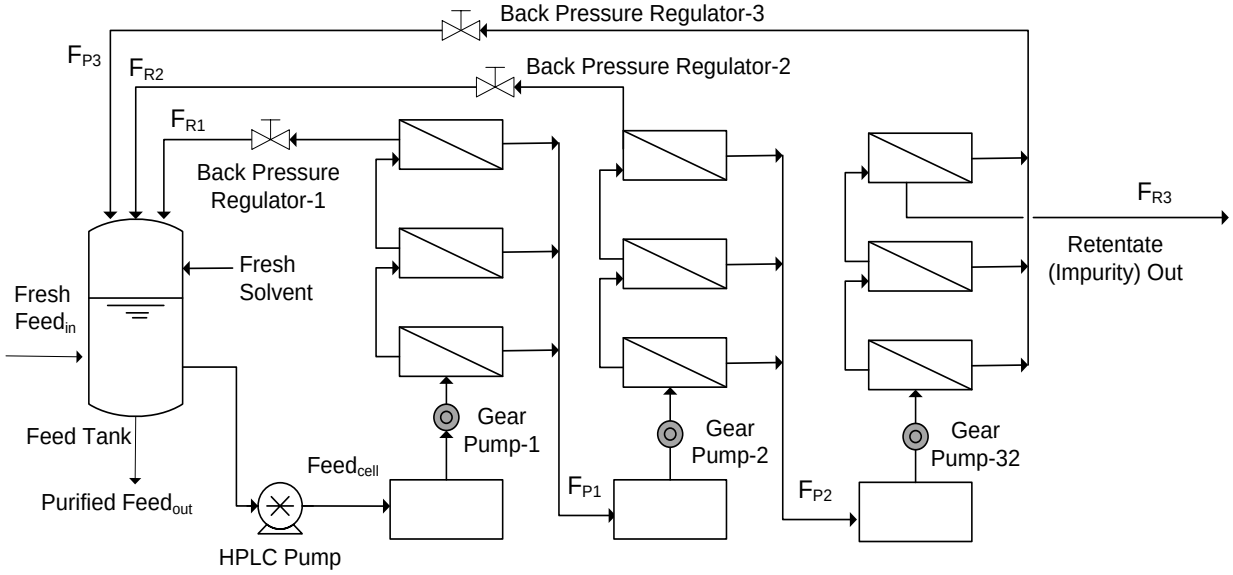

Figure 3.7 - Scheme of the continuous two-stage cascade with the main equipment and streams highlighted. Legend: $Feed_{in}$ – Feed flow-rate in (to be purified); $Feed_{out}$ – Feed flow-rate out (purified); $Feed_{cell}$ – Feed flow-rate to the first stage; F_{R1} – Retentate flow-rate from stage 1; F_{P1} – Permeate flow-rate from stage 1; F_{P2} – Permeate flow-rate from stage 2; F_{R2} – Retentate flow-rate from stage 2; F_{P3} – Permeate flow-rate from stage 3; F_{R3} – Retentate flow-rate from stage 3

Mass balances for each stage were developed to modulate this system.

$$\frac{dC_{R1,i}}{dt} = \left(\frac{1}{V_1}\right).\ [Feed_{in}.\ C_{i,0} - F_{P1}.C_{R1,i}.(1 - R_{1,i}) + F_{R2}.\ C_{R2,i} + F_{P3}.C_{P3,i} - Feed_{out}.\ C_{out,i}]$$

Equation III.36

$$\frac{dC_{R2,i}}{dt} = \left(\frac{1}{V_2}\right).[\ F_{P1}.\ C_{R1,i}.(1 - R_{1,i}) - F_{P2}.\ C_{R2,i}.(1 - R_{2,i}) - F_{R2}.\ C_{R2,i}\ ]$$

Equation III.37

$$\frac{dC_{R3,i}}{dt} = \left(\frac{1}{V_3}\right).[\ F_{P2}.\ C_{R2,i}(1\text{-}R_{2,i})\ -\ F_{P3}.C_{P3,i} - F_{R3}.\ C_{R3,i}]$$

Equation III.38

with $C_{P3,i} = C_{R3,i}.(1\text{-}R_{3,i})$ and where V_1 is the feed tank plus the first-stage volume, V_2 is the second-stage volume, V_3 is the third-stage volume, and F_j, represents the flow-rate, being j the correspondent stream as shown in *Figure 3.7*.

Considering steady state, the concentration profiles can be obtained analytically. Since $C_{P1,i} = C_{R1,i}.(1\text{-}R_{1,i}) = C_{Feed_{cell},i}.(1\text{-}R_{1,i})$ and the $Feed_{cell}$ stream concentration will reach the same value as $Feed_{out}$ concentration when reaching steady state, $C_{P1,i} = C_{out,i}.(1\text{-}R_{1,i})$ and $C_{R1,i} = C_{out,i}$.

$$C_{out,i} = \left(\frac{Feed_{in}.\ C_{i,0} + F_{P3}.C_{R3,i}\ (1 - R_{3,i}) + F_{R2}.\ C_{R2,i}}{Feed_{out} + F_{P1}(1\text{-}R_{1,i})}\right)$$

Equation III.39

$$C_{R2,i} = \left(\frac{(Feed_{in}.\ C_{i,0} + F_{P3}.C_{R3,i}(1 - R_{3,i}))\ .\ F_{P1}.\ (\ 1\text{-}R_{1,i}\ )}{Feed_{out}\ .\ F_{R2} + Feed_{out}\ .\ F_{P2}(1 - R_{2,i}) + F_{P1}(1 - R_{1,i}).F_{P2}(1 - R_{2,i})}\right)$$

Equation III.40

$$C_{R3,i} = \left(\frac{Feed_{in}.\ C_{i,0} + \prod_{j=1}^{2}.F_{Pj}(1\text{-}R_{j,i})}{Feed_{out}\ .\ (F_{R2}\ .\ F_{R3} + F_{P3}(1 - R_{3,i})\ .\ F_{R2} + F_{P2}(1 - R_{2,i})\ .\ F_{R3} + \prod_{j=2}^{3}.F_{Pj}(1 - R_{j,i})) + \prod_{j=1}^{2}.F_{Pj}(1 - R_{j,i})\ .\ F_{R3}}\right)$$

Equation III.41

The results from the equations above can be verified using the mass balance to the feed tank and a global mass balance:

Mass balance to the feed tank:
$Feed_{in}.\ C_{i,0} + F_{R1}.\ C_{R1,i} + F_{R2}.\ C_{R2,i} + F_{P3}.C_{P3,i} = Feed_{out}.\ C_{out} + F_{Feedcell}.\ C_{Feedcell,i}$

Equation III.42

Global mass balance:
$Feed_{in}.\ C_{i,0} = Feed_{out}.\ C_{out} + F_{R3}.\ C_{R3,i}$

Equation III.43

Feed utilization is once again defined as above, *Equation III.30,* and the recycle ratio (R_c), in this case, is defined separately for each stage:

Second stage:

$$R_C = \frac{F_{P2}}{F_{P1}} = \frac{B_2.\ \Delta P_2}{B_1.\ \Delta P_1}$$

Equation III.44

Third stage:

$$R_C = \frac{F_{P3}}{F_{P2}} = \frac{B_3.\ \Delta P_3}{B_2.\ \Delta P_2}$$

Equation III.45

CHAPTER IV

RESULTS AND DISCUSSION

4.1 Solvent choice

To proceed with the desirable purification of the API amoxicillin from the impurity, 4-hydroxy-L-phenylglycine, it was necessary to choose the solvent to be used in the nanofiltration process.

Taking into account the literature data, vide *Table 3.1,* and some experimental trials made previously in this group (vide *Table 4.1*) with numerous potential organic solvents commonly used in OSN, the range of ideal solvents to use in this process was reduced to four possible solvents: water, acetone, ethanol and methanol.

Table 4.1 – Results summary of the solvents tested in the laboratory previously.

Solvent	Soluble at 1 g.L^{-1}, at 20ºC	Stable for 48 h at 20ºC
Water	✓	✓
Methanol	✓	degradation
Acetone	✓	✕
DMF	✓	degradation
DCM	✕	n.a. [#]
MeCN	✕	n.a. [#]
EtOAc	✕	n.a. [#]
THF	✕	n.a. [#]
Toluene	✕	n.a. [#]

[#]n.a. = not available
✓= yes; ✕= no

The study of the solubility and stability of the compound of interest (amoxicillin) in these solvents was conducted in order to understand the behaviour of the compound and choose the more suitable solvent for the OSN process.

4.1.1 Amoxicillin solubility and stability study

Solutions of amoxicillin were prepared separately in water, acetone, ethanol and methanol and left stirring in a carousel for 24 h at approximately 20ºC. This experience was repeated once using the same conditions. The results from the HPLC analysis (calibration curve presented in the appendix I). of the samples taken are presented in *Table 4.2*.

Table 4.2. - Comparison of the results obtained for the amoxicillin solubility. Solutions prepared with 10g.L^{-1} of amoxicillin in the different solvents.

Solubility (g.L^{-1}) at 20ºC	Literature Data (*Table 3.1*)	Experimental Data (after 24 h) [*]
Water	3.43	2.82 ± 0.02
Acetone	not available	1.41 ± 0.02
Ethanol	3.40	0.39 ± 0.02
Methanol	7.50	3.69 ± 0.02

[*] Average of two experiences performed and error values represent one standard deviation from the mean.

From *Table 4.2* it is possible to verify that water was the solvent with closer results to the literature data; ethanol and methanol solubility values were much lower than the expected. One of the possible factors for the discrepancy of values is that the literature data obtained for the solubility are for the tri-hydrate amoxicillin compound and in this research work the non-hydrate amoxicillin was used. The API has a reasonable solubility in water, and therefore the presence of three molecules of water in the compound molecular structure can have a significant effect in the solubility of the molecule. Nevertheless, this factor alone could not explain the decreased to less than half of the solubility values for the ethanol and methanol. A possible reason will be described in the stability study.

Solutions of amoxicillin were prepared separately in water, acetone, ethanol and methanol to study the stability of the API over time in the different solvents. Samples of all solutions were taken for over two weeks and analyzed.

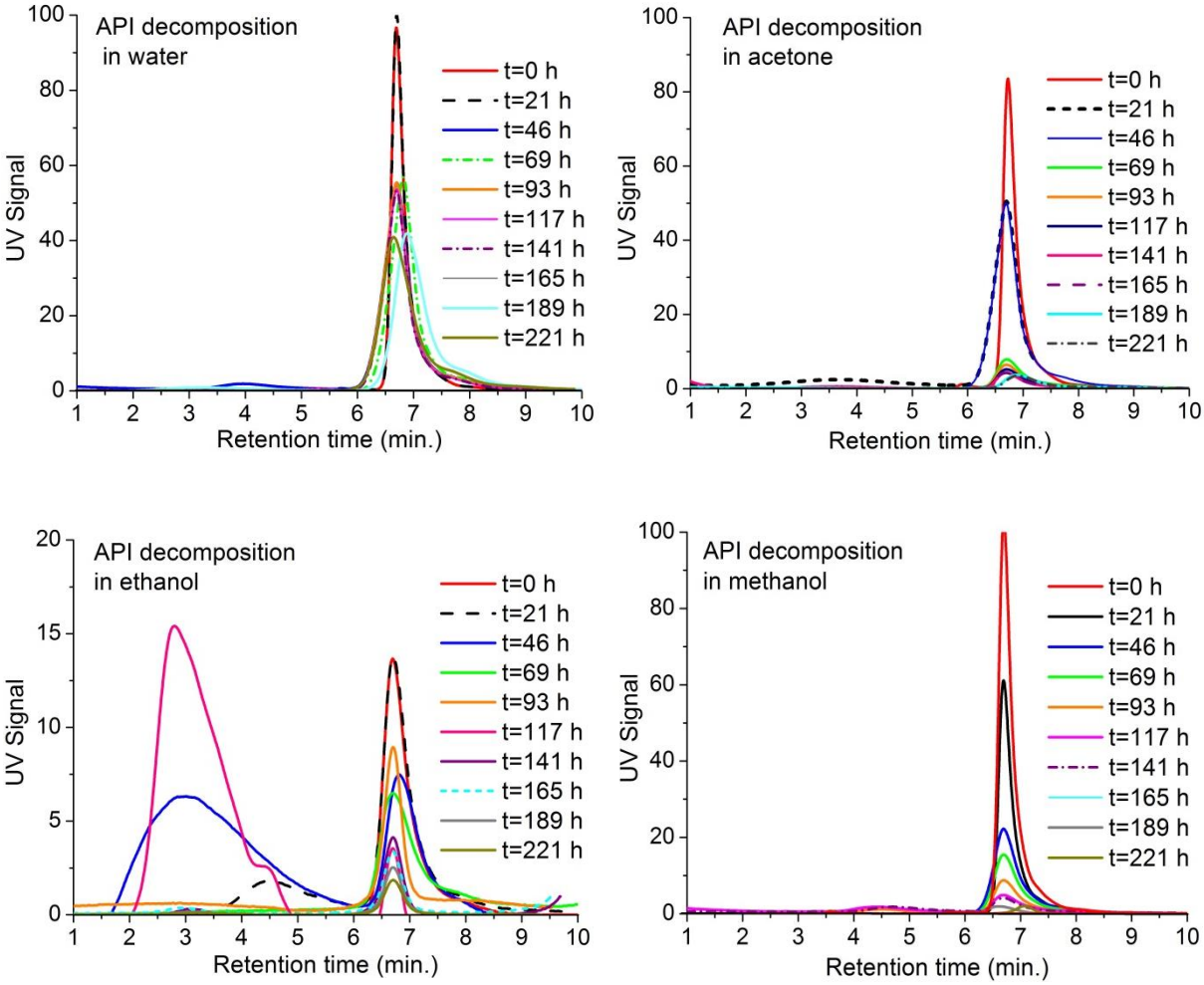

Figure 4.1 – UV signal, from the HPLC analysis, of the samples taken over time for each solution. Solutions prepared with 1g.L^{-1} of amoxicillin in the different solvents.

From *Figure 4.1* it is perceptible the loss of the API over time in all mixtures. After 21 h it can be seen for all mixtures, with the exception of the water mixture, a decrease in 40% or more from the initial amoxicillin concentration.

It was expected that ethanol would dissolve the API almost as well as water giving the fact that they have similar solubilities (vide *Table 4.2*). In all experimental trials, the amoxicillin powder dissolved after 15 min. of stirring at 22 ºC with the exception of the trials using the ethanol mixture. However, it was impossible to dissolve the 1 g.L^{-1} of amoxicillin in ethanol which means that the solubility is below 1 g.L^{-1}. Examining *Figure 4.1* it was noticeable from the beginning of the experiment that the API signal from the ethanol mixture was always significantly lower when compared to the other solvents. This brings an uncertainty about the ethanol solubility value from the literature data and corroborates the experimental data obtained in the solubility study described above. In addition, it was also noticeable another peak after 117 h that was no longer visible after 141 h but could be related to the formation of a decomposition product.

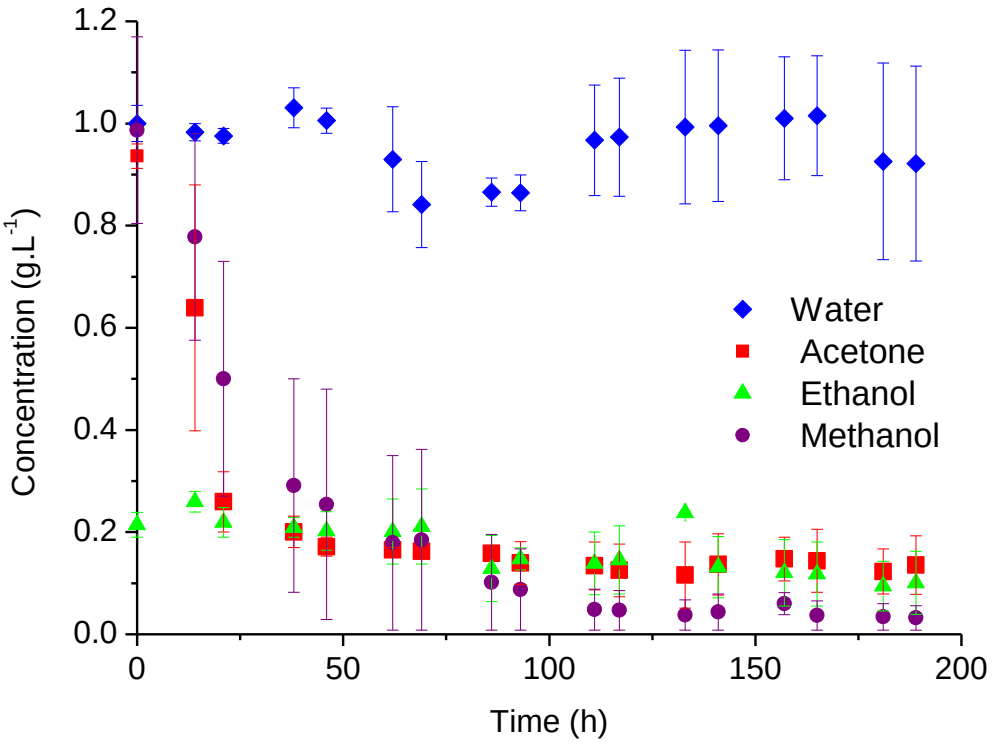

Figure 4.2 - Concentration of amoxicillin over time in the different solvents. Solutions prepared with 1 g.L^{-1} of amoxicillin. These results represent an average of two experiments and the error bars are the standard deviation of the mean.

Analyzing the concentration profiles over time for each solvent (*Figure 4.2),* it was possible to realize that the decomposition of amoxicillin over time had the slowest decrease when compared with the other solvents. After a period of 200 h water had a decrease in concentration of less than 10% while the other solvents had a decrease higher than 80%. It can also be noticed that the API had a low concentration in ethanol since time 0 h., probably due to its low solubility (as mentioned before).

The API concentration in acetone and methanol had a very quick decrease in concentration in the first 25 h. For acetone it was visible to the naked eye, in less than 24 h, the appearance of a white powder in the solution; this could be due to decomposition or precipitation. The solution was filtered to maximize the sample collection but the powder, even in much smaller quantities, continued to appear. Comparing the concentration profiles between methanol and acetone, methanol had an accentuated decrease of the API concentration over time, but not as pronounced as in the acetone mixture. This fast decrease in concentration can be the explanation for the low solubility values of methanol obtained experimentally. Since the solubility samples were taken after 24 h, at that point the amoxicillin concentration had already decreased approximately to half of the initial value.

Considering both studies and the information collected, the solvent chosen was water given the fact it had reasonable solubility and the best stability when compared with the other solvents. Even using water as a solvent, decomposition occurred and the stability of amoxicillin could be a serious issue in the membrane purification step.

In previous studies, it was showed that the amoxicillin solubility and stability is highly dependent on temperature and pH (Shaohua Feng, 2006; Francesco Crea, 2012; Morton, 2001; Vahdat, 2007; Sabegh, 2012). Solubility increases and stability decreases rapidly with the increase of temperature. In terms of pH conditions, it is known that the solubility increases significantly with higher (>8) and lower pH (<2) being the API stable in acid conditions. Nevertheless, the behavior of the amoxicillin with pH is complex and the literature data available is not enough to fully understand the pH effect. Being one of the key parameters for the success of the OSN purification process titration curves of both compounds were analyzed and a dissociation study was performed.

4.2 Isoelectric point determination

For better understanding of the behavior of the compounds with the pH, titrations of both compounds (Amoxicillin and 4-hydroxy-L-phenylglycine) were conducted. The standard solutions were prepared based on the study developed by Francesco Crea et al. in 2012.

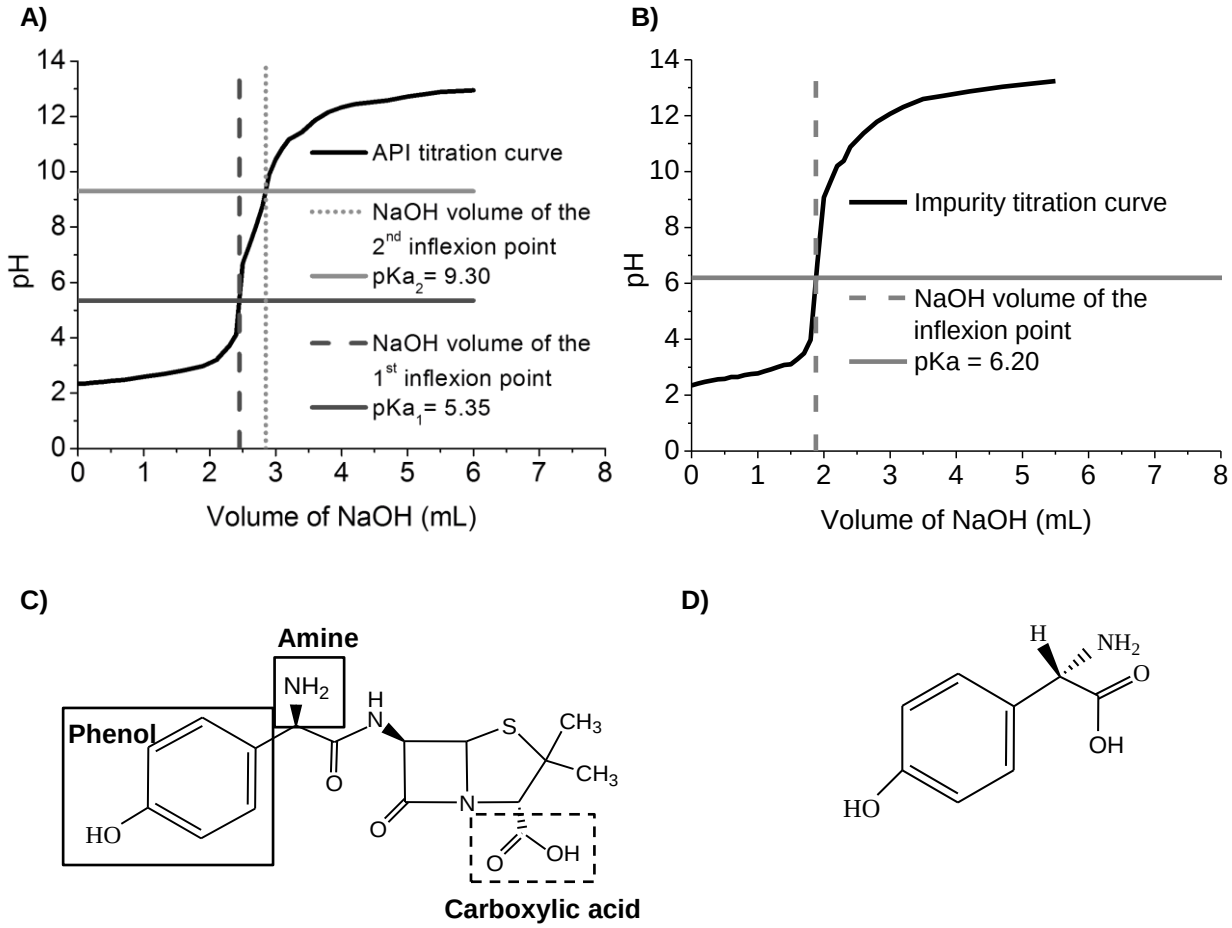

Figure 4.3 – Isoelectric point determination: A) Titration curve of amoxicillin a T=20ºC. Experimental conditions: C_{API}= 1.32 mmol.L^{-1}; C_{NaOH}= 49.65 mmol.L^{-1}; $V_{iniz.}$ = 10 mL; B) Titration curve of 4-hydroxy-L-phenylglycine a T=20ºC. Experimental conditions: C_{API}= 1.43 mmol.L^{-1}; C_{NaOH}= 49.65 mmol.L^{-1}; $V_{iniz.}$ = 10 mL; C) Molecular structure and ionizable groups from amoxicillin; D) Molecular structure of 4-hydroxy-L-phenylglycine.

The titration data was analyzed using a derivation method of finite elements and it was possible to determinate the NaOH volumes used in the inflexion point and as well as the exact pKa (see appendix II for calculations).

Comparing the amoxicillin titration curve obtained with the literature data, two of the three inflexion points were obtained: one possibly corresponding to the amine group (pKa ~ 7.00) and a second one possibly from the phenol group (pKa ~ 9.50) (Francesco Crea, 2012; Morton, 2001). From the literature data and observing the API structure in *Figure 4.3 (C)*, it was expected a third inflexion point corresponding to the carboxylic acid group (pKa ~ 3). One explanation for the non-appearance of this inflexion point could be related to the fact that the pKa of carboxylic acid group is at a value close to the initial pH of the titration curve which could explain its absence from the titration curve.

No literature data was found about the acting groups of the 4-hydroxy-L-phenylglycine compound. Nevertheless, amoxicillin molecule is very similar in terms of groups but the interaction with each other could be different. From the titration curve it was possible to identify a pKa of 6.20 for 4-hydroxy-L-phenylglycine.

After obtaining the isoelectric points of each compound there was the possibility of separating them using the ionic interactions and properties.

Ferreira F. C. A. in 2004 deducted an equation that allows the calculation of the concentration of the neutral and ionic species for a given pH and therefore allows the study of the dissociation profiles of the different species in a solution. From *Equations III.4 and III.5*, described in sub-section 3.1.2.3.1, it was possible to study the dissociation profiles of each compound and compared them to see if the pH factor can favor the separation process.

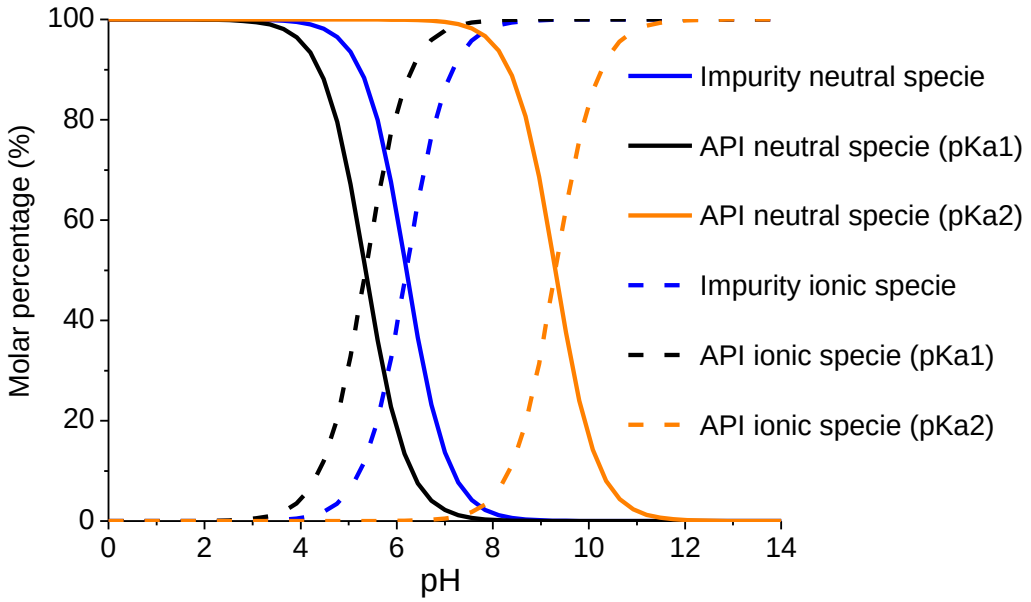

Figure 4.4 - Dissociation profiles of the amoxicillin and 4-hydroxy-L-phenylglycine, considering 100% molar percentage in the beginning (see appendix III for calculations).

In numerous studies it was observed that membranes in general have a tendency to have a higher rejection for dissociated species than non-dissociated species (Manttari Mika, 2006). Nevertheless, this tendency can easily change depending on the membrane characteristics, such as charge or cross-linking degree, or even the model mixture used.

In *Figure 4.4*, starting with an acidic pH of 2.0, both compounds are in completely neutral form (100% molar percentage). Approaching a pH of approximately 5.0, 25% of amoxicillin (50% of the first ionized group) and 50% of the impurity compound were dissociated. Reaching a pH around 9.0, the impurity is completely dissociated, but only the first ionized group of amoxicillin is completely dissociated.

Being a binary mixture of two very similar compounds with no exhaustive background in the membrane investigation technology, it would be of extreme interest to execute a more detailed study of their behavior with the change of pH and the effect in their separation results. Besides, diafiltrations trials should be performed for each compound separately and as a mixture (varying the pH conditions) to understand the possible interactions with the workable membrane (usage of a different membrane as control).

For this study, it was thought that the most promising condition to perform the diafiltrations trials would be to use a pH of approximately 9, since with this pH it can be obtain a higher difference, in terms of dissociation groups, between the two compounds. The acidic conditions (pH 2.00 and 5.00) were also investigated in terms of rejection for the separation process.

Varying the pH was thought to be a crucial parameter and could make the difference between a suitable or unsuitable separation process using OSN for this study case.

4.3 Membrane screening

In order to identify the most suitable membrane for this separation process different types of membranes were tested: PBI, PI, PEEK, TFNF-DL, M130 and Duramem®200 (membrane description in sub-section 3.1.3). The choice of the membranes was based on their molecular weight cut-off, performance and interaction with water and also previous studies conducted with the API amoxicillin and other similar compounds using membrane technology (Sterlitech Corporation and Evonik Industries via online; Valtcheva, 2012; Shahtalebi, 2011).

The membrane screening was conducted in two different set-ups: dead-end measurements and m-CSTR upside down measurements, as described in sub-section 3.1.4.

In both set-ups, parameters such pressure and solution pHs were studied in the different membranes. The pressures tested were 10, 20 and 30 bar and the solution pH tested were 2.0, 4.9 (pH of the solution containing the two compounds) and 8.6. The temperature was kept constant at 22ºC in all trials.

A solution containing 1g.L^{-1} of amoxicillin and 0.03 g.L^{-1} (30 ppm) of 4-hydroxy-L-phenylglycine (impurity) was used to conduct the experiments. This solution had an initial pH of approximately 4.8 (at 22 ºC) and the solvent used was water (as concluded in the sub-section 4.1).

When evaluating a membrane performance the two most important parameters are rejection and permeability. Permeability is often considered a critical variable; however, a high permeability is not always necessary or even desirable. In fact, especially in the pharmaceutical industry, it is often more important to achieve a high yield and level of purity, because complete retention of a particular solute is the main objective. Since there is always a trade-off between permeability and rejection, one must select the membrane that match as close as possible the specific process requirements. As a rule of thumb, the rejection of the smaller compound should not exceed 80% for the process to be practical and feasible. All rejections presented in this chapter were obtained by *Equation III.7* using the calibration curves presented in the appendix I.

4.3.1 Dead-end measurements

The set-up configuration used for these measurements is described in the sub-section 3.1.4.1 As mentioned before, prior to any diafiltration, the system was washed with water to wash away membrane preservatives or any remaining impurities from the previous filtrations and also to conditioned the membrane. The total solution volume used for the filtration trials was 50 mL. The mass balance error for the solution concentration in all trials was of 9 ± 6% for the API and 10± 8% for the impurity.

The effect of operating pressure on solute rejection has been studied extensively by many authors (Bowen, 2002; Peeva and Livingston, 2004). In NF, solute rejection is usually observed to increase with rising pressure. Therefore, firstly the membranes were first screened by varying the system pressure (measurements at 10, 20 and 30 bar), maintaining temperature and pH conditions constant.

Knowing the molecular structures of the mixture compounds it is expected that the solutes rejections will be very similar. Therefore, and considering the analysis performed in section 4.2, experimental trials were performed by changing the pH of the solution (to a pH of 2.0, 4.8 and 8.6). These experiments were performed for the membranes selected in the initial trials: PBI22, PBI20, TFNF-DL and PI(1:4) membranes.

4.3.1.1 Pressure effect

The results from the trials performed at 10 bar are presented in *Table 4.3*.

Table 4.3 - Summary of the screening results conducted using water as solvent with a pressure of 10 bar and a temperature of 22ºC.

Membrane [a]	Rejection (%)		Flux [b] ($L.m^{-2}.h^{-1}$)
	API	Impurity	
PBI26 [c]	-	-	-
PBI22- A(1)	**97.78**	**90.18**	**19.7 ± 2.1**
PBI22- A(2)	**98.83**	**95.25**	**11 ± 1**
PBI20- A(1)	**96.85**	**90.16**	**11.9 ± 0.7**
PBI20- A(2)	**88.12**	**73.96**	**15.7 ± 0.7**
PBI17- A(1)	44.8	25.99	43 ± 8
PBI17- A(2)	19.2	11.04	53.8 ± 12.2
PI(1:4)- A	67.12	47.4	5.9 ± 0.9
PI(1:4)- B(1)	77.39	55.03	4.2 ± 0.3
PI(1:3)	61.45	44.92	13.4 ± 1.7
PI(1:2)	60.03	49.35	30.8 ± 0.8
PEEK [c]	-	-	-
TFNF-DL- A	**99.36**	**95.07**	**34.3 ± 1.5**
TFNF-DL- B	**98.04**	**94.17**	**32.6 ± 2.1**
M130	63.01	52.96	32 ± 3
DM200	59.64	52.08	31.9 ± 2.8

a Letter indicates the membrane batch; number in parenthesis indicates the membrane coupon
b Error values represent the standard deviation of the mean.
c Membrane with negligible flux.

From the initial trials presented above, it can be seen that the PBI26 and PEEK membranes did not have any rejection or flux results and this was due to their very low flux.

It is also possible to see that PBI17 membrane had low rejections and high fluxes for both compounds, which could mean an inappropriate MWCO for the case study having all solutes been permeated through the membrane.

PI membranes had low fluxes and API rejections not high enough to achieve a satisfactory yield.

For the M130 and Duramem®200 membranes there was a trade-off between permeability and rejection. Although their flux was more than satisfactory to work with, their rejections were very low for the API (around 60%).

PBI22, PBI20 and TFNF-DL were the best membranes having high rejections for the API (close to 99%) and reasonable fluxes (around 12 $L.m^{-2}.h^{-1}$ for the PBI membranes and 34 $L.m^{-2}.h^{-1}$ for the TFNF-DL membranes). PBI20- A(2) had lower rejections values which could be related to a defect in the membrane surface.

Both PBI (PBI26 to PBI17) and PI (PI(1:4) to PI(1:2)) membranes showed consistency and the expected trend as the proportion of polymer in the dope decreased, the rejection of the membrane decreased and its permeability increased correspondingly. This trend towards tighter membranes with higher polymer fraction has been observed previously (See Toh, Ferreira and Livingston, 2007).

Evaluating these initial trials it can be concluded that the difference between the compounds rejections was very similar which will constitute the main limitation for the separation process.

The results from the trials performed at 20 bar are described in *Table 4.4*.

Table 4.4 - Summary of the screening results conducted using water as solvent with a pressure of 20 bar and a temperature of 22ºC.

Membrane [a]	Rejection (%)		Flux [b] ($L.m^{-2}.h^{-1}$)
	API	Impurity	
PBI26 [c]	-	-	-
PBI22- A(1)	**98.45**	**92.05**	**25 ± 1**
PBI22- A(2)	**99.13**	**96.6**	**20.9 ± 0.5**
PBI20- A(1)	**97.77**	**93.62**	**19.9 ± 0.5**
PBI20- A(2)	**88.60**	**73.21**	**27.5 ± 1.4**
PBI17- A(1)	45.49	35.01	62.7 ± 6.7
PBI17- A(2)	27.05	29.05	79 ±16
PI(1:4)- A	**91.02**	**79.51**	**10.7 ± 0.6**
PI(1:4)- B(1)	**93.08**	**78.94**	**7.9 ± 1.9**
PI(1:3)	72.74	49.05	22.8 ± 0.5
PI(1:2)	63.95	48.57	51 ± 2
PEEK [c]	-	-	-
TFNF-DL- A	**96.88**	**92.91**	**63 ± 9**
TFNF-DL- B	**98.74**	**95.11**	**59 ± 3**
M130	74.06	60.33	45 ± 1
DM200	58.57	52.98	46.1 ± 0.5

a Letter indicates the membrane batch; number in parenthesis indicates the membrane coupon.
b Error values represent the standard deviation of the mean.
c Membrane with very low flux.

As seen for 10 bar pressure, PBI26 and PEEK membranes continued to have insufficient flux to obtain any results.

As expected, almost in all membranes the flux and rejection values increased with pressure. Even so, for the PBI17, M130 and DM200 membranes this increase was not enough to make them one of the possible membranes to be used.

On the contrary, the PI(1:4) membrane showed 90% rejection for the API, which was not enough for a suitable purification process but could be an option to considerer if the rejection increased again when using a higher pressure .

The best results in terms of rejection were obtained for the PBI22 and TFNF-DL membranes, which presented even higher fluxes when comparing with the ones obtained at 10 bar. The membrane TFNF-DL- A did not follow this trend but it could be related to the damage of the membrane surface during prior to its insertion in the cell.

The increasing of the API rejection with pressure was a positive achievement but the rejection of impurity increased proportionally, i.e., the difference of rejection remained constant.

The results from the trials performed at 30 bar are described in *Table 4.5*.

Table 4.5 - Summary of the screening results conducted using water as solvent with a pressure of 30 bar and a temperature of 22ºC.

Membrane [a]	Rejection (%)		Flux [b] ($L.m^{-2}.h^{-1}$)
	API	Impurity	
PBI26 [c]	-	-	-
PBI22- A(1)	**98.60**	**94.05**	**31 ± 5**
PBI22- A(2)	**99.22**	**96.88**	**28.1 ± 0.8**
PBI20- A(1)	**98.68**	**95.63**	**25 ± 3**
PBI20- A(2)	**91.40**	**78.21**	**31 ± 4**
PBI17- A(1)	26.89	20.2	163.8 ± 28.5
PBI17- A(2)	25.68	29.24	106.3 ± 4.8
PI(1:4)- A	**96.68**	**94.81**	**13.2 ± 1.7**
PI(1:4)- B(1)	**94.93**	**84.6**	**11.6 ± 0.8**
PI(1:3)	78.76	62.19	32 ± 3
PI(1:2)	75.61	64.16	51.5 ± 6.1
PEEK [c]	43.3	41	0.27 [f]
TFNF-DL- A	**97.68**	**92.29**	**85 ± 10**
TFNF-DL- B	**99.02**	**95.50**	**81 ± 15**
M130	79.03	68.12	60 ± 2
DM200	66.39	59.62	72.6 ± 7.4

a Letter indicates the membrane batch; number in parenthesis indicates the membrane coupon
b Error values represent the standard deviation of the mean.
c Membrane with very low flux.
f Only one value available

Using a pressure of 30 bar it was possible to measure the flux for PEEK membrane, but as can be seen this membrane had low rejections and a flux that was not workable from a practical point of view.

PBI26 membrane did not show any flux and for that reason it was discarded.

PBI17,PI(1:3), PI(1:2), M130 and DM200 membranes demonstrated in all trials to have poor rejections for both compounds so they were also put aside as suitable membranes for this separation case.

By increasing the applied pressure, PI(1:4) membrane gained interest since its API rejection increased from approximately 70%, at 10 bar, to approximately 96%, at 30 bar. Membrane PI(1:4)-B(1) presented the highest difference between solute rejections, 10 p.p., considering all experimental trials.

Membranes that showed better performance and could be applied to this process were PBI20, PBI22 and TFNF-DL. TFNF-DL had higher flux compared with PBI membranes but the rejections are similar.

Ideally an API rejection of 100 % and a low or medium rejection for the impurity would be preferable. Similarly to many other studies of NF, as the membrane gets tighter, the rejection of the smaller compound increased in parallel with that of the larger one. Thus, if the membrane is tight enough for the rejection of the larger species to approach 100%, then the rejection of the smaller one would also become higher with reduced permeability. This parallel increase in rejection is also observed when increasing the pressure, but it reaches a point that the API rejection is not significantly affected by the increase of pressure and only the impurity rejection continues to increase, resulting in an even lower difference between their rejections. This can be seen in *Table 4.5* for PBI22 and PBI20 membranes. In this particular case it would be more logical to use lower pressures (20 bar for example) since the API rejection was practically the same but the difference of solute rejections was higher.

In summary, it was possible to have a considerable high rejection of API (99%), using the PBI and TFNF-DL membranes, but with a high impurity rejection as well (95%). A maximum of 10 p.p. difference between solutes rejections was obtained using the PI(1:4) membrane, but the API rejection was 5 p.p. lower when compared with the other suitable membranes (94%).

PBI22, PBI20, TFNF-DL and PI(1:4) membranes were selected to proceed with the optimization study by changing the pH of the model mixture.

4.3.1.2 Separation optimization based on solution pH effect

The experiments using PBI membranes were not performed at 30 bar because as it was seen the difference between solutes rejections was higher at lower pressures. In addition, PBI membranes are sensitive at higher pressures because of compaction (Valtcheva, 2012).

Table 4.6 - Summary of the screening results conducted using water as solvent at 22ºC.

Membrane [a]	P (bar)	Rejection (%)		Flux [b] ($L.m^{-2}.h^{-1}$)	Solution pH (at 20ºC)
		API	Impurity		
PBI22- B	10	99.08	95.61	13.6 ± 1.6	5.1
	20	99.38	97.24	22.1 ± 0.8	-
	20	99.11	95.58	20.1 ± 0.6	2.0 [c]
	20	**98.05**	**88.18**	**20.5 ± 1.9**	**8.7** [d]
PBI20- B	10	94.22	85.97	16.3 ± 1.6	4.8
	20	95.43	90.81	24.0 ± 1.8	-
	20	95.20	90.01	22.31 ± 1.5	2.0 [c]
	20	**97.75**	**86.63**	**12.99 ± 0.68**	**8.6** [d]
PI(1:4)- B(2)	10	70.26	49.26	5.3 ± 0.4	5.1
	20	73.12	61.06	10.2 ± 0.7	-
	30	81.27	73.02	13.5 ± 0.8	-
	30	82.95	76.67	13.5 ± 0.6	2.0 [c]
	30	**86.48**	**71.93**	**13.3 ± 0.6**	**8.7** [d]
TFNF-DL- B	10	98.61	94.17	30.6 ± 3.1	4.9
	20	99.04	95.11	51 ± 13	-
	30	99.02	94.3	77 ± 13	-
	30	98.83	94.18	101.6 ± 20.3	2.3 [c]
	30	**98.92**	**89.65**	**89.3 ± 10.8**	**8.7** [d]

a Letter indicates the membrane batch; number in parenthesis indicates the membrane coupon
b Error values represent the standard deviation of the mean.
c Change of pH with HCl (0.8M) with a dilution effect of .20% for both compounds
d Change of pH with NaOH (0.1M) with a dilution effect of .20% for both compounds

Analyzing all the results obtained, a clear effect in the rejection of the compounds was observed when changing the solution pH to 8.7. A decrease in the rejection of the impurity occurred due to pH change which increased the difference in rejection of both solutes (positive effect).

Rejections and fluxes obtained in all trials before the change of pH were consistent with the previous results, with the exception of the PI(1:4) membrane, probably due to a defect in the membrane surface.

For the mixtures at pH 4.9 and 8.6 but at the same pressure one can verify that the difference in rejection between the solutes was the double when changing the pH from 4.9 to 8.6. The maximum different obtained between the compounds rejections was of approximately 10 p.p. in all membranes except for the PI(1:4) membrane.

When changing the pH to 8.6 it was noticeable a decrease in flux when using PBI membranes, which was expected from previous studies (Valtcheva, 2012). The PBI20- B had a more significant decrease in flux when changing the solution pH to 8.6. This decrease in flux could be due to compaction, fouling effects, like membrane adsorption or pore blocking.

For the TFNF-DL membranes the effect was the opposite, the flux increased with the change of pH. If the membrane is charged, as it happens with PBI membranes, by changing the pH of the solution interactions between the compound and the membrane could have occurred which could explain the change in performance. Other possibility could be an eventual increase in the pore swelling and consequently a higher permeability (Manttari Mika, 2006).

From the results it was clear that by changing the pH to 8.6 the separation process was optimized. In summary, it was possible to have a high rejection of API (98-99%) using the PBI22 and TFNF-DL membranes and a difference of 10 p.p. between the rejection of API and impurity, which was not possible by maintaining the pH constant.

Considering all the results from the membrane screening using dead-end measurements it was possible to select the most suitable membranes and conditions for the following filtrations studies: PBI22 membrane using a pressure of 20 bar and TFNF-DL using a pressure of 30 bar, both using optimized pH conditions.

4.3.2 m-CSTR upside down measurements

It is known that the dead-end filtration mode has a lot of fouling and concentration polarization problems as described in sub-section 1.2.3. A cross-flow mode is preferably used in diafiltrations being less susceptive to these problems and normally better rejections are obtained.

Therefore, a more exhaustive screening using a set-up with an m-CSTR upside down cell was performed for PBI22 and TFNF-DL. It is important to run diafiltrations tests in this mode to confirm the results obtained with the previous set-up and to see if there is any possibility to improvement.

The system proposed for this screening is illustrated in *Figure 4.5* and described in detail in the sub-section 3.1.4.2. The flow was supplied using only a single pump and the pressure was regulated using a backpressure regulator in the downstream. The retentate from the membrane cell was recycled and each component of the system was stirred vigorously to guarantee that the compounds are well mixed and minimize any adverse concentration polarization effects inside the membrane cells. Furthermore, this system operates in a self-regulating manner, so no external control was required once the process starts.

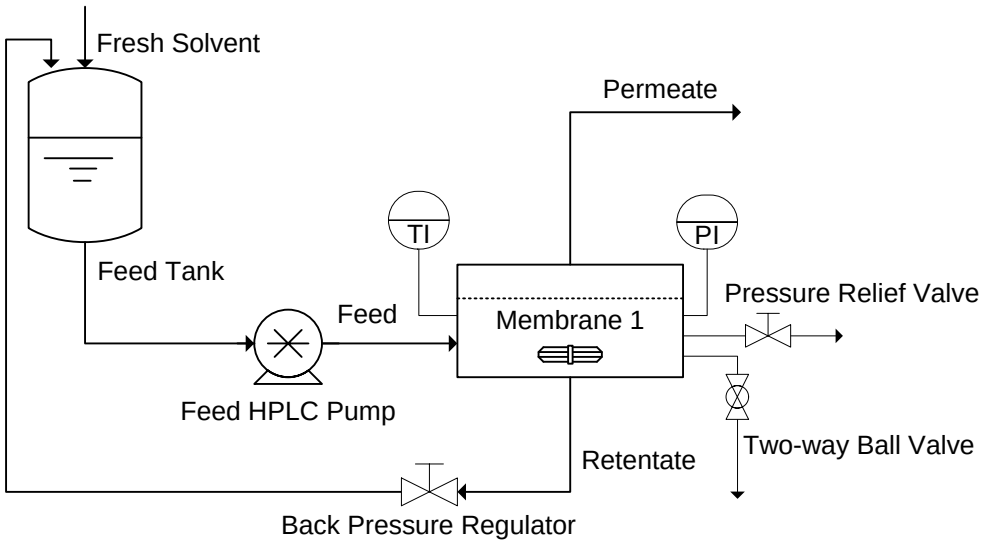

Figure 4.5 - Process diagram of the single membrane system (PI: Pressure gauge; TI: Temperature indicator).

As mentioned before, prior to any diafiltration, the system was washed with water to achieve steady state flux and also to wash away membrane preservatives and any remaining impurities from the previous filtrations The total solution volume used for the filtration trials was 200 mL. The mass balance error for the solution concentration in all trials was of 16 ± 14% for the API and 12 ± 19% for the impurity.

Firstly, diafiltrations without changing the solution pH were conducted for each trial to condition the membrane and to have comparative rejection values. The initial solution was always drained from the cell to conduct the pH exchange and the membrane clean with water for more than 1h before proceeding with the filtration with a basic pH.

4.3.2.1 PBI22 screening results

Table 4.7 - Summary of the screening results conducted using water as solvent at 20 bar at 22ºC. Pure solvent average flux is 52.5 ± 2.5 L.m^{-2}.h^{-1}.

Membrane [a]	Filtration time (h)	Rejection (%)		Flux [b] (L.m^{-2}.h^{-1})	Solution pH (measured at 20ºC)
		API	Impurity		
PBI22- C (1)	0	-	-	-	5.1
	1	**94.28**	**93.88**	31.4± 0.4 (at 27ºC)	4.3
	cleaned with 500 mL of water				
	0	-	-	-	8.6 [c]
	1	98.83	95.29	26.5± 0.8	-
	4	98.60	95.92	-	-
	5	**98.87**	**96.19**	26.79± 0.27	8.2
PBI22- C (2)	0	-	-	-	5.0
	1	**93.17**	**88.98**	24.26± 1.21	4.0
	cleaned with 500 mL of water				
	0	-	-	-	8.6 [c]
	1	96.16	77.71	23.4± 0.7	-
	4	93.86	81.48	-	-
	5	**94.00**	**82.62**	18.5± 0.3	7.9
PBI22- D	0	**-**	-	-	5.0
	1	**96.23**	**89.17**	25.21± 0.59	4.1
	cleaned with 500 mL of water				
	0	**-**	-	-	8.7 [c]
	3	92.69	71.26	26.79± 0.58	
	4	91.86	73.38	-	-
	5	**92.64**	**74.28**	26.5± 0.7	8.0

a Letter indicates the membrane batch; number in parenthesis indicates the membrane coupon
b Error values represent one standard deviation of the mean.
c Change of pH with NaOH (0.1M) with negligible dilution effect (2% for both compounds).

From *Table 4.7* it can be seen that the permeate flux was, from the beginning, smaller than the pure solvent flux. This difference was already observed by many authors for different solute-solvent systems (Yang et al., 2001; Whu, Baltzis and Sirkar, 2000; Gibbins et al., 2002), and can have several causes, such as osmotic pressure, concentration polarization or hindered diffusion within the pores. Analyzing the fluxes at a normal pH and comparing with dead-end results (*Table 4.5* and *4.6*), it can be seen that all trials were consistent (see sub-section 4.3.1). Only the flux obtained for the PBI22-C(1) membrane was higher but this has to do with the high temperature of the measurement (27ºC). Temperature is one of the factors that influence the permeability flow since with its increase the pores

tend to be more flexible and the solvent viscosity tends to decrease, facilitating the permeability of the solution.

As seen in the dead-end measurements (*Table 4.6*), the PBI22 membrane permeate flux dropped from 22.1 ± 0.8 to 20.5 ± 1.9 $L.m^{-2}.h^{-1}$ when changing the pH to basic conditions (see sub-section 4.3.1.2). The PBI22 – C(2) membrane was the only one with a drastic drop of flux along the diafiltration process when changing the pH to 8.6 (from 24.26 ± 1.21 to 18.5 ± 0.3 $L.m^{-2}.h^{-1}$). This could be attributed to membrane compaction. However, membrane compaction is normally accompanied by an increase in the rejection which was not observed. Thus, it was more likely that the flux continued to drop due to fouling effects, like membrane adsorption or pore blocking. At the end of the trial considerable quantities of white powder were observed close to the edges of the membrane and in the inner o-rings. This phenomenon could be the reason for the drastic drop in flux and will be discussed in sub-section 4.3.2.2.1.

Comparing both systems for PBI22 membranes it was observed a considerable difference between the rejections values obtained. With the use of a cross-flow mode system it was expected that the rejection of solutes would increase or maintain the same tendency of values observed before (in the range of 98-99% for the API; and for the impurity 94-96% with normal pH and 88-89% with basic pH). Observing *Table 4.7*, it can be seen that the rejections values for both compounds in the different pH conditions dropped in all membranes tested.

Considering the PBI22- C(1) membrane before the pH change, the API rejection was lower and the difference between solute rejection almost disappeared. When modifying the pH the API rejection increased to a coherent value having in consideration the previous results and it was practically constant over the diafiltration process. Nevertheless, a significant decrease of the impurity rejection was not observed as before, not having an improvement in the difference between solute rejections.

For the PBI22- C(2) membrane it was observed the same low rejection for API (93.17%) that increased after changing the pH to 8.6 (same trend as PBI22-C(1)). As expected from the dead-end measurements, the impurity rejection went down in 10 p.p. corroborating the positive effect of the pH in the separation.

In PBI22- D membrane, the initial rejection was satisfactory but when changing the pH, a significant drop in 5 p.p was observed. In the previous membrane (PBI22-C(2)), the impurity rejection went down , with a decrease of 20 p.p.. This higher decreased in the impurity rejection probably was due to the parallel decreased in the API rejection.

Previous studies using PBI membranes showed decreases in rejections during the diafiltration process due to interactions between the cross-linker present in the membrane and the filtration solvent (Valtcheva, 2012). A parallel project was being performed by co-workers at the Andrews Livingston Group, Piers Gaffney and Jeong Kim, with a similar problem using cross-linked PBI membranes. Their objective was to remove byproducts from a chain reaction using an OSN process. Unfortunately the byproducts rejections were being too high, even when using a suitable MWCO. They hypothesized that the anionic byproducts could be ion exchanging with the original bromide counter-ions within the PBI membrane from the cross-linking reaction. Therefore, they added a salt to the solution allowing the exchange of the byproduct ions associated with the ions in solution, being then capable to remove effectively the byproducts from the solution.

The cross-linker of the PBI membrane used in this work, as indicated in sub-section 3.1.3.1, was dibroxylene (DBX). Analyzing the pH measurements in all trials, it can be seen a decrease in the solution pH in all membranes after performing the diafiltrations trials. An interaction with the cross-linker certainly would have this effect since the cross-linker is formed by bromide groups that are negatively charged. Since the mixture compounds seem to be sensitive to the pH conditions, as shown before, this variability of the pH could be the reason for the inconsistent performance in the different diafiltration trials. Nevertheless, depending on the cross-linking degree, the membrane can have more or less bromide groups, which could mean a higher or lower interaction with the module mixture. Combining this with the variability originated from the preparation steps, such as the dope solution and casting of the membrane, a significant effect in the membrane performance could be expected.

Understand and control this interaction phenomena is crucial for the use of this membranes in this specific separation process. Currently, PBI membranes are being considered as a solution for many problems in OSN processes such as basic and acidic conditions.

4.3.2.2 TFNF-DL screening results

Table 4.8 - Summary of the screening results conducted using water as solvent at 20 and 30 bar at 22ºC. Pure solvent average flux is 160.7 ± 0.1 L.m^{-2}.h^{-1} at 20bar and 225.0 ± 15.2 L.m^{-2}.h^{-1} at 30 bar.

Membrane [a]	Filtration time (h)	Rejection (%)		Flux [b] (L.m^{-2}.h^{-1})	Solution pH (measured at 20ºC)
		API	Impurity		
TFNF-DL- C	0	-	-	-	4.8
	1	**92.08**	**84.48**	25.2± 0.5	4.7
20 bar	**cleaned with 500 mL of water**				
	0	-	-	-	8.7 [c]
	1	95.95	68.08	95± 6	-
	4	97.07	74.15	-	-
	5	**96.87**	**74.29**	99± 4	8.6
TFNF-DL- D	0	-	-	-	4.7
	1	**97.51**	**94.40**	26.8± 0.8	4.7
30 bar	**cleaned with 500 mL of water**				
	0	-	-	-	8.7 [c]
	1	97.89	84.57	68± 3	-
	4	98.90	85.89	-	-
	5	**98.93**	**86.20**	68± 2	8.5
TFNF-DL- E	0	-	-	-	4.7
	1	**97.23**	**93.01**	26.25± 0.54	4.8
30 bar	**cleaned with 500 mL of water**				
	0	-	-	-	8.7 [c]
	1	98.94	85.89	64± 3	
	4	99.11	86.07	-	-
	5	**99.12**	**87.80**	64.3± 0.0	8.6

a Letter indicates the membrane batch; number in parenthesis indicates the membrane coupon
b Error values represent the standard deviation of the mean.
c Change of pH with NaOH (0.1M) with negligible dilution effect (2% for both compounds).

A trial using a pressure of 20 bar was performed to allow a latter comparison between the results from TFNF-DL and PBI22 membranes under the same conditions.

As observed with PBI22 membranes, the permeate flux was also, from the beginning, smaller than the pure solvent flux (vide *Table 4.8*). As explained before, osmotic pressure, concentration polarization or hindered diffusion within the pores can be the causes of this flux decrease. In addition, as seen in the dead-end measurements (vide *Table 4.6*), the permeate flux increased when changing the pH conditions to 8.7.

In the dead-end measurements, an API rejection of 99%, using a 30 bar pressure, was obtained and a difference between solute rejections of approximately 10 p.p. was observed when increasing the solution pH to 8.7. Comparing these results with the ones described in *Table 4.8*, it can be seen that they are reasonably consistent which proves the membrane reproducibility.

It is important to notice that in these trials the solution pH did not change during the diafiltration, as it happened with PBI22 membranes, which corroborates the justification given above to the inconsistent results obtained for the PBI trials.

In the previous trials, using the dead-end system, it was possible to obtain a flux around 80 L.m^{-2}h^{-1} in a standard pH (≈ 4.9) and a flux of 90 L.m^{-2}h^{-1} using the module mixture with a basic pH (≈8.6), both at 30 bar. A significant decrease in the permeate flux was observed for the trials using standard pH (comparing dead-end with cross-flow) and for the trials using pH of 8.6 (comparing dead-

end with cross-flow); this decrease was of 55% and 36%, respectively. At the end of the each membrane experimental trial, a considerable amount of white powder was observed close to the edges of the membrane sheet and in the inner o-rings, as observed with the PBI22- C(2) membrane in the previous sub-section 4.3.2.1. This powder precipitation could be related to the flux drop observed in some trials. Considering the quantities and the consistence of the powder observed, it was thought to be amoxicillin precipitation. Since this phenomenon was occurring with some frequency and in considerable amounts, analyzes of the powder were performed in order to verify what was causing this precipitation phenomena.

4.3.2.2.1 Precipitated powder analysis

At the end of each membrane trial, the precipitated powder was thoroughly collected from the edge of the membrane and the o-rings, dried and weighted (process description in sub-section 3.1.4.2.1). An aqueous solution with a concentration of approximately 1 $g.L^{-1}$ (in two of the three trials was used a lower concentration due to the poor quantities of powder available) was prepared and a sample collected for HPLC analysis (calibration curves are presented in appendice I).

In *Figure 4.6* are shown the HPLC UV signals of the mixture compounds, amoxicillin and 4-hydroxy-L-phenylglycine, in 1 $g.L^{-1}$ aqueous solution, for comparison purposes.

A)

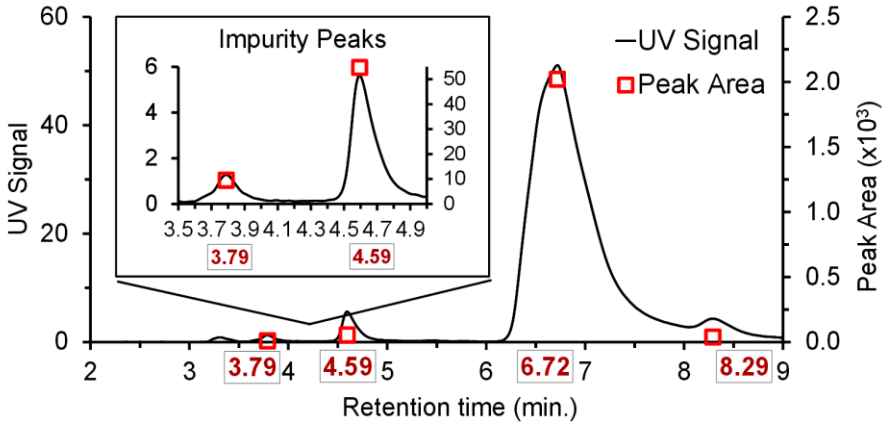

B)

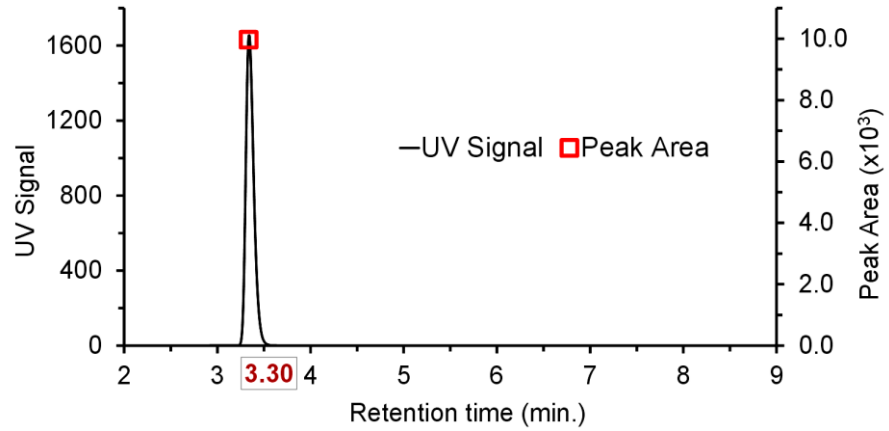

Figure 4.6 – HPLC UV signal from the mixture compounds in 1 $g.L^{-1}$ aqueous solution: A) amoxicillin (90.0% pure); B) 4-hidroxy-L-phenylglycine (99.0% pure). The red points indicate the different peak areas and the label values the retention times of those peaks.

Figure 4.6 A) shows the amoxicillin peak after 6.72 minutes with a UV signal of approximately 50 units. It was possible to identify four extra peaks, in which only three have a quantifiable area. Since the purchased powder was only 90.0% pure, these other peaks most likely correspond to those impurities present in the original powder. Observing the *Figure 4.6 B)* it can be seen a clear peak of the impurity of study that appears after 3.30 minutes.

Having the signal profiles of the original compounds, a comparison with the precipitated powder collected from the diafiltration using the TFNF-DL membrane can be made.

In *Figure 4.7* the HPLC UV signals from the precipitated powder collected in the screening trials for each TFNF-DL membrane are shown.

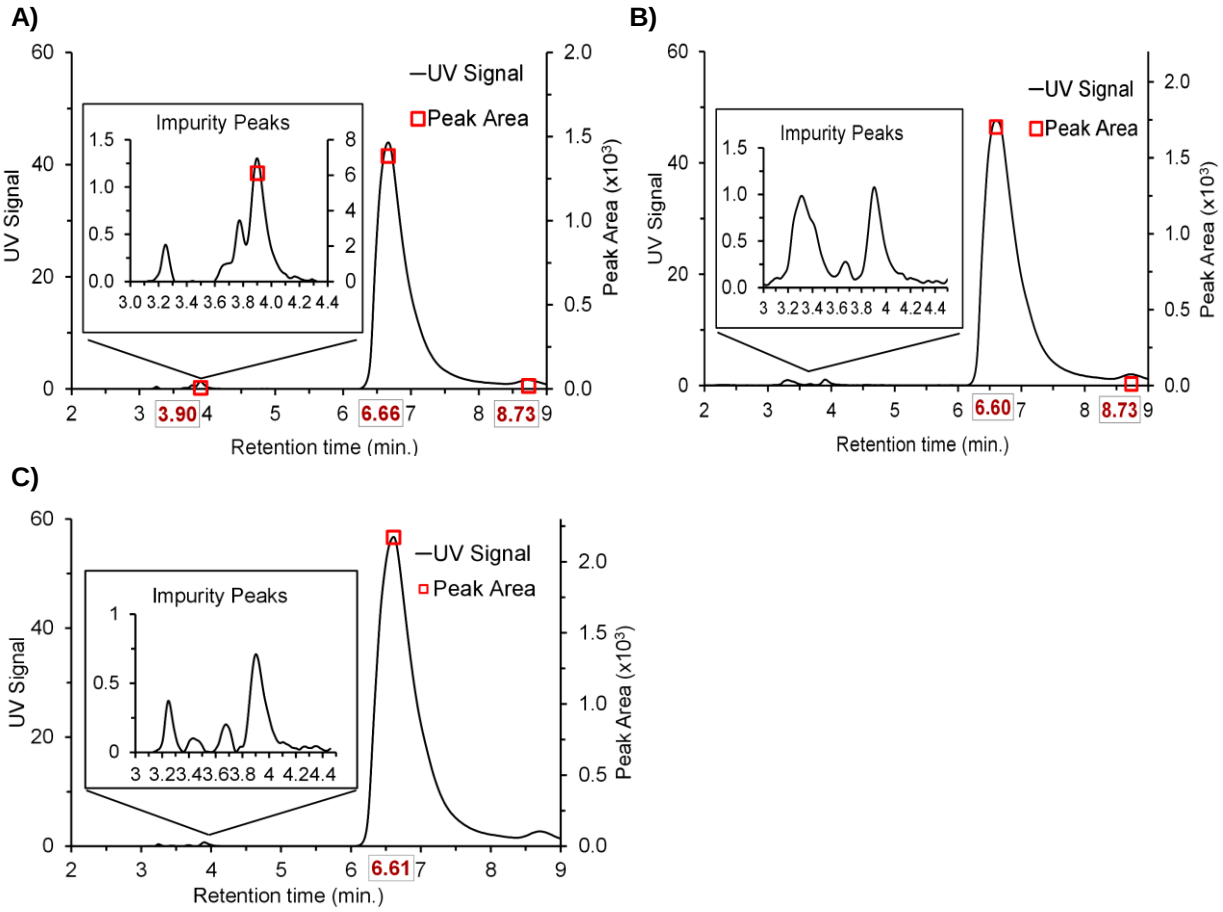

Figure 4.7 - HPLC UV signal results from the powder analysis. A) powder from TFNF-DL- C membrane trial at 0.7 g.L^{-1}; B) powder from TFNF-DL- D membrane trial at 0.9 g.L^{-1}; C) powder from TFNF-DL- E membrane trial at 1 g.L^{-1}. The red points indicate the different peak areas and the label values the retention times of those peaks. The peaks without red points are the ones with dispersible areas (≤ 2).

It can be seen from *Figure 4.7* that the samples were prepared in different concentrations. The objective was to prepare solutions with 1 g.L^{-1} being easier the comparison with the analysis to the original powder. The reason for this was that not enough powder was available due to difficulties in collecting the powder from the cell.

Comparing *Figures 4.6* and *4.7,* it was concluded that the powder collected was in fact amoxicillin. This indicates that for some reason the product of interest was precipitating during the diafiltration process. Nevertheless, all impurity peaks had a much lower signal area compared with the amoxicillin peak. Using the calibration curves in appendice I, it was possible to verify the amoxicillin concentration in the samples and therefore estimate the powders purity. For the samples represented in *Figure 4.7 A)* and *B)* was obtained a purity of 99.03% and 99.22% respectively. For the sample corresponding to the image *C)*, a purity above 100% was obtained, probably due to an experimental error made when preparing the 1 g.L^{-1} solution.

MIT co-workers had observed that the compound 4-hidroxy-L-phenylglycine (impurity) tends to crystallize in the same conditions as the API due to their similar properties. Since the powder collected had very low content of this impurity, it was though that the precipitation could be due to solubility reasons. Concentration polarization in the membrane interface or even insufficient mixing in some dead areas of the membrane cell could be the reason for an increase in concentration, reaching the amoxicillin solubility limit.

Thus, the mass transfer coefficient for amoxicillin was estimated for the diafiltration process performed. From the *Equations III.8* to *III.11*, described in the sub-section 3.1.4.2.2, the approximated amoxicillin mass transfer coefficient in the diafiltration process was calculated, having a value of 1.62×10^{-7} m.s^{-1}, which is considerably low (standard order of magnitude between 10^{-5} and 10^{-6} in membrane systems).

Peeva et al. studied the effect of concentration polarization on flux in OSN (Peeva and Livingston, 2004). The model developed and the corresponding mathematical equations are described in sub-section 3.1.4.2.3. Defining the permeability, molal volume, rejections and feed concentration for the solute and solvent, it was possible to calculate the solute concentration at the membrane interface profile with the mass transfer coefficient in a determinate system. Using MATLAB® to solve the non-linear algebraic *Equations III.15* to *III.17* and considering the results and conditions from the TFNF-DL-E trial in the upside-down cell (vide *Table 4.8*), the membrane interface concentration profile of amoxicillin in the range of the mass transfer coefficients estimated above was obtained.

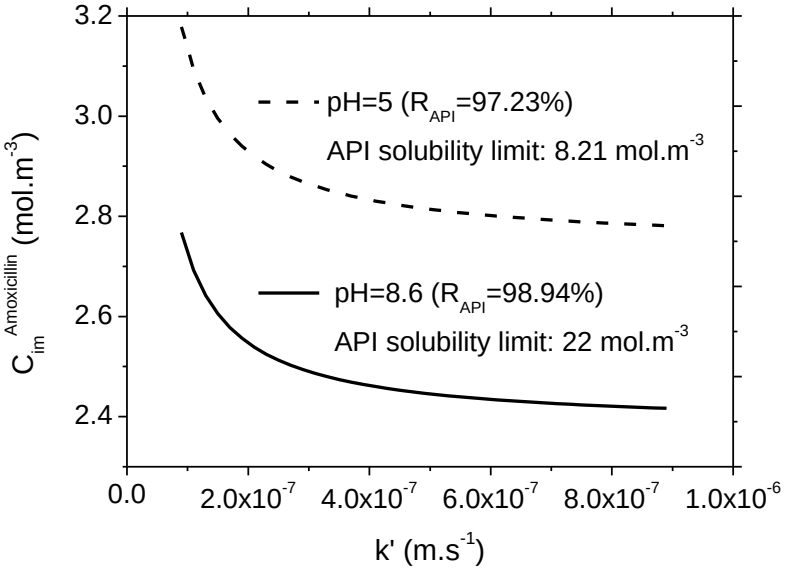

Figure 4.8 – Concentration profile for the API in the membrane interface, C_{im}, as a function of the mass transfer coefficient. Profiles for the experimental trial using the TFNF-DL – E for both pH conditions considering a retentate API concentration of 2.74 mol.m^{-3} (1 g.L^{-1}) and a solvent rejection of 1%.

From *Figure 4.8* it can be seen that the concentration of the API in the membrane interface increases with the decrease of the mass transfer coefficient. Considering the mass transfer coefficient estimated previously, 1.62×10^{-7} m.s^{-1}, a concentration in the range of 3 mol.m^{-3} was obtained from the concentration profile. Since the solubility limit in water for the API is approximately 3 g.L^{-1} (8.21 mol.m-3) for pH 5 and 8 g.L-1 (22 mol.m-3) for pH 8.6; the increase at the concentration in the membrane interface described by the module is not sufficient to cause the powder precipitation.

As it was mentioned before, an inconstant hydrodynamic profile in the cell could be also causing this phenomenon. Because the stir is situated at the bottom and center of the cell, in some areas the mixing might not be sufficient to have a homogeneous solution. These called dead areas are normally situated close to the upper side and in the radial perimeter of the membrane cell. The precipitation powder appeared exactly in those areas, so possibly this insufficient mixing could be contributing to this precipitation.

No further investigation of this phenomenon was continued, but it seems that this precipitation could be crucial for the implementation of the process itself.

4.3.3 Membrane screening conclusion

From all the screening trials, the TFNF-DL membrane was the most promising for the separation process in study showing consistency and reproducibility even when changing the set-up process. This membrane had the best results using higher pressures (30 bar) and achieving an API rejection of 99% with a very satisfactory flux of approximately 65 $L.m^{-2}.s^{-1}$. When working in basic conditions (pH of 8.7), it was observed, like the other studied membranes, an increase in the difference between the solutes rejections; a maximum difference of 10 p.p was achieved. Although it was possible to optimize the separation manipulating the pH conditions, the difference between the solutes rejections were still very similar which constitutes a hurdle to the separation process.

A system mass balance calculation demonstrates that to achieve a clean and efficient separation using diafiltration, two conditions need to be met: the difference in rejection between the two solutes needs to be large and the rejection of the bigger compound should be close to 100%. None of these conditions were achieved in the previous studies. It is common that in the field of membrane separation, the limiting factor is the membrane performance itself, with insufficient separation even after screening and optimization. It is for this reason that membrane cascades were originally proposed to overcome this fundamental material limitation. In the next section different cascade systems and conditions will be simulated and compared for the case in study. With a suitable cascade system possibly the issues described above can be mitigated and a separation with high purity and reasonable yield accomplished.

4.4 Process modelling

With the results obtained from the membrane screening, it was possible to simulate the behaviour of the separation process using different system configurations. The main goal was to use a cascade configuration, improving the separation process, and incorporate the system in a continuous process of amoxicillin purification.

Firstly, a simulation using a semi-batch system was conducted considering only one stage and then two stages. The two stage membrane cascade system was then adapted to a continuous system and simulated using two different configurations in the same conditions. All the different separation configurations were modelled by equating a mass balance for each stage. The concentration profiles of the product and impurity were calculated in MATLAB® using the process models described in sub-sections 3.2.1 and 3.2.2. The concentration profiles were then used to determine the yield and purity profiles. Different parameters such as the feed flow rate into the system ($Feed_{in}$), the stages effective pressures (ΔP), the recycle ratio (Rc) and feed utilization ratio (FU) were studied in detail. A three continuous cascade, using the most suitable continuous membrane cascade configuration, was also simulated in steady state using MS Excel Solver™. In this way, the increase of the number of stages in the separation was also investigated (described in sub-section 3.2.2.2).

In *Table 4.9* are described the parameters considered for all simulations, based on the semi-batch experimental trial using the commercial membrane TFNF-DL-E described in *Table 4.8*.

Table 4.9 - Summary of the parameters considerations based on the semi-batch experimental trial using the TFNF-DL-E membrane.

Parameter	Value considered	Unit
Effective pressure in stage 1	30	bar
Model mixture pH	8.7	-
Working temperature	22	ºC
Permeability	2.14[a]	$L.m^{-2}.h^{-1}.bar$
API rejection	99.12	%
Impurity rejection	87.80	%
Membrane area in stage 1	$51x10^{-4}$	m^2
Membrane area in stage 2	$51x10^{-4}$	m^2
Membrane area in stage 3	$51x10^{-4}$	m^2
Initial concentration of API	1.00	$g.L^{-1}$
Initial concentration of Impurity	0.03	$g.L^{-1}$
Initial API purity	97.09	%
Volume in stage 1	0.10	L
Volume in stage 2	0.10	L
Volume in stage 3	0.10	L

a Correspondes to a flux average of 64 $L.m^{-2}.h^{-1}$ at 30 bar obtained after 5 h of experiment.

Two system limitations had to be considered in the simulations: for cascade systems the effective pressure of the following stage had always to be lower than the previous stage (ΔP1> ΔP2> ΔP3), to guarantee the existence of retentate flow-rate in all stages; and the amoxicillin concentration in the purified out stream cannot be above 8 $g.L^{-1}$ due to the solubility limit at the workable conditions. This boundary condition is of great importance and can seriously affect the liability of the process since the fundamental concept of the system configuration is to concentrate the product of interest in the feed tank. These two considerations are the system restrains.

4.4.1 Semi-Batch mode

4.4.1.1 One stage system

With the configuration and correspondent mathematical equations described in the sub-section 3.2.1 for a single stage and the considerations described in *Table 4.9* a characterization of the system was performed using MATLAB®.

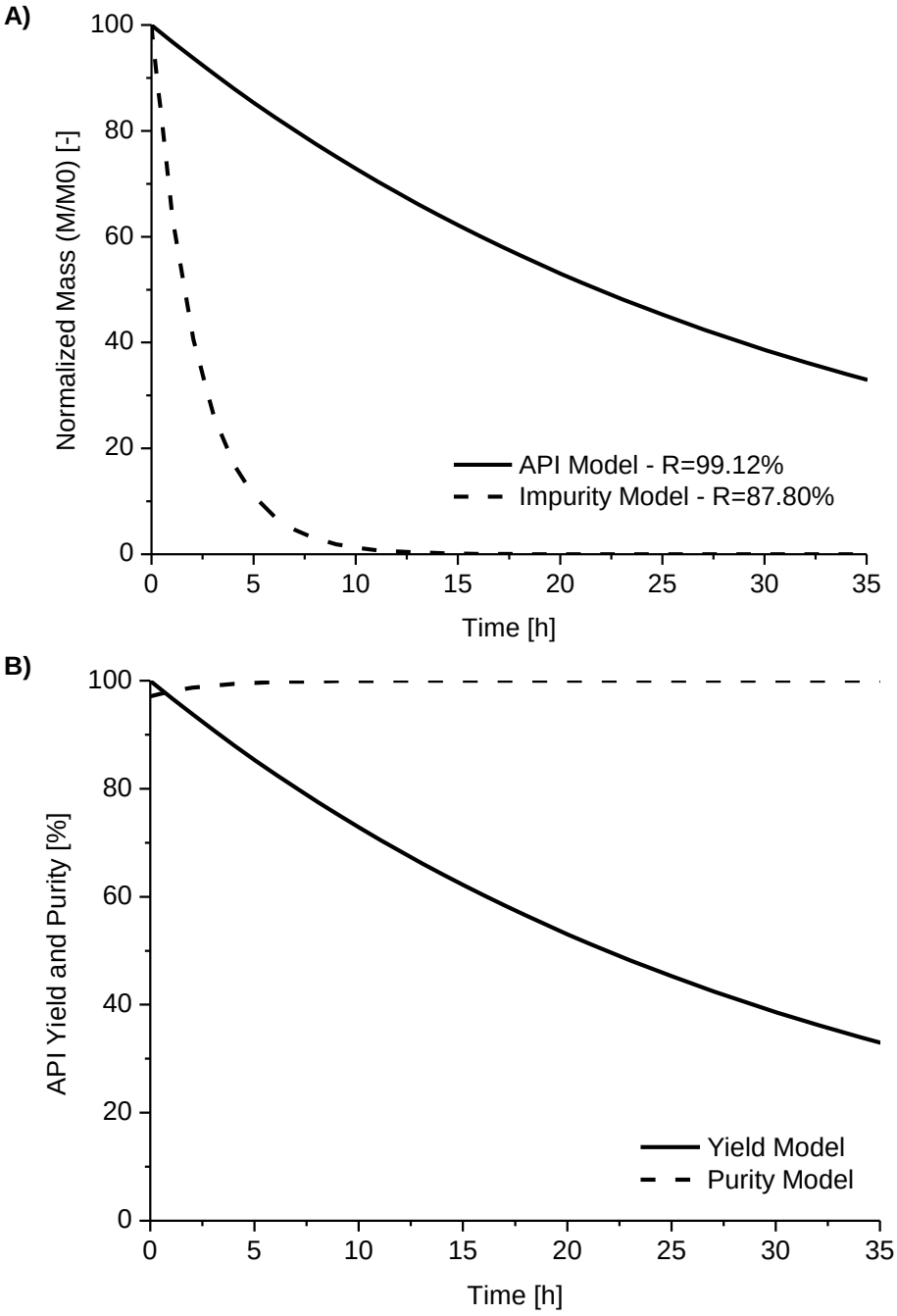

Figure 4.9 – Single-stage semi-batch system: A) Mass profiles over filtration time for both compounds in the retentate stream; B) Yield and purity profiles for the API, amoxicillin.

From *Figure 4.9* it can be seen that the mass of each compound remaining in the retentate stream followed the expected trend. A substantial decrease over time for the amoxicillin mass profile was observed; even if the rejection was 99% this would result in a loss of product and an accentuate decrease in yield. From an initial purity of 97.09%, a final purity of 99.99% could be achieved for the API after 35 (25 vols) but with a very low yield of 33%. The trade-off between purity and yield is too high limiting the purification process.

Once again it can be seen that the limiting factor was the membrane performance itself, with insufficient separation even after screening and optimization.

A cascade system was then considered to further optimize the purification process.

4.4.1.2 Two stage system

With the configuration and mathematical equations described in the sub-section 3.2.1 and the considerations described in *Table 5.1* a characterization of the two stage semi-batch system was performed using MATLAB®. Since the modulation was performed following the assumption that the rejection and permeability values were the same in both stages, a pressure of 25 bar for the second stage was chosen to perform the simulation and consequently a Rc of 0.17 was established.

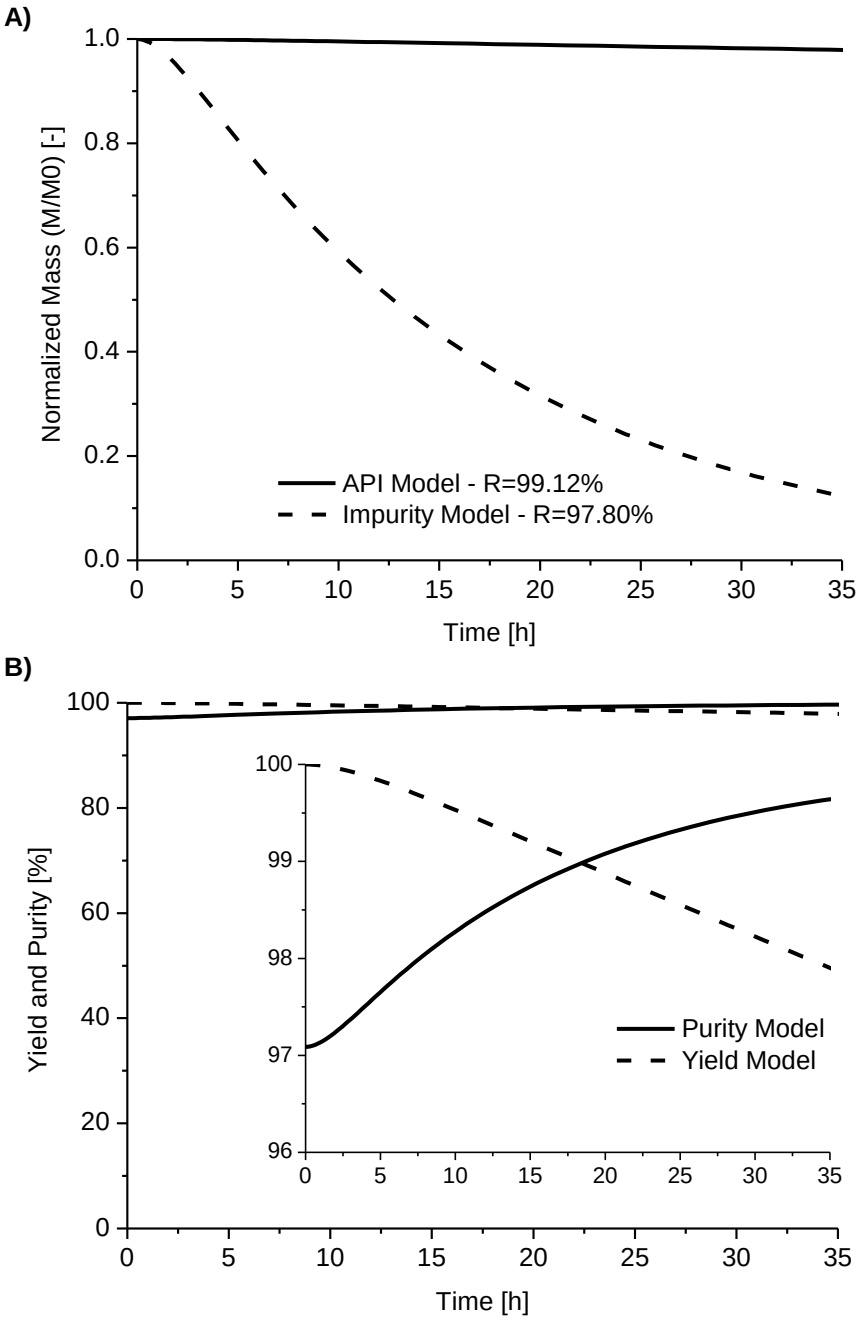

Figure 5.1 – Two-stage semi-batch system considering an effective pressure in the second stage of 25 bar and a Rc = 0.17: A) Total normalized mass profiles over filtration time for both compounds in the retentate stream; B) Yield and purity profiles for the API, amoxicillin, and the correspondent zoom.

Comparing *Figures 4.9* and *5.1* it can be seen a clear process optimization using the cascade system. After 35 h (25 vols) a purity and a yield of 99.65% and 97.86%, respectively, was achieved in opposite to 99.99% purity and 33% yield using a single stage system. A purity of 99.99% with a yield of 94.24% can be obtained but a diafiltration time of 92 h (69 vols) would be necessary, which would not be sustainable.

The effect of the recycle ratio (Rc) was also study in detail. As mentioned before, Rc is an independent variable that can be controlled using the back-pressure regulators, and its value can be adjusted from zero to as high as the membrane can withstand.

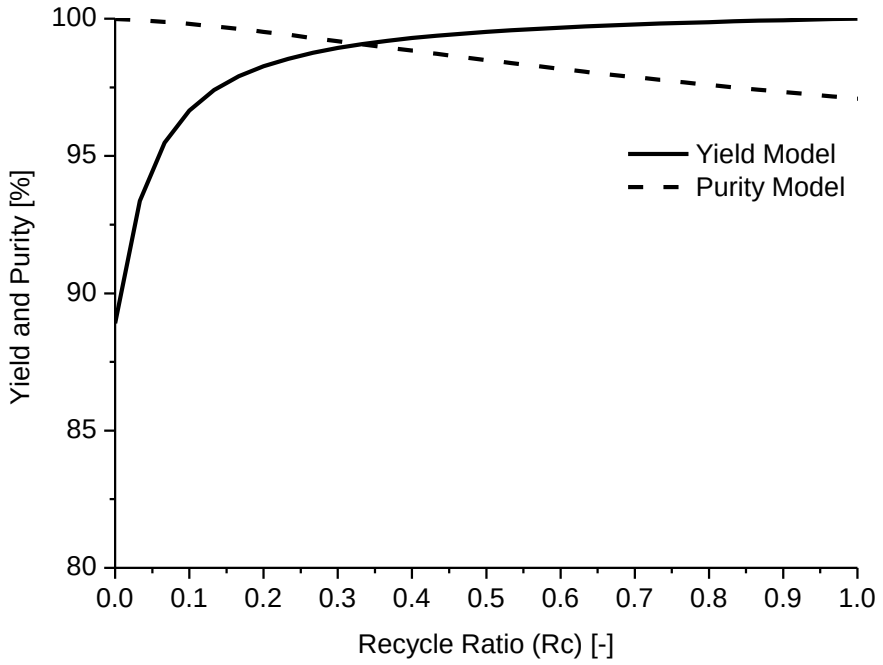

Figure 5.2 – Modeled effect of recycle ratio, Rc, on the API yield and purity of amoxicillin in a two-stage cascade after 35 h (25 vols) obtained using MATLAB®.

From *Figure 5.2* it can be seen that the Rc parameter has a significant impact in the purity and yield. Increasing the Rc will increase the API yield but inevitably decrease the purity.

Without recycling, the compounds that permeate through the first stage would accumulate in the second stage over time. Then, as the concentrations in the second stage increase, both compounds start to permeate the second membrane identically to the single-stage process, and the absolute mass loss increases accordingly. The reason for the dramatic improvement in yield with increasing the Rc is that the concentration of the compounds in the second stage is low, thus minimizing the yield loss through the second membrane. On the other hand, the purity decreased significantly with increasing Rc. When working with only a 10 p.p difference between rejections, more impurity is retained in the retentate stream and therefore its concentration in the feed tank will increase with the Rc. In addition, when increasing the Rc the concentration in the second stage is minimized slowing down the impurity removal rate (Kim J.and livingston, 2013). Therefore, two-stage system takes more time/vols to achieve the same purity as single-stage.

4.4.2 Continuous mode

The main goal was to incorporate this separation step in a continuous industrial process. Two different configurations were studied in detail and will be explained in more detail in the next sub-sections. In both configurations, it was considered that a continuous flow of the feed to be purified was pumped to the feed tank and the purified stream would come out of the feed tank as well; the permeate stream was fed to the next stage. A mathematical model describing the two different configurations was developed and used for preliminary selection of operational parameters. In sub-section 3.2.2 the two configurations schemes are described as well as the correspondent mathematical equations; both configurations are an adaptation of the semi-batch two-stage cascade system presented in the previous sub-section.

The effect of various parameters, such as the flow rate of the feed into the tank and the effective pressure in each stage, was proved to be of great importance to the separation process. In addition, as expected, two very important parameters were also important the Rc and the feed utilization ratio, FU, both defined in the in sub-section 3.2.2.

4.4.2.1 Configuration I

In configuration I, all the retentate streams from both stages are recycle back to the feed tank (scheme and mathematical equations presented in sub-section 3.2.2.1). To understand the critical parameters and optimal conditions to work a system characterization was performed. Parameters such as the flow rate of the feed into the feed tank, the difference between the effective pressure of the two stages, the Rc and the FU were study in detail. The FU ratio parameter it is dependent on the feed flow rate and the purified feed flow rate used in the system.

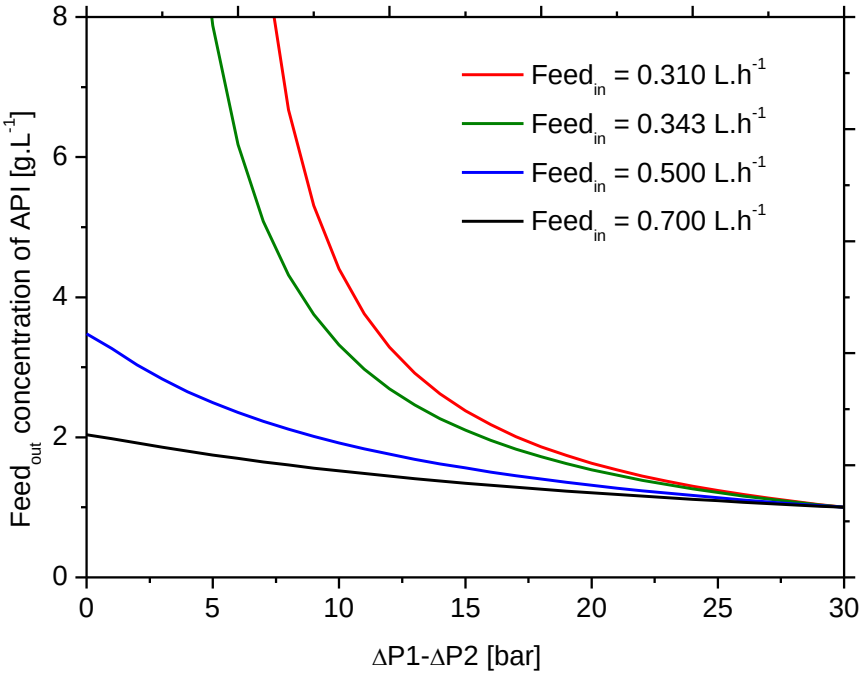

Figure 5.3 – Concentration profile of the API in the purified outlet stream ($Feed_{out}$) obtained using MATLAB®, considering a ΔP1 of 30 bar and varying the feed flow rate ($Feed_{in}$) and the effective pressure of the second stage (ΔP2) parameters. A permeability of 2.14 L.m^{-2}.h^{-1}.bar, an API rejection of 99.12% and an impurity rejection of 87.80% were used based on the TNFN-DL-E membrane trials.

From *Figure 5.3* it can be seen that the $Feed_{in}$ and the difference between the stages effective pressures are critical parameters to the process. The amoxicillin concentration in the purified stream increases with the decrease of the difference between stage pressures. A pressure lower or equal to 10 bar is necessary to obtain suitable concentrations of the API in the purified stream (which means a minimum pressure of 20 bar in the second stage). It was also observed an increase in the amoxicillin concentration in the purified stream ($Feed_{out}$) with the decrease in the $Feed_{in}$. With a feed flow rate of 0.700 L.h^{-1} the maximum API concentration obtained was approximately of 2 g.L^{-1}. When decreasing

to a feed flow rate of 0.343 $g.L^{-1}$ or higher was obtain a concentration equal or even higher to 8 $g.L^{-1}$. Concentrations higher than 8$g.L^{-1}$ were not presented in the graph since the solubility of API at the assumed conditions are 8 $g.L^{-1}$.

The purity and yield profiles were analyzed varying the difference between stage effective pressures and the feed flow rate.

A)

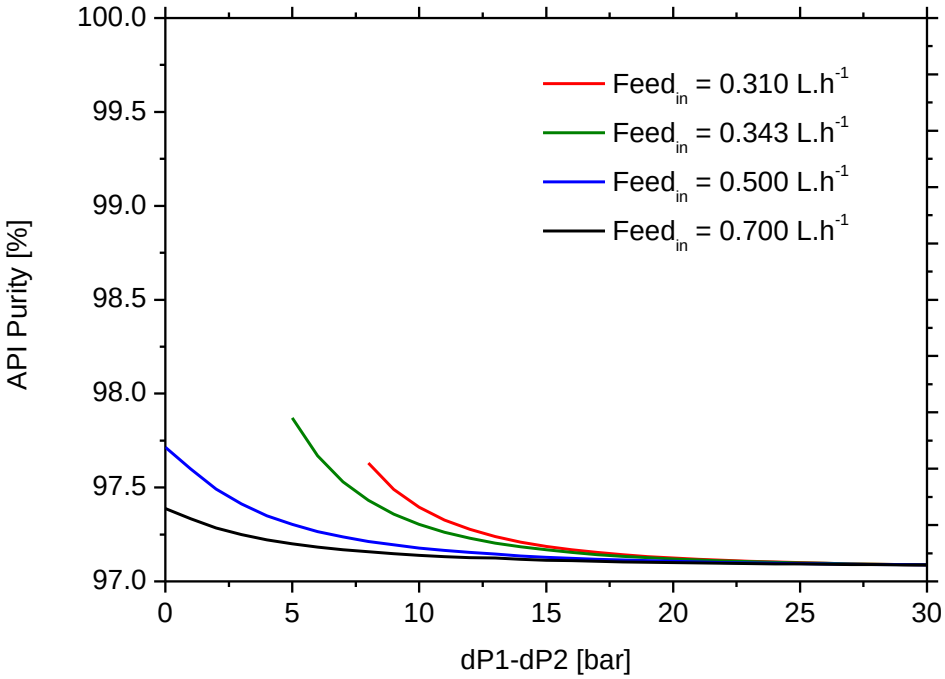

B)

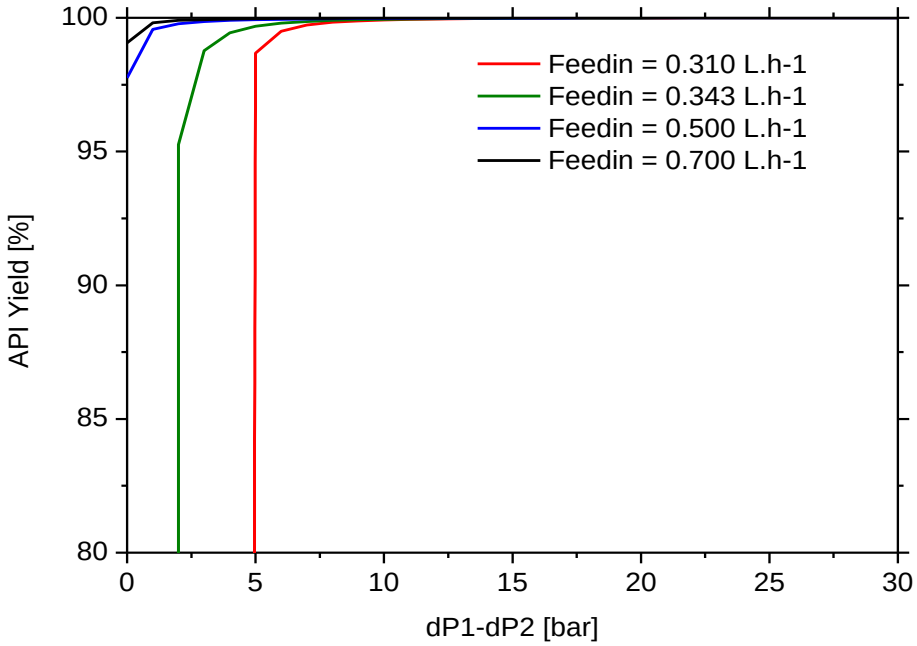

Figure 5.4 – Purity (figure A) and yield (figure B) profiles of the API in the purified outlet stream ($Feed_{out}$) obtained using MATLAB®, considering a ΔP1 of 30 bar and varying the feed flow rate ($Feed_{in}$) and the effective pressure of the second stage (ΔP2) parameters. A permeability of 2.14 $L.m^{-2}.h^{-1}.bar$, an API rejection of 99.12% and an impurity rejection of 87.80% were used based on the TNFN-DL-E membrane trials.

Figure 5.4 shows that the highest API purity does not correspond to the lowest feed flow rate due to the solubility limit restriction. As observed in *Figure 5.3,* the tendency for better results when decreasing the difference between stages effective pressure was maintained.

As expected the API yield profile follows the opposite trend of the purity profile, decreasing significantly with the decrease in the difference between stage pressures. The lower the $Feed_{in}$ the higher pressure difference can be used without compromising in a great extent the purity. Nevertheless, in terms of yield the pressure conditions need further investigation.

The Rc and feed utilization parameters (FU) profiles were also investigated.

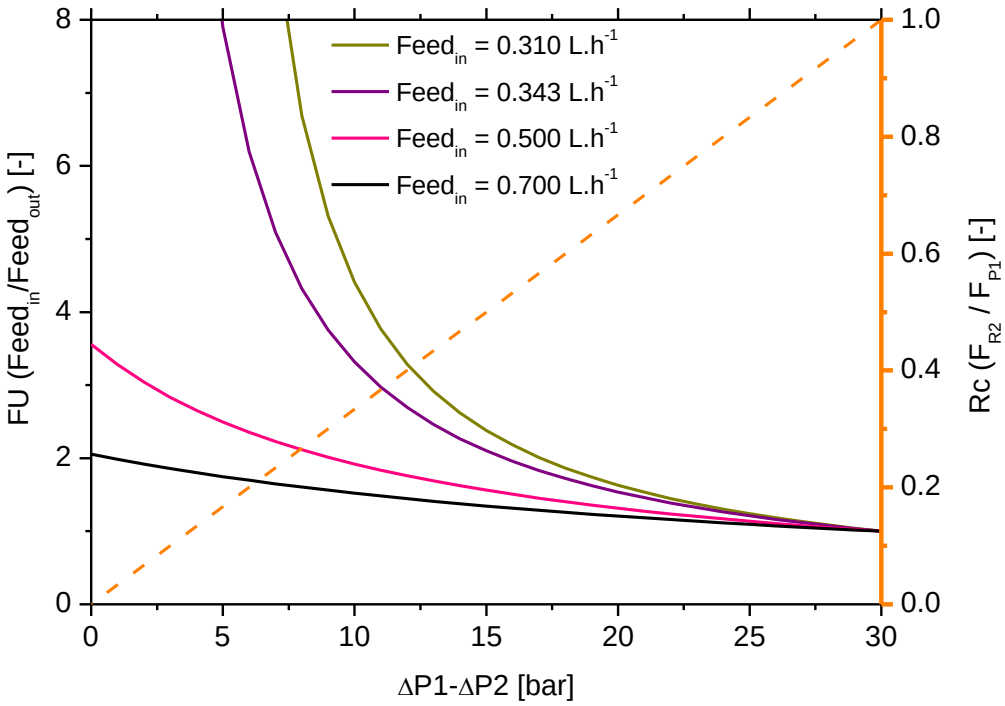

Figure 5.5 – Behavior of the feed utilization (FU) and Recycle ratio (Rc) with the difference of effective pressure between the two stages (ΔP1-ΔP2) obtained using MATLAB®. A ΔP1 of 30 bar, permeability of 2.14 L.m^{-2}.h^{-1}.bar, an API rejection of 99.12% and an impurity rejection of 87.80% were used based on the TNFN-DL-E membrane trials.

In the *Figure 5.5* it is represented the profiles of FU (read in the left Y axis) and Rc (read in the right Y axis) as a function of the difference between the stage pressures. The FU increases with the decrease in the difference between stage pressures and in the $Feed_{in}$. Therefore, to achieve higher concentrations of the API in the purified out stream, higher FU are necessary. This means that more feed is necessary to be kept in the system for the process to run effectively and will correspond to a lower quantity of solution coming out as purified stream.

The profile of the Rc was also studied and since this parameter is independent of the $Feed_{in}$, it was only represented one profile curve in *Figure 5.5*. The Rc has the opposite tendency comparing to the FU, it decreases when decreasing the difference between the stage pressures. Therefore, to have higher concentrations of API in the $Feed_{out}$, low Rcs are necessary, as observed in the previous semi-batch two stages configuration. Since both compounds have a high rejection with the TFNF-DL membrane (only 10 p.p. difference), the separation is not so effective and more impurity is kept in the system when increasing the Rc, as explained in sub-section 4.4.1.2. The Rc and FU are directly related since both are dependent of the effective pressure in the second stage and this has to be considered.

From *Figure 5.3*, *5.4* and 5.5 it was possible to understand the relevant parameters and the limitations of the configuration. A number of simulations with MATLAB® using different combination of parameters are presented in *Table 5.1* to evaluate the most suitable combination of parameters in order to perform the purification process.

Table 5.1 - Values for independent and dependent variables, obtained using MATLAB®, in order to optimize the conditions (considering a permeability of 2.14 $L.m^{-2}.h^{-1}.bar$, an API rejection of 99.12% and an impurity rejection of 87.80%). Boundary condition established: API maximum concentration = 8 $g.L^{-1}$.

Independent Variables			Dependent Variables					
ΔP1 [bar]	ΔP2 [bar]	$Feed_{in}$ [$L.h^{-1}$]	API $C_{Feedout}$ [$g.L^{-1}$]	Impurity $C_{Feedout}$ [$g.L^{-1}$]	API Purity [%]	API Yield [%]	FU [-]	Rc [-]
30	22	0.310	6.68	0.16	97.63	99.83	6.69	0.27
30	23	0.310	9.00	0.20	97.84	99.73	9.02	0.23
30	**25**	**0.343**	**7.88**	**0.17**	**97.87**	**99.68**	**7.90**	**0.17**
30	26	0.343	10.86	0.20	98.17	99.43	10.92	0.13
30	29	0.500	3.27	0.08	97.60	99.56	3.28	0.03
30	29	0.700	1.98	0.05	97.33	99.81	1.99	0.03

From *Table 5.1* it can be identified the optimal process parameters taking into account the restrictions and conditions established. The values marked in red were excluded since the API concentration in the purified out stream was above the amoxicillin solubility limit. The best parameters combination was obtained using a feed flow rate of 0.343 $L.h^{-1}$, a 30 bar effective pressure for the first stage and 25 bar in the second stage, obtaining a purity of 97.87% and a yield very close to 100%. As expected, the Rc a small value of 0.17 and the FU had a significant high value of approximately 8. Nevertheless, it can also be notice that FU has the same values as the API $Feed_{out}$ concentration (FU ≈ $C_{Feedout}$.).

Establishing the optimal process parameters, Concentration profile of API and impurity as well as the yield and purity for API were simulated and are represented in *Figures 5.6* and *5.7*.

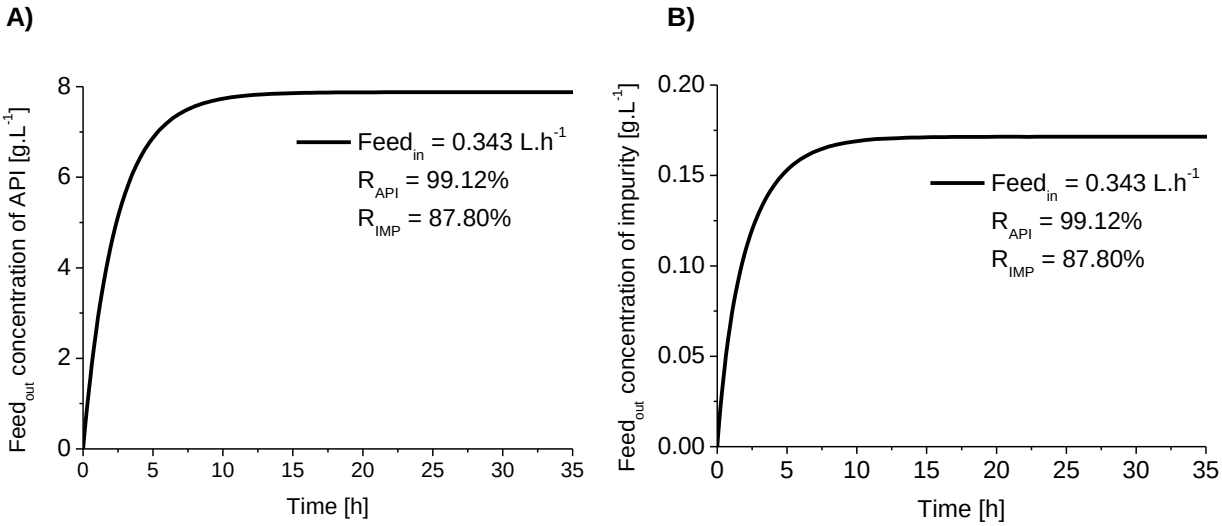

Figure 5.6 – Concentrations in the purified stream over time (h) obtained using MATLAB®: A) API profile; B) Impurity profile Parameters considered: ΔP1= 30 bar; ΔP2= 25 bar; $Feed_{in}$ = 0.343 $L.m^{-2}.h^{-1}$ and a permeability of 2.14 $L.m^{-2}.h^{-1}.bar$. The recycle ratio and the feed utilization of the systems are respectively Rc= 0.17 and FU= 7.90 (vide *Table 5.1*).

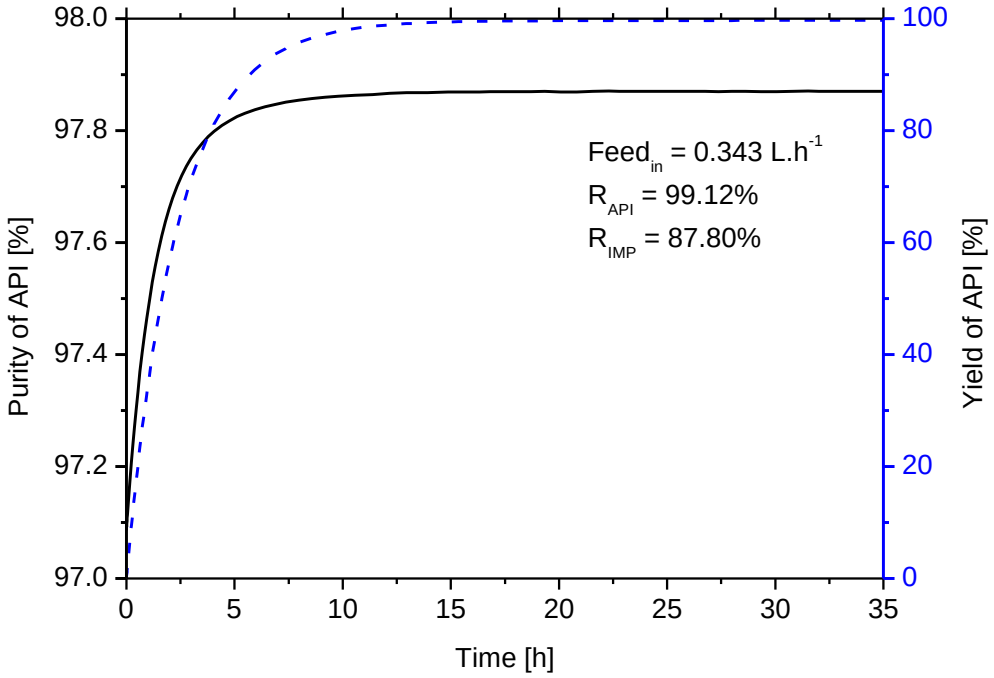

Figure 5.7 – Profiles of the API purity and yield obtained using MATLAB®. Parameters considered: ΔP1= 30 bar; ΔP2= 25 bar; Feed$_{in}$ = 0.343 L.m^{-2}.h^{-1} and a permeability of 2.14 L.m^{-2}.h^{-1}.bar. The recycle ratio and the feed utilization of the systems are respectively Rc= 0.17 and FU= 7.90 (vide *Table 4.9*).

In less than 35 h (25 vols) it was achieved an amoxicillin purity of 97.80% (read in the left Y axis) with a workable yield of approximately 98% (read in the right Y axis), from an initial API purity of 97.09%. The purity obtained does not yet reach the initial goal of 99.70% purity (3 ppm of impurity in the solution).

Restrictions in terms of the similarity in the rejection of solutes and API solubility limits are detrimental factors hindering a higher success in the purification process. Therefore, other configurations were studied to possibly achieve better results.

An increase from two to three stages was performed and analyzed in steady state using MS Excel Solver^{TM}. Considering the results obtained in the TFNF-DL-.E trial (a permeability of 2.14 L.m^{-2}.h^{-1}.bar, an API rejection of 99.12%, an impurity rejection of 87.80% and considering an effective pressure of 30 bar for the first stage) it was obtained a higher API yield of 99% but the API purity dropped to 97.45% considering a lower feed flow rate of 0.247 L.h^{-1}.

Since the solute rejections were both very high, a high percentage of the impurity was being retained in the membrane as well. Therefore, it was thought that the recycle of the retentate streams back to the feed tank could be a configuration impediment to achieve higher purities. A change in configuration was considered and different options were study. A configuration where instead of recycling the retentate streams back to the feed tank these were recycled directly into the feed of the first stage (Feed$_{cell}$ represented in the configurations shemes). Simulations in steady state using MS Excel Solver^{TM} were performed and the results shown no improvement in the purity of the product. Considering the results obtained for the TFNF-DL-.E trial (a permeability of 2.14 L.m^{-2}.h^{-1}.bar, an API rejection of 99.12%, an impurity rejection of 87.80% and considering an effective pressure of 30 bar for the first stage) using a feed flow rate of 0.200 L.h^{-1}, was obtained a higher API purity of 97.99% but the API yield dropped to 92.99%. Higher purities could be obtained but with a pronounced drop in the product yield. For instance to obtain a purity of 99.32% the yield would correspond to 48.84%. Finally it was thought to recycle the permeate streams, instead of the retentate streams, because impurity concentration is lower (see sub-section 3.2.2.2). Being the first stage the main responsible for the separation itself and since this stream switch would have a negative effect in the API yield (the retentate has higher concentrations of the API), it was thought to switch only the retentate and permeate streams of the second stage. The promising results from this configuration are discussed in the next sub-section.

4.4.2.2 Configuration II

In configuration II, the permeate stream from the second stage was recycled back to the feed tank instead of the retentate stream (configuration and mathematical equations presented in sub-section 3.2.2.2). To understand the critical parameters and optimal conditions to work in this configuration a system characterization was performed. Parameters such as the $Feed_{in}$, the difference between the effective pressure of the two stages and, the Rc and the FU were studied in detail.

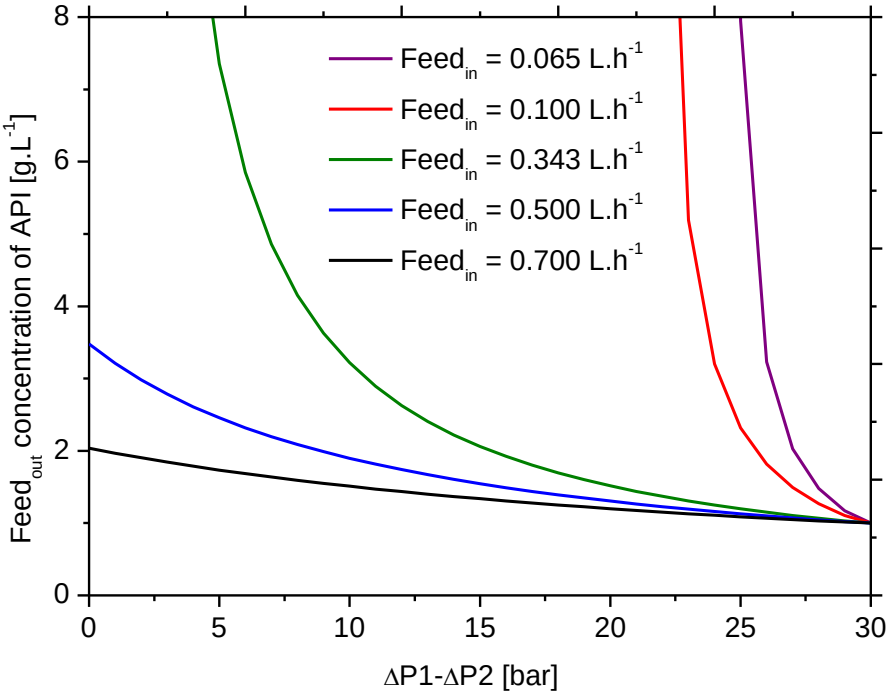

Figure 5.8 – Concentration profile of the API in the $Feed_{out}$ obtained using MATLAB®, considering a ΔP1 of 30 bar and varying the $Feed_{in}$ and ΔP2 parameters. A permeability of 2.14 L.m^{-2}.h^{-1}.bar, an API rejection of 99.12% and an impurity rejection of 87.80% were considered.

From *Figure 5.8* it can be seen that the $Feed_{in}$ and the difference between the stages pressures are critical parameters to the process. The amoxicillin concentration in the purified stream increases with the decrease of the difference between stage pressures. Depending on the feed flow rate, the optimal difference between stages effective pressure changes significantly. When considering feed flow rates equal or higher than 0.343 L.h^{-1} the difference in pressure should not be higher than 7 bar, but when considering lowest feed flow rates the difference in pressures could be between 22 and 27 bar. It was also observed an increase in the amoxicillin concentration in the purified stream with the decrease of the $Feed_{in}$. Considering a feed flow rate of 0.700 L.h^{-1} the maximum API concentration obtained was approximately of 2 g.L^{-1}. When decreasing to a flow rate of 0.100 g.L^{-1} or lowest it was possible to obtain concentration around 8 g.L^{-1} (we cannot go higher than this value). Higher concentrations that 8g.L^{-1} are not presented in the figure since cannot be obtained due to the API solubility limit in the considered conditions.

The purity and yield profiles were analyzed varying the difference between stage effective pressures and the feed flow rate.

A)

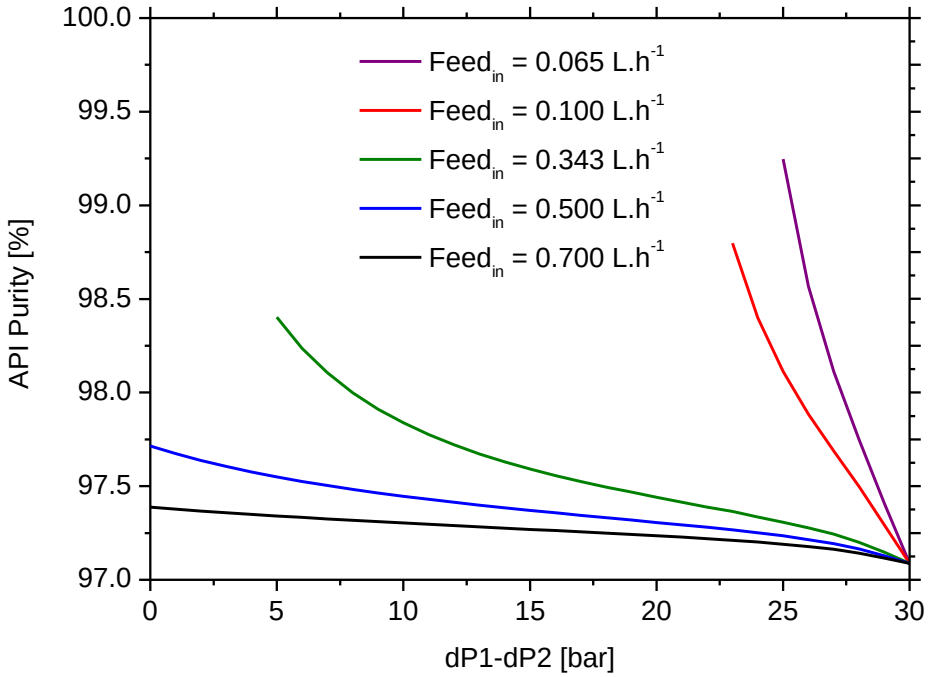

B)

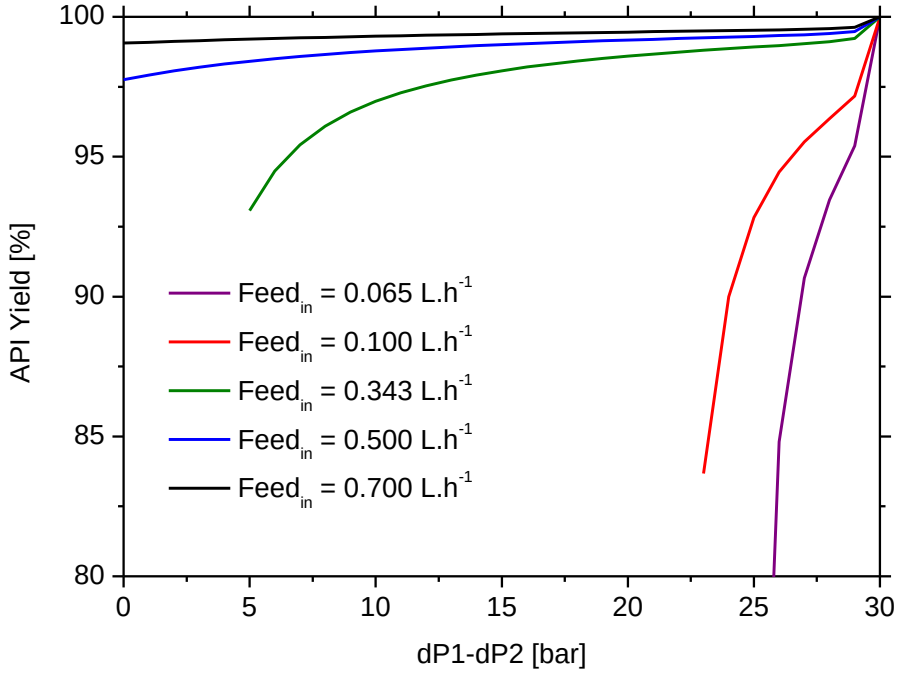

Figure 5.9 – Purity (figure A) and yield (figure B) profiles of the API in the purified out stream ($Feed_{out}$) obtained using MATLAB®, considering a ΔP1 of 30 bar and varying the feed flow rate ($Feed_{in}$) and the effective pressure of the second stage (ΔP2) parameters. A permeability of 2.14 $L.m^{-2}.h^{-1}.bar$, an API rejection of 99.12% and an impurity rejection of 87.80% were used based on the TNFN-DL-E membrane trials.

From *Figure 5.9* it can be seen that the highest API purity corresponds to the lowest feed flow rate. As observed in *Figure 5.8*, the feed flow rate and the effective pressure difference between stages have a considerable impact in the purity and yield results. The API yield profile follows the opposite trend to the purity, decreasing significantly with the decrease in the difference between stage pressures. With lowest feed flow rates it was possible to obtained better purification results, but to be sustainable in terms of yield the pressure conditions have to be carefully chosen. With this configuration, the API yield is much more affected comparing with the previous configuration, especially when working with lower feed flow rates.

The Rc and FU parameters profiles were also investigated and are represented in *Figure 6.1*.

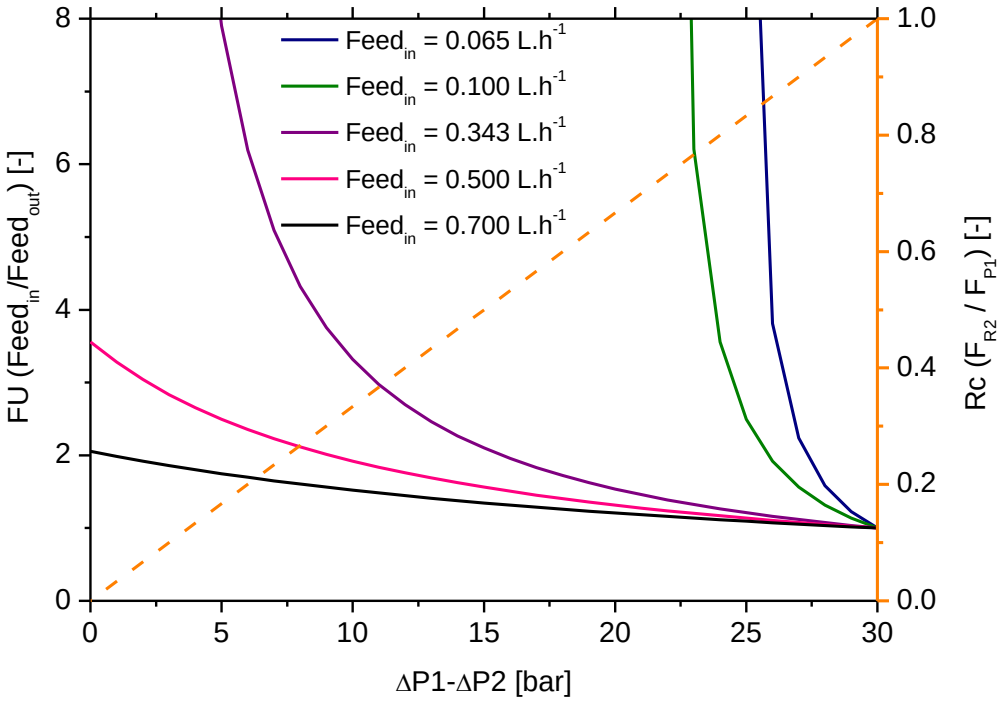

Figure 6.1 – Behavior of the feed utilization (FU) and recycle ratio (Rc) with the difference of effective pressure between the two stages (ΔP1-ΔP2) obtained using MATLAB®. A ΔP1 of 30 bar, permeability of 2.14 L.m^{-2}.h^{-1}.bar, an API rejection of 99.12% and an impurity rejection of 87.80% were considered.

Figure 6.1 shows the profiles of the FU (read in the left Y axis) and the Rc (read in the right Y axis) with the difference between the stages effective pressures. The FU increases with the decrease in the difference between stage pressures and by decreasing the Feed$_{in}$. This means that to have higher concentrations of the API in the purified stream higher FU is necessary. As in configuration I, lower quantities of solution will be coming out as purified stream due to this high FU by the system.

The profile of the Rc was also studied and since this parameter is independent of the Feed$_{in}$, only one profile curve is presented in *Figure 6.1*. The Rc has the opposite tendency comparing to FU it decreases when decreasing the difference between the stage pressures. But unlike configuration I, depending on the feed flow rate considered, the optimal value for the recycle ratio is significantly different. When considering feed flow rates equal or higher than 0.343 L.h^{-1} the Rc should not be higher than 0.2, but when considering lower feed flow rates the optimal values for the Rc are between 0.7 and 0.9.

From *Figure 5.8*, *5.9* and 6.1 it was possible to understand the relevant parameters and the limitations of the configuration. A number of simulations with MATLAB® using different combination of parameters are presented in *Table 5.2* to evaluate the most suitable combination of parameters in order to perform the purification process.

Table 5.2 - Values for independent and dependent variables, obtained using MATLAB®, in order to optimize the conditions (considering a permeability of 2.14 L.m^{-2}.h^{-1}.bar, an API rejection of 99.12% and an impurity rejection of 87.80%). Boundary condition established: API maximum concentration = 8 g.L^{-1}.

Independent Variables			Dependent Variables					
ΔP1 [bar]	ΔP2 [bar]	Feed$_{in}$ [L.h^{-1}]	API C$_{Feedout}$ [g.L^{-1}]	Impurity C$_{Feedout}$ [g.L^{-1}]	API Purity [%]	API Yield [%]	FU [-]	Rc [-]
30	24	0.065	32685.05[a]	0.09	100.00	347165.47[a]	0.00[b]	0.80
30	25	0.065	7.95	0.06	99.25	62.13	12.80	0.83
30	22	0.100	13.73	0.08	99.41	56.66	24.22	0.73
30	23	0.100	5.19	0.06	98.80	83.68	6.21	0.77
30	4	0.343	9.90	0.14	98.62	90.67	10.92	0.13
30	**5**	**0.343**	**7.36**	**0.12**	**98.40**	**93.07**	**7.90**	**0.17**
30	1	0.500	3.21	0.08	97.67	97.92	3.28	0.03
30	1	0.700	1.97	0.05	97.38	99.09	1.99	0.03

a Values considering FU=0 but in reality FU<0 which will implicate a negative concentration in the Feed$_{out}$ stream (verified using steady state).
b. Negative values (in the MATLAB code was defined to take the value 0)

From *Table 5.2* it can be identified the optimal process parameters taking into account the restrictions and conditions established. The values marked in red were excluded since the API concentration in the purified out stream was above the amoxicillin solubility limit. The best API purity obtained was 99.25% but since the API yield has a poor value of 62.13% this result was also discarded. Considering a 30 bar effective pressure for the first stage and 5 bar in the second stage and a feed flow rate of 0.343 L.h^{-1}, a purity of 98.40% with a satisfactory yield of 93.07% was achieved. As mentioned before, a lost in yield was expected but the trade-of between purity and yield has to be balance to obtain a suitable process. For the same conditions (Feed$_{in}$ = 0.343 L.h^{-1}) the FU had a significant high value of approximately 8 and the recycle ratio a small value of 0.17, as observed in the previous configuration I.

Establishing the optimal process parameters, the concentration purity and yield profiles were simulated in MATLAB® and are represented in the *Figures 6.2* and *6.3*.

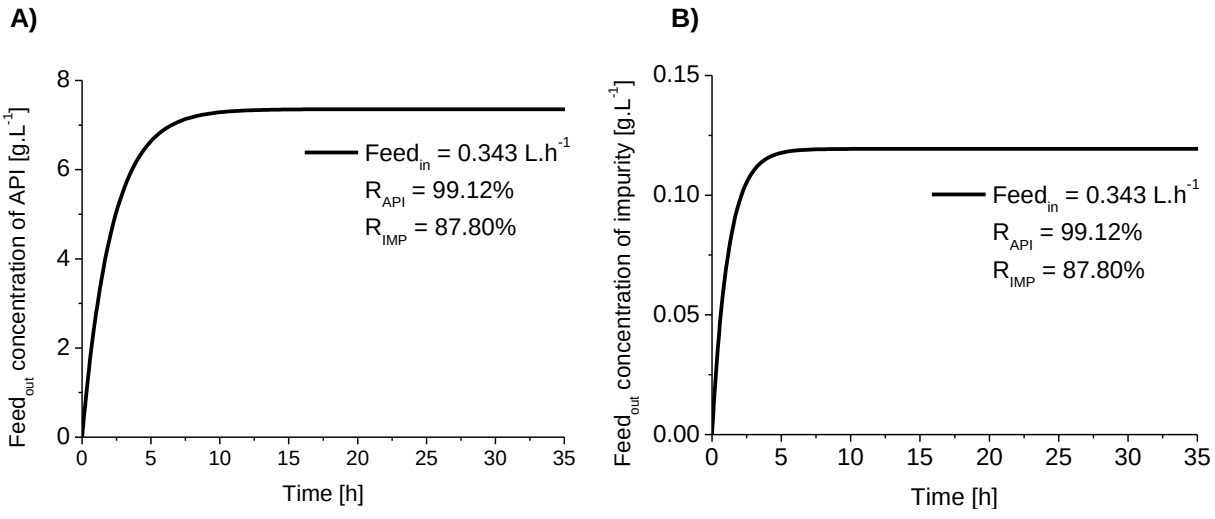

Figure 6.2 – Concentrations in the purified stream over time (h) obtained using MATLAB®: A) API profile; B) Impurity profile. Parameters considered: ΔP1= 30 bar; ΔP2= 5 bar; Feed$_{in}$ = 0.343 L.m^{-2}.h^{-1} and a permeability of 2.14 L.m^{-2}.h^{-1}.bar. The recycle ratio and the feed utilization of the systems are respectively Rc= 0.17 and FU= 7.90 (vide *Table 5.2*).

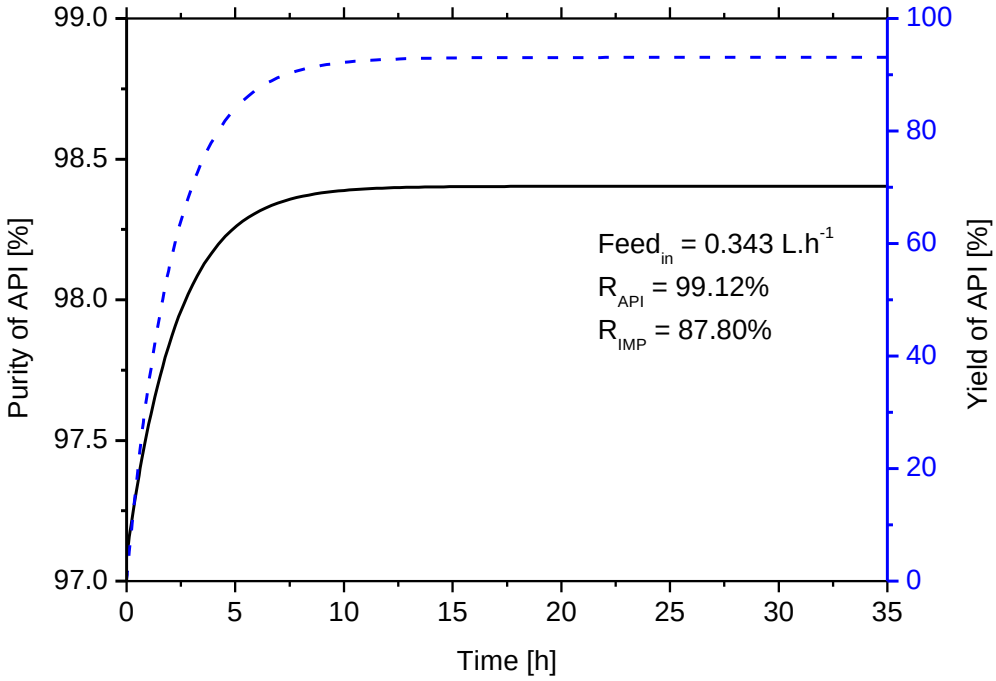

Figure 6.3 – Profiles of the API purity and yield obtained using MATLAB®. Parameters considered: ΔP1= 30 bar; ΔP2= 5 bar; Feed$_{in}$ = 0.343 L.m^{-2}.h^{-1} and a permeability of 2.14 L.m^{-2}.h^{-1}.bar. The recycle ratio and the feed utilization of the systems are respectively Rc= 0.17 and FU= 7.90 (vide *Table 4.9*).

In less than 35 h (25 vols), from an initial API purity of 97.09%, a purity of 98.40% (read in the left Y axis) was achieved with a workable yield of 93.07% (read in the right Y axis). The purity obtained was closer to the initial goal of 99.70% purity (3 ppm of impurity in the solution) but the loss in product was 5 p.p. higher comparing with the previous configuration I.

An increase from two to three stages was performed and analyzed in steady state using MS Excel Solver™ to see if it was possible to achieve better results especially in terms of API yield. Due to the API yield limitations referenced before, in the three stage cascade only the last retentate stream from the third stage was switched with the permeate stream, being this one recycled back to the feed tank (configuration and mathematical equations presented in sub-section 3.2.2.2). The simulation of the different parameters is presented in *Table 5.3*.

Table 5.3 - Values for independent and dependent variables, obtained using MS Excel Solver™, in order to optimize the conditions (considering a permeability of 2.14 L.m^{-2}.h^{-1}.bar, an API rejection of 99.12% and an impurity rejection of 87.80%). Boundary condition established: API maximum concentration = 8 g.L^{-1}.

Independent Variables				Dependent Variables						
ΔP1 [bar]	**ΔP2 [bar]**	**ΔP3 [bar]**	**Feed$_{in}$ [L.h^{-1}]**	**API $C_{Feedout}$ [g.L^{-1}]**	**Impurity $C_{Feedout}$ [g.L^{-1}]**	**API Purity [%]**	**API Yield [%]**	**FU [-]**	**Rc Stage 2 [-]**	**Rc Stage 3 [-]**
30	25	20	0.065	12.47	0.64	99.05	97.42	12.8	0.17	0.8
30	15	10	0.065	12.72	0.22	98.31	99.44	12.8	0.5	0.67
30	10	5	0.065	12.76	0.27	97.96	99.72	12.8	0.67	0.5
30	**25**	**20**	**0.069**	**7.49**	**0.12**	**98.65**	**98.54**	**7.59**	**0.17**	**0.8**
30	15	10	0.069	7.58	0.16	97.93	99.69	7.6	0.5	0.67
30	5	10	0.069	7.59	0.18	97.65	99.84	7.6	0.67	0.5
30	25	20	0.100	2.49	0.06	97.7	99.67	2.5	0.17	0.8
30	15	10	0.100	2.49	0.07	97.33	99.93	2.5	0.5	0.67
30	10	5	0.100	2.49	0.07	97.24	99.96	2.5	0.67	0.5
30	25	20	0.343	1.21	0.03	97.19	99.95	1.2	0.17	0.8
30	15	10	0.343	1.21	0.04	97.12	99.99	1.2	0.5	0.67
30	10	5	0.343	1.21	0.04	97.11	99.99	1.2	0.67	0.5
30	25	20	0.500	1.14	0.03	97.16	99.96	1.1	0.17	0.8
30	15	10	0.500	1.14	0.03	97.11	99.99	1.1	0.5	0.67
30	10	5	0.500	1.14	0.03	97.1	99.99	1.1	0.67	0.5
30	25	20	0.700	1.09	0.03	97.14	99.99	1.1	0.17	0.8
30	15	10	0.700	1.09	0.03	97.1	99.99	1.1	0.5	0.67
30	10	5	0.700	1.09	0.03	97.09	99.99	1.1	0.67	0.5

From *Table 5.3* it can be seen that the separation process could be improved with a three stage cascade system but in very limited conditions. Once again the values marked in red were excluded due to solubility limit restrictions. Considering a 30 bar effective pressure in for the first stage, a 25 bar in the second stage, a 20 bar in the third stage and a feed flow rate of 0.069 L.h^{-1} it was possible to obtain a purity of 98.65% with a yield of 98.65%. With this increase in the number of stages the API purity increased but more important an increase in almost 6 p.p. of the API yield was achieved.

This increase in the number of stages cannot be generalized since it will deeply depend on the configuration considered. Even with this third stage continuous configuration other possible switches of permeate and retentate streams are possible to be made and their study could show an improvement or not in the process purification. As observed in configuration I (sub-section 4.4.2.1) the increase in the number of stages it is not always favorable in this study case.

4.4.3 Process modelling conclusion

The performance of the different system configurations used to purify the model mixture of amoxicillin and 4-hidroxy-L-phenylglycine using TFNF-DL membrane is summarized in *Table 5.4*.

Table 5.4 - Comparison between the performances of the different systems configurations described previously. A permeability of 2.14 L.m^{-2}.h^{-1}.bar, an API rejection of 99.12% and an impurity rejection of 87.80% were considered.

System configuration	Conditions	Purity [%]	Yield [%]	FU [-]	Rc stage 2 [-]	Rc stage 3 [-]
Semi-batch single stage	ΔP1 = 30 bar	99.99	33.00	-	-	-
Semi-batch two stage	ΔP1 = 30 bar ΔP2 = 25 bar	**99.65**	**97.86**	**-**	**0.17**	-
Continuous two stage - configuration I	ΔP1 = 30 bar ΔP2 = 25 bar, $Feed_{in}$ = 0.343 L.h^{-1}	97.87	99.68	7.9	0.17	-
Continuous two stage - configuration II	ΔP1 = 30 bar ΔP2 = 5 bar $Feed_{in}$ = 0.343 L.h^{-1}	98.4	93.07	7.9	0.17	-
Continuous three stage - configuration II	ΔP1 = 30 bar ΔP2 = 25 bar ΔP3 = 20 bar $Feed_{in}$ = 0.343 L.h^{-1}	97.19	99.95	1.2	0.17	0.8
	ΔP1 = 30 bar ΔP2 = 25 bar ΔP3 = 20 bar $Feed_{in}$ = 0.069 L.h^{-1}	**98.65**	**98.54**	**7.6**	**0.17**	**0.8**

It can be concluded that the semi-batch two stage membrane system configuration was the one with better purity and yield results from all of the configurations proposed, achieving a 99.65% purity with a 97.86% in yield.

In all configurations it was observed a big trade-off between purity and yield. The key to a suitable process is to balance both parameters to achieve a considerable high purity with a suitable loss of yield. By changing the process configuration or by adding more stages to the cascade system it was possible to decrease the influence of this trade-off in the continuous configurations. It is important to notice that the increase in the number of stages does not always improves this separation, it dependents on the configuration considered. More investigation should be performed in this area to have a more general conclusion.

High FU and low Rc are required, which is not the ideal for a cascade system and can bring several limitations to the separation process in terms of flow rate of the purified out stream and loss of product due to concentration polarization problems in the membrane.

CHAPTER V

CONCLUSION REMARKS AND FUTURE WORK

OSN processes attracted a lot of attention as an alternative process for purification of APIs. This separation process offers unique advantages over conventional separation methods such as mild temperatures and can be employed for thermolabile compounds like APIs. In addition, it is energy efficient and can be also used for solvent recovery. This work had the objective to explore the potential of membrane technology in the amoxicillin antibiotic purification from the enzymatic synthesis sub-product 4-hidroxy-L-phenylglycine with an initial concentration of 30 ppm (97.09% purity) to a value equal or less than 3 ppm (99.70 % purity).

Characterization studies of the main product were conducted. Solubility and stability studies were performed in order to choose the most suitable solvent. From four different solvents tested in detail, water was the one presenting better results and therefore the solvent used in the following studies. The API showed to be a labile compound to work with because of the low solubility and the fast decomposition solvents tested. A dissociation study was also performed for both compounds and from this analysis a route to explore the dissociation as a function of pH could be implemented in the process optimization. A basic pH of approximately 9 was thought to be the most promising pH condition to perform the filtration experiments.

A membrane screening using dead-end and m-CSTR measurements was performed varying the pressure (10, 20 and 30 bar) and pH (2, 5 and 8.7) parameters in six membrane types (PBI, PI, PEEK, TFNF-DL, M130 and Duramem®200). Higher pressures showed to improve the rejections and fluxes results and the change in the solution pH to a value of 8.7 improved the difference in the rejection of the solutes showing to be a crucial parameter in the process optimization. The best results were obtained using the TFNF-DL membrane (in m-CSTR measurements) at 30 bar and in basic conditions, having an API rejection of 99.12%, an impurity rejection of 87.80% and a flux of 64.4 $L.m^{-2}.h^{-1}$ (2.14 $L.m^{-2}.h^{-1}.bar$). From the screening results one can conclude that the main obstacle for the purification process was the membrane performance itself, with insufficient separation between the compounds (a maximum of 10 p.p. was achieved).

With the results obtained from the membrane screening, it was simulated the behaviour of the separation process using different systems (semi-bath and continuous) and configurations. The membrane cascade configuration improved the separation process but the API solubility limit and the trade-off between purity and yield were serious limitations to the continuous cascade system. Feed flow rate, difference between stages effective pressures, FU and Rc were parameters that showed to have an important effect in the purification process results. High FU and low Rc were necessary conditions to obtain higher purities; nevertheless, further experimental investigation is needed to account for the concentration polarization effects.

A maximum purity of 99.65% with a yield of 97.86% was obtained with the semi-batch two-stage cascade system being really close to the purity goal (99.70%). The application of a continuous configuration showed to be limited and conditioned. The most suitable result was obtained with the configuration II using a three stage cascade system. Implementing a $Feed_{in}$ of 0.069 $L.h^{-1}$ it could be achieved a purity of 98.65% and a yield of 98.56% which is below the initial goal: 99.70%. Therefore it is necessary a more exhaustive investigation in terms of configuration and performed more experimental testes.

With this study it was demonstrated that the amoxicillin purification needs further investigation at different levels. In future works it is important to investigate other alternatives in terms of membrane cascade configuration. In addition, experimental data is required to validate the mathematical models developed in this research work. The amoxicillin precipitation in the membrane cell observed in this work should be carefully studied and taken into account since it could be of great importance in a system implementation and performance. The membrane cascade purification of the API is extremely dependent on the membrane selectivity, and further investigation related to the membrane needs to be performed to have a better resolution between the two compounds. The study of the model mixture and its interaction with the PBI membrane cross-linker could be also an important investigation in order to understand this phenomena and see if it is possible to improve this membrane performance. Being the search of the ideal membrane a very hard goal to achieve, another possible line of work could pass through a molecular manipulation of the molecular weight of one of the compounds using for example ligands (similar to the catalytic techniques). Other techniques such as molecular imprinting method (both API and impurity are very similar which could be an obstacle for using this technique) and zeolites could also be investigated for comparison or even incorporated in the purification process.

CHAPTER VI

REFERENCES

Aerts S., Buekenhoudt A., Weyten H., Gevers L.E.M., Vankelecom I.F.J., Jacobs P. A., (2006) The use of solvent resistant nanofiltration in the recycling of the Co- Jacobsen catalyst in the hydrolytic kinetic resolution (HKR) of epoxides, *Journal of Membrane. Science*, 280, 245–252.

Agrawal, R. & Xu, J. (1996) Gas separation membrane cascades II. Two-compressor cascades. *Journal of Membrane Science*. 112 (2), 129-146.

Alemzadeh, G. B. (2010). Enzymatic Synthesis of Amoxicillin with Immobilized Penicillin G Acylase. Sharif University of Technology.

Arunima Saxena, B. P. (2009). Membrane-based techniques for the separation and purification of proteins:An overview. *Advances in Colloid and Interface Science* 145, 1–22.

Baker, R. W (2004). *Membrane Technology and Applications, 2nd edn.* (pp. ch.1, pp. 1-21). John Wiley and Sons Ltd

Bellona, C. & Drewes, J. E. (2005) The role of membrane surface charge and solute physico-chemical properties in the rejection of organic acids by NF membranes. *Journal of Membrane Science*. 249 (1–2), 227-234.

Benedict, M., Pigford, T. H. & Levi, H. W. (1981) *Nuclear Chemical Engineering.* 2nd edition. , McGraw-Hill.

Bhanushali, D., Kloos, S. & Bhattacharyya, D. (2002) Solute transport in solvent-resistant nanofiltration membranes for non-aqueous systems: experimental results and the role of solute–solvent coupling. *Journal of Membrane Science*. 208 (1–2), 343-359.

Boam, A. & Nozari, A. (2006) Fine chemical: OSN – a lower energy alternative. *Filtration & Separation*. 43 (3), 46-48.

Boeren M., D. P. (s.d.). *Amoxicillin, stability and solubility*. Eurovet Animal Health, Handelsweg, 25, 5531 AE Bladel, the Netherlands.

Bowen W.R., J.S. Welfoot. (2002).*Chemical Engineering Science* (57), 1121-1137.

Bruggink, A. (2001). *Synthesis of β-lactam Antibiotics: Chemistry, Biocatalysis & Process Integration*, Kluwer Academic Publishers.

Cai Shan-Ying, H. C.-Q.-Z. (2003). Chromatographic determination of high-molecular weight impurities in amoxicillin. *Journal of Pharmaceutical and Biomedical Analysis* 31, 589 - 596.

Chandon, P., Kovarski, O., & J. L. (2007). Marketing strategies in the competition between branded and generic antibiotics (A), Clamoxyl in 1996 – Report by INSEAD, France.

Chemical Book. (2008). Obtained in Febuary of 2013, http://www.chemicalbook.com/ProductChemicalPropertiesCB1765553_EN.htm.

Chemical - Buyers. (2012). Obtained in Febuary of 2013, http://www.chemical-buyers.com/cas-324/32462-30-9.html.

Coulson & Richardson's (2002). *Chemical Engineering - Particle Technology and Separation Processes* (5 th ed., Vol. 2). Butterworth Heinemann.

Cuperus, F. P. & Smolders, C. A. (1991) Characterization of UF membranes: Membrane characteristics and characterization techniques. *Advances in Colloid and Interface Science*. 34 (0), 135-173

Daniel J. DeNoon (2012). *The 10 Most Prescribed Drugs: Most-Prescribed Drug List Differs From List of Drugs With Biggest Market Share*. Obtained in August 2013, http://www.webmd.com/news/20110420/the-10-most-prescribed-drugs

Dave Mihalovic (Naturopathic doctor who is specialized in vaccine research, cancer prevention and natural approach to treatment) (2012). *The 7 most prescribed drugs in the world and their natural counterparts*. [Online] Obtained in August of 2013, http://www.balance7.com/the-7-most-prescribed-drugs-in-the-world-and-their-natural-counterparts/.

Dijkstra, M. F. J., Bach, S. & Ebert, K. (2006) A transport model for organophilic nanofiltration. *Journal of Membrane Science*. 286 (1–2), 60-68.

Dunn, P. J., Wells, A. & Williams, M. T. (2010) *Green Chemistry in the Pharmaceutical Industry*. Weinheim, Wiley-VCH.

Elin M. Rundquist, C. J. (2012). Organic solvent nanofiltration: a potencial alternative to distillation for solvent recovery from crystallisation mother liquors. *The Royal Society of Chemistry*, 2197-2205.

Evangelista, F. (1987) Approximate design method for reverse osmosis plants equipped with imperfectly rejecting membranes. *Industrial & Engineering Chemistry Research*. 26 (6), 1109-1116.

Evonik Industries. About DuraMem and PuraMem. Obtained in August of 2013, http://duramem.evonik.com/product/duramem-puramem/en/about/pages/default.aspx.

Falciani M. R. (1979). *Patente N.º 133,442*. Italy.

Ferreira, F. C. (2004). PhD Thesis. *Membrane aromatic recovery system (MARS): theoretical analysis and industrial applications*. Imperial college of London.

Fiona M. MacKenzie Aberdeen (Royal Infirmary, Scotland) (2012). ARPAC *Patterns of Antibiotic Use in European Hospitals*. Obtained in August 2013, http://www.infectiologie.com/site/medias/JNI/2005/CP/cp9-1-mackenzie.pdf

Foulstone, M. (1982). Assay of Amoxicillin and Clavulanic Acid, the components of Augmentin. In Biological Fluids with HPLC, *Ant. Ag. Chem*., Vol.22, (pp. pp. 753-762,).

Francesco Crea, D. C. (2012). Modeling solubility, acid–base properties and activity coefficients of coefficients of amoxicillin, ampicillin and (+)6-aminopenicillanic acid, in NaCl(aq) at different ionic strengths and temperatures. *European Journal of Pharmaceutical Sciences* , 47, 661-677.

Geens, J., Hillen, A., Bettens, B., Van der Bruggen, B. & Vandecasteele, C. (2005) Solute transport in non-aqueous nanofiltration: effect of membrane material. *Journal of Chemical Technology & Biotechnology*. 80 (12), 1371-1377.

Gibbins, E., D'Antonio, M., Nair, D., White, L. S., Freitas dos Santos, L. M., Vankelecom, I. F. J. & Livingston, A. G. (2002) Observations on solvent flux and solute rejection across solvent resistant nanofiltration membranes. *Desalination*. 147 (1–3), 307-313.

Grossman, J. H., & Glenn A. Hardcastle, J. (1975). *Patente N.º 558,763*. Bristol-Myers Company, New York (N.Y).

Guidechem ICP. (2010-2013). Obtained in Febuary of 2013, http://www.guidechem.com/reference/dic-21540.html.

Halle, E. V. & Shacter, J. (2000) Diffusion Separation Methods. In: Anonymous Kirk-Othmer *Encyclopedia of Chemical Technology*. , John Wiley & Sons, Inc.

Hiral Khoda (Pharmacist Lead DH Advisory) (2011). Committee on Antimicrobial Resistance and Healthcare Associated Infection (ARHAI). *European antibiotics awareness day 2011 evaluation – Report.* Obtained in August 2013, https://www.gov.uk/government/publications/european-antibiotic-awareness-day-2011-campaign-evaluation-published

Hwang, S. & Kammermeyer, K. (1965) Operating lines in cascade separation of binary mixtures. The Canadian *Journal of Chemical Engineering*. 43 (1), 36-39.

Hwang, S. T. & Kammermeyer, K. (1975) *Membranes in Separations*. , Wiley.

IMS Health (intelligence applied) (2012). Obtained in August 2013, http://www.imshealth.com.

Infobanc (2009). Obtained in August 2013, http://infobanc.com/market_reports/amoxicillin-export-market-analysis.pdf,DGCIS.

Justin Chun-Te Lin, A. L. (2007). Nanofiltration membrane cascade for continuous solvent exchange. *Chemical Engineering Science*, 2728-2736.

Keurentjes, J. T. F., Linders, L. J. M., Beverloo, W. A. & Van 'T Riet, K. (1992) Membrane cascades for the separation of binary mixtures. *Chemical Engineering Science*. 47 (7), 1561-1568.

Kessels, G. (1993). *Patente N.º 5210288*. Garrucha, Spain

Kim J. F., Freitas da Silva A. M., Valtcheva, I. B. & Livingston, A. G. (2013). When the membrane is not enough: A simplified membrane cascade using Organic Solvent Nanofiltration (OSN). *Separation and Purification Technology 116* , 277–286.

KOCH Membrane Systems Inc. (2013). *KOCH membrane systems*. [Online] Obtained in August of 2013, http://www.kochmembrane.com/Resources/Technical-Documents.aspx

KOCH Membrane Systems Inc. (2013). *KOCH membrane systems*. Obtained in August of 2013,http://www.kochmembrane.com/PDFs/KMS_Amino_Acid_Production_Application.aspx

Krass, A. S. (1983) *Uranium enrichment and nuclear weapon proliferation*. New York, International Publications Service, Taylor & Francis.

La-Scalea M. A., C. M. (2005). Molecular volume calculation using AM1 semi-empirical method toward diffusion coefficients and electrophoretic mobility estimates in aqueous solution. *Journal of Molecular Structure: THEOCHEM 730*, 111–120.

Lai, J. C. (2009). Penicillins: Their Chemical History and Legal Disputes in *New Zealand. Chemistry in New Zealand*, 116-124.

Lightfoot, E. N. (2005) Can Membrane Cascades Replace Chromatography? Adapting Binary Ideal Cascade Theory of Systems of Two Solutes in a Single Solvent. *Separation Science and Technology*. 40 (4), 739-756.

Lightfoot E.N., Root T.W., O'Dell J. L, (2008) *Biotechnol Progr* 24, 599-605.

Lin, J. C. T., Peeva, L. G. & Livingston, A. G. (2006) Separation of pharmaceutical process-related impurities by an organic solvent nanofiltration membrane cascade. *AIChe Annual Meeting*. 2006, San Francisco pp.12-17.

Luciana R.B. Gonçalves, R. L. (2005). Mathematical modeling of batch and semibatch reactors for the enzymic synthesis of amoxicillin. *Process Biochemistry* 40, 247-256, Elsevier Ltd.

Magalhães M.J, Borschiver S. (2012). Amoxicillin and Ampicillin - Import trends and increasing use in Brazil. *Chemistry Today*, Vol. 30(5), 91-98.

Manttari Mika, A. P. (2006). Effect of pH on hydrophilicity and charge and their effect on the filtration efficiency of NF membranes at different pH. *Journal of Membrane Science 280*, 311–320

Maskan, F., Wiley, D. E., Johnston, L. P. M. & Clements, D. J. (2000) Optimal design of reverse osmosis module networks. *AIChE Journal*. 46 (5), 946-954.

McCandless, F. P. (1985) A comparison of some recycle permeators for gas separations. *Journal of Membrane Science*. 24 (1), 15-28.

McCandless, F. P. (1990) Comparison of countercurrent recycle cascades with continuous membrane columns for gas separations. *Industrial & Engineering Chemistry Research*. 29 (10), 2167-2170.

McCandless, F. P. & Herbst, S. (1990) Counter-current recycle membrane cascades for the separation of the boron isotopes in BF3. *Journal of Membrane Science*. 54 (3), 307-319.

Mitesh Shah. J. (2010). Troikaa Pharmaceuticals Ltd. *Report on market survey of azithromycin and amoxicillin with clavulanic acid*. Obtained in August 2013, http://www.slideshare.net/miteshjshah/market-survey-on-azithromycin-and-amoxicillin-with-clavulanic-acid

Morton, J. M. N. (2001). *Phsycochemical Properties of Amoxicillin and Clavulanic Acid*.

Mulder, M. (1996). In *Basic Principles of Membrane Technology 2nd edn.* Kluwer Academic Publications

Mulherkar, P. & Van Reis, R. (2004) Flex test: a fluorescent dextran test for UF membrane characterization. *Journal of Membrane Science*, 236 (1–2), 171-182.

Mullin, J. W. (2001). *Crystallization*, 4th ed.; Butterworth-Heinemann: Oxford

Myerson, A. S. (2002). *Handbook of Industrial Crystallization*, 2nd ed.; Butterworth- Heinemann: Oxford.

Nair D., Scarpello J.T., White L.S., Santos L.M.F.D., Vankelecom I.F.J., A.G.Livingston, (2001) Semi-continuous nanofiltration-coupled Heck reactions as a new approach to improve productivity of homogeneous catalysts, *Tetrahedron Lett*.42, 8219–8222.

Ohno, M., Morisue, T., Ozaki, O. & Miyauchi, T. (1978) Gas Separation Performance of Tapered Cascade with Membrane. *Journal of Nuclear Science and Technology*. 15 (6), 411-420.

Olander, D. R. (1981). The Theory of Uranium Enrichment by Gas Centrifuge. *Progress in Nuclear Energy*, 8, 1-33.

O'Neil, M.J., ed. (2001) The Merck Index, 13th Ed., Whitehouse Station, NJ, Merck & Co., page 96; monograph 582

Peeva, L., Burgal, J. d., Vartak, S., & Livingston, A. G. (2013). Experimental strategies for increasing the catalyst turnover number in a continuous Heck coupling reaction. *Journal of Catalysis (306)*, 190-201.

Peeva L., Gibbins E., Livingston A.G.. (2004). *Journal of Membrane Science,* 236, 121-136.

Peeva, L. & Livingston, A. G. (2004). Effect of concentration polarisation and osmotic pressure on flux in organic solvent nanofiltration. *Journal of Membrane Science 236* , 121–136.

Peng, H. & Tremblay, A. Y. (2008) The selective removal of oil from wastewaters while minimizing concentrate production using a membrane cascade. *Desalination*. 229 (1–3), 318-330.

Perry´s, H. R (1999). *Chemical Engineering Handbook 7th edn.* Mcgraw-Hill companies, Chapter 5, 52-59

Raviña, E. (2011). *The Evolution of Drug Discovery: From Traditional Medicines to Modern Drugs,* John Wiley and Sons Ltd.
Richard Bowen, W. & Doneva, T. A. (2000) Atomic force microscopy studies of nanofiltration membranes: surface morphology, pore size distribution and adhesion. *Desalination*. 129 (2), 163-172.

Roberge D.M, Ducry L.,Bieler N.,Cretton P.,Zimmermann B., (2005). *Chemical Engineering & Technology* 28, 318-323.

Robinson, J. P., Tarleton, E. S., Millington, C. R. & Nijmeijer, A. (2004) Solvent flux through dense polymeric nanofiltration membranes. *Journal of Membrane Science*. 230 (1–2), 29-37.

Rundquist, E. M., Pink, C. J. & Livingston, A. G. (2012) Organic solvent nanofiltration: a potential alternative to distillation for solvent recovery from crystallisation mother liquors. *Green Chemistry*. 14 (8), 2197-2205.

Sabegh, M. A., Rajaei, H., Hezave, A. Z., & Esmaeilzadeh, F. (2012). Amoxicillin Solubility and Supercritical Carbon Dioxide. *Journal of chemical and engineering data* (57), 2750−2755.

Scarpello, J., Nair, D., Santos, L. F., White, L., & Livingston, A.G. (2002). The separation of homogeneous organometallic catalysts using solvent resistant nanofiltration. *Journal of Membrane Science* (203), 71-85.

Screewathanawut I., F. W., Bhole, Y. S., Ormerod, D., Horvath, A., Boam, A. T. & Livingston, A. G. (2010). Demonstration of Molecular Purification in Polar Aprotic Solvents by Organic Solvent Nanofiltration. *Organic Process Research and Development*, 600-611.

See Toh Y.H., Ferreira F.C. & Livingston A.G.. (2007). The influence of membrane formation parameters on thefunctional performance of organic solvent nanofiltration membranes *Journal of Membrane Science* 299(1-2), 236-250.

See Toh, Y. H., Loh, X. X., Li, K., Bismarck, A. & Livingston, A. G. (2007) In search of a standard method for the characterisation of organic solvent nanofiltration membranes. *Journal of Membrane Science*. 291 (1–2), 120-125.

See Toh, Y. H., Silva, M. & Livingston, A. G. (2008) Controlling molecular weight cut-off curves for highly solvent stable organic solvent nanofiltration (OSN) membranes. *Journal of Membrane Science*. 324 (1–2), 220-232.

Shahtalebi A., M. S. (2011). Application of nanofiltration membrane in the separation of amoxicillin from pharmaceutical wastewater. Iran. J. *Environ. Health. Sci. Eng*.,Vol. 8, No. 2, pp. 109-116.

Shaohua Feng, N. S. (2006). Crystallization of Amoxicillin Trihydrate in the Presence of Degradation. *Organic Process Research & Development*, 10, 1212-1218.

Siew W. E., A. G. (2012). Molecular separation with an organic solvent nanofiltration cascade – augmenting membrane selectivity with process engineering. *Chemical Engeneering Science*, 90, 299-310.

Slater C. S., M. J. (2010). In A. W. P.J. Dunn, *Green Chemistry in Pharmaceutical Industry* (pp. ch.3, pp 49-82). Wiley-VCH Verlag GmBH and Co., Weinheim.
Sterlitech Corporation. Bench scale equipment - Flat sheet membranes.Obtained in August of 2013, http://www.sterlitech.com/bench-scale-equipment/flat-sheet-membranes.html.

Székely G., Bandarra J., Heggie W., Ferreira F.C., Sellergren B., (2011). *Separation and Purification Technology* .

Székely, G. (2012). *Degenotoxification of pharmaceuticals by molecular imprinting and organic solvent nanofiltration.* Hungary.

Vahdat L., V. S. (2007). Kinetics of amoxicillin and clavulanate degradation alone and in combination in aqueous solution under frozen conditions. *International Journal of Pharmaceutics* 342, 95–104.

Valtcheva, I. B., Kumbharkar, S. C., Kim, J. F., Peeva, L. G. & Livingston, A. G. (2012) Development of organic solvent nanofiltration membranes for the application in extreme pH conditions. *Euromembrane*. 23-27 September, London.

Van der Bruggen, B., Geens, J. & Vandecasteele, C. (2002) Influence of organic solvents on the performance of polymeric nanofiltration membranes. *Separation Science and Technology*. 37 (4), 783-797.

Van der Bruggen, B., Mänttäri, M. & Nyström, M. (2008) Drawbacks of applying nanofiltration and how to avoid them: A review. *Separation and Purification Technology*. 63 (2), 251-263.

Vandezande, P., Gevers, L. E. M. & Vankelecom, I. F. J. (2008) Solvent resistant nanofiltration: separating on a molecular level. *Chemical Society Reviews*. 37 (2), 365-405.

Vandezande P., L. E. (2007). Solvent resistant nanofiltraton: separating on a molecular level. *The Royal Society of Chemistry*, 365-405.

Vankelecom, I. F. J., De Smet, K., Gevers, L. E. M., Livingston, A., Nair, D., Aerts, S., Kuypers, S. & Jacobs, P. A. (2004) Physico-chemical interpretation of the SRNF transport mechanism for solvents through dense silicone membranes. *Journal of Membrane Science*. 231 (1–2), 99-108.

Vanneste, J., De Ron, S., Vandecruys, S., Soare, S. A., Darvishmanesh, S. & Van der Bruggen, B. (2011) Techno-economic evaluation of membrane cascades relative to simulated moving bed chromatography for the purification of mono- and oligosaccharides. *Separation and Purification Technology*. 80 (3), 600-609.

Vanneste J., Ormerod D., Theys G., Van Gool D., Van Camp B., Darvishmanesh S., Van der Bruggen B., (2012). *Journal of Chemical Technology and Biotechnology*

Veterinary Substances Data Base (VSDB) (05 de August de 2011). Obtained in Febuary of 2013, http://sitem.herts.ac.uk/aeru/vsdb/Reports/1741.htm.

Villani, S. & Becker, E. W.,. (1979) *Uranium enrichment*. Berlin; New York, Springer-Verlag

Whu, J. A., Baltzis, B. C. & Sirkar, K. K. (2000) Nanofiltration studies of larger organic microsolutes in methanol solutions. *Journal of Membrane Science*. 170 (2), 159-172.

Yan, Z. & Kao, Y. (1989) Comparative study of two-membrane permeators for gas separations. *Journal of Membrane Science*. 42 (1–2), 147-168.

Yang, X. J., Livingston, A. G. & Freitas dos Santos, L. (2001) Experimental observations of nanofiltration with organic solvents. *Journal of Membrane Science*. 190 (1), 45-55.

Zhang Ye-Wang, R.-J. L.-M. (2010). One-pot, two-step enzymatic synthesis of amoxicillin by complexing with Zn^{2+}. *Appl Microbiol Biotechnol*, 49–55.

CHAPTER VII

APPENDIX

Appendix I – HPLC calibration curves

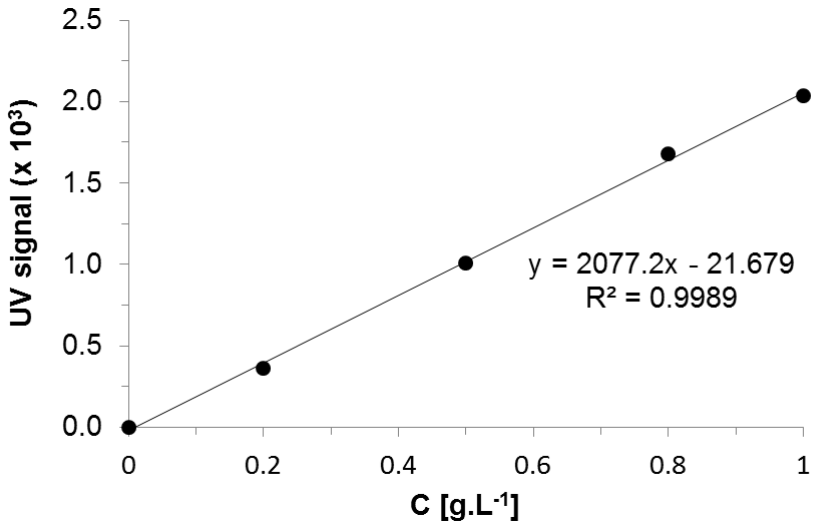

Figure I.1 - Calibration curve for amoxicillin in water (30ºC, retentation time = 10 min.).

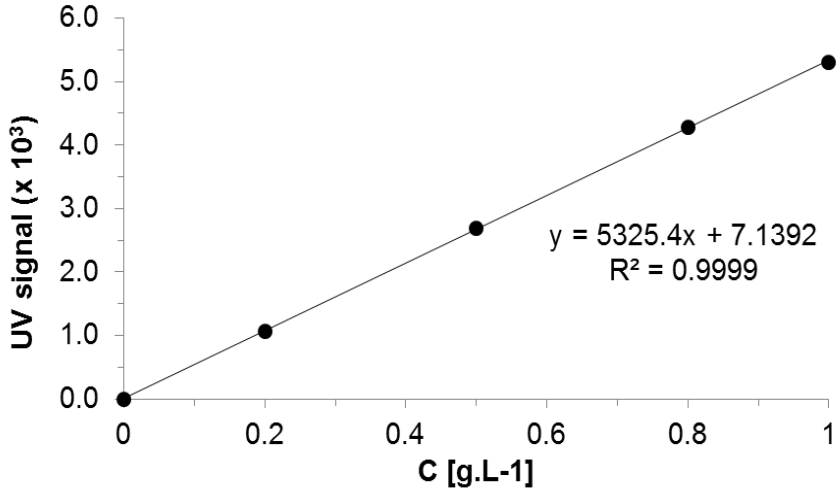

Figure I.2 - Calibration curve for amoxicillin in water (30ºC, retentation time = 10 min.).

Appendix II – Calculations for the titration curves.

Table II.1 - Derivative method finite elements - amoxicillin

V NaOH (mL)	pH (20ºC)	Volume médio NaOH (mL)	DpH/DV	Média do Volume médio (mL)	D2pH/D2V
0	0	-	-	-	-
0.1	2.347	0.05	46.9400	-	-
0.2	2.372	0.15	0.1667	0.1	-467.733
0.4	2.415	0.30	0.1433	0.225	-0.1037
0.5	2.44	0.45	0.0556	0.375	-0.23407
0.7	2.482	0.60	0.0700	0.525	0.027513
1	2.594	0.85	0.1318	0.725	0.085193
1.3	2.692	1.15	0.0852	1	-0.04655
1.6	2.82	1.45	0.0883	1.3	0.002353
1.9	2.982	1.75	0.0926	1.6	0.002685
2.1	3.197	2.00	0.1075	1.875	0.007962
2.3	3.715	2.20	0.2355	2.1	0.060931
2.4	4.117	2.35	0.1711	2.275	-0.0283
2.5	6.686	2.45	1.0486	2.4	0.365628
2.6	7.325	2.55	0.2506	2.5	-0.31919
2.7	8.023	2.65	0.2634	2.6	0.004926
2.8	8.762	2.75	0.2687	2.7	0.001974
2.9	9.9	2.85	0.3993	2.8	0.046632
3	10.45	2.95	0.1864	2.9	-0.0734
3.1	10.842	3.05	0.1285	3	-0.01931
3.2	11.172	3.15	0.1048	3.1	-0.00767
3.3	11.298	3.25	0.0388	3.2	-0.02062
3.4	11.434	3.35	0.0406	3.3	0.000554
3.6	11.87	3.50	0.1246	3.425	0.024518
3.8	12.16	3.70	0.0784	3.6	-0.01283
4	12.335	3.90	0.0449	3.8	-0.00882
4.2	12.445	4.10	0.0268	4	-0.00451
4.7	12.585	4.45	0.0315	4.275	0.001083
5	12.72	4.85	0.0278	4.65	-0.00078
5.5	12.882	5.25	0.0309	5.05	0.000598
6	12.945	5.75	0.0110	5.5	-0.00362

Table II.2 - Derivative method finite elements - 4-hidroxy-L-phenylglycine

V NaOH (mL)	pH (20ºC)	Volume médio NaOH(mL)	DpH/DV	Média do Volume médio (mL)	D2pH/D2V
0	2.35	-	-	-	-
0.1	2.42	0.05	1.4400	-	-
0.2	2.48	0.15	0.3933	0.1	-10.46666667
0.3	2.52	0.25	0.1720	0.2	-1.106666667
0.4	2.57	0.35	0.1257	0.3	-0.154285714
0.5	2.59	0.45	0.0422	0.4	-0.208730159
0.6	2.65	0.55	0.1145	0.5	0.144646465
0.7	2.65	0.65	0.0092	0.6	-0.175524476
0.8	2.72	0.75	0.0867	0.7	0.110622711
0.9	2.75	0.85	0.0412	0.8	-0.056862745
1	2.78	0.95	0.0284	0.9	-0.014172687
1.1	2.86	1.05	0.0733	1	0.044912281
1.2	2.93	1.15	0.0583	1.1	-0.01370224
1.3	3	1.25	0.0616	1.2	0.002782609
1.4	3.08	1.35	0.0585	1.3	-0.00237037
1.5	3.1	1.45	0.0131	1.4	-0.032439336
1.6	3.29	1.55	0.1239	1.5	0.073845013
1.7	3.5	1.65	0.1261	1.6	0.001368524
1.8	3.98	1.75	0.2737	1.7	0.086855106
1.9	6.72	1.85	1.4795	1.8	0.66985843
2	9.08	1.95	1.2118	1.9	-0.140876099
2.1	9.64	2.05	0.2717	2	-0.470043777
2.2	10.2	2.15	0.2623	2.1	-0.004467493
2.3	10.4	2.25	0.0827	2.2	-0.081663143
2.4	10.9	2.35	0.2094	2.3	0.055084798
2.6	11.4	2.50	0.1976	2.425	-0.004850186
2.8	11.8	2.70	0.1507	2.6	-0.018022792
3	12.1	2.90	0.0983	2.8	-0.018737457
3.2	12.3	3.10	0.0797	3	-0.006199481
3.5	12.6	3.35	0.0839	3.225	0.001303311
3.8	12.7	3.65	0.0315	3.5	-0.014963928
4.2	12.9	4.00	0.0410	3.825	0.002481869
4.7	13	4.45	0.0366	4.225	-0.001034506
5.2	13.2	4.95	0.0263	4.7	-0.002205657
5.5	13.2	5.35	0.0133	5.15	-0.00252264

Appendix III – Dissociation profiles

Table III.1 - Molar percentage with pH of the amoxicillin for the pKa1

PH (20ºC)	Molar percentage - Dissociated Specie	Molar percentage - Neutral Specie
0	1.00E+02	4.47E-04
0.28	1.00E+02	8.51E-04
0.56	1.00E+02	1.62E-03
0.84	1.00E+02	3.09E-03
1.12	1.00E+02	5.89E-03
1.4	1.00E+02	1.12E-02
1.68	1.00E+02	2.14E-02
1.96	1.00E+02	4.07E-02
2.24	9.99E+01	7.76E-02
2.52	9.99E+01	1.48E-01
2.8	9.97E+01	2.81E-01
3.08	9.95E+01	5.34E-01
3.36	9.90E+01	1.01E+00
3.64	9.81E+01	1.91E+00
3.92	9.64E+01	3.58E+00
4.2	9.34E+01	6.61E+00
4.48	8.81E+01	1.19E+01
4.76	7.96E+01	2.04E+01
5.04	6.71E+01	3.29E+01
5.32	5.17E+01	4.83E+01
5.6	3.60E+01	6.40E+01
5.88	2.28E+01	7.72E+01
6.16	1.34E+01	8.66E+01
6.44	7.52E+00	9.25E+01
6.72	4.09E+00	9.59E+01
7	2.19E+00	9.78E+01
7.28	1.16E+00	9.88E+01
7.56	6.13E-01	9.94E+01
7.84	3.23E-01	9.97E+01
8.12	1.70E-01	9.98E+01
8.4	8.90E-02	9.99E+01
8.68	4.68E-02	1.00E+02
8.96	2.45E-02	1.00E+02
9.24	1.29E-02	1.00E+02
9.52	6.76E-03	1.00E+02
9.8	3.55E-03	1.00E+02
10.08	1.86E-03	1.00E+02
10.36	9.77E-04	1.00E+02
10.64	5.13E-04	1.00E+02
10.92	2.69E-04	1.00E+02
11.2	1.41E-04	1.00E+02
11.48	7.41E-05	1.00E+02

11.76	3.89E-05	1.00E+02
12.04	2.04E-05	1.00E+02
12.32	1.07E-05	1.00E+02
12.6	5.62E-06	1.00E+02
12.88	2.95E-06	1.00E+02
13.16	1.55E-06	1.00E+02
13.44	8.13E-07	1.00E+02
13.72	4.27E-07	1.00E+02
14	2.24E-07	1.00E+02

Table III.2 - Molar percentage with pH of the amoxicillin for the pKa2

PH (20ºC)	Molar percentage - Dissociated Specie	Molar percentage - Neutral Specie
0	1.00E+02	5.01E-08
0.32	1.00E+02	9.55E-08
0.64	1.00E+02	1.82E-07
0.96	1.00E+02	3.47E-07
1.28	1.00E+02	6.61E-07
1.6	1.00E+02	1.26E-06
1.92	1.00E+02	2.40E-06
2.24	1.00E+02	4.57E-06
2.56	1.00E+02	8.71E-06
2.88	1.00E+02	1.66E-05
3.2	1.00E+02	3.16E-05
3.52	1.00E+02	6.03E-05
3.84	1.00E+02	1.15E-04
4.16	1.00E+02	2.19E-04
4.48	1.00E+02	4.17E-04
4.8	1.00E+02	7.94E-04
5.12	1.00E+02	1.51E-03
5.44	1.00E+02	2.88E-03
5.76	1.00E+02	5.50E-03
6.08	1.00E+02	1.05E-02
6.4	1.00E+02	1.99E-02
6.72	1.00E+02	3.80E-02
7.04	9.99E+01	7.24E-02
7.36	9.99E+01	1.38E-01
7.68	9.97E+01	2.62E-01
8	9.95E+01	4.99E-01
8.32	9.91E+01	9.46E-01
8.64	9.82E+01	1.79E+00
8.96	9.66E+01	3.35E+00
9.28	9.38E+01	6.20E+00
9.6	8.88E+01	1.12E+01
9.92	8.07E+01	1.93E+01
10.24	6.86E+01	3.14E+01

10.56	5.34E+01	4.66E+01
10.88	3.76E+01	6.24E+01
11.2	2.40E+01	7.60E+01
11.52	1.42E+01	8.58E+01
11.84	8.01E+00	9.20E+01
12.16	4.37E+00	9.56E+01
12.48	2.34E+00	9.77E+01
12.8	1.24E+00	9.88E+01
13.12	6.56E-01	9.93E+01
13.44	3.46E-01	9.97E+01
13.76	1.82E-01	9.98E+01
14.08	9.54E-02	9.99E+01

Table III.3 - Molar percentage with pH of the 4-hidroxy-L-phenylglycine

PH (20ºC)	Molar percentage - Dissociated Specie	Molar percentage - Neutral Specie
0	1.00E+02	6.31E-05
0.28	1.00E+02	1.20E-04
0.56	1.00E+02	2.29E-04
0.84	1.00E+02	4.37E-04
1.12	1.00E+02	8.32E-04
1.4	1.00E+02	1.58E-03
1.68	1.00E+02	3.02E-03
1.96	1.00E+02	5.75E-03
2.24	1.00E+02	1.10E-02
2.52	1.00E+02	2.09E-02
2.8	1.00E+02	3.98E-02
3.08	9.99E+01	7.58E-02
3.36	9.99E+01	1.44E-01
3.64	9.97E+01	2.75E-01
3.92	9.95E+01	5.22E-01
4.2	9.90E+01	9.90E-01
4.48	9.81E+01	1.87E+00
4.76	9.65E+01	3.50E+00
5.04	9.35E+01	6.47E+00
5.32	8.84E+01	1.16E+01
5.6	7.99E+01	2.01E+01
5.88	6.76E+01	3.24E+01
6.16	5.23E+01	4.77E+01
6.44	3.65E+01	6.35E+01
6.72	2.32E+01	7.68E+01
7	1.37E+01	8.63E+01
7.28	7.68E+00	9.23E+01
7.56	4.18E+00	9.58E+01
7.84	2.24E+00	9.78E+01
8.12	1.19E+00	9.88E+01

8.4	6.27E-01	9.94E+01
8.68	3.30E-01	9.97E+01
8.96	1.73E-01	9.98E+01
9.24	9.11E-02	9.99E+01
9.52	4.78E-02	1.00E+02
9.8	2.51E-02	1.00E+02
10.08	1.32E-02	1.00E+02
10.36	6.92E-03	1.00E+02
10.64	3.63E-03	1.00E+02
10.92	1.91E-03	1.00E+02
11.2	1.00E-03	1.00E+02
11.48	5.25E-04	1.00E+02
11.76	2.75E-04	1.00E+02
12.04	1.45E-04	1.00E+02
12.32	7.59E-05	1.00E+02
12.6	3.98E-05	1.00E+02
12.88	2.09E-05	1.00E+02
13.16	1.10E-05	1.00E+02
13.44	5.75E-06	1.00E+02
13.72	3.02E-06	1.00E+02
14	1.58E-06	1.00E+02

Appendix IV – HPLC UV signals of the mixture model

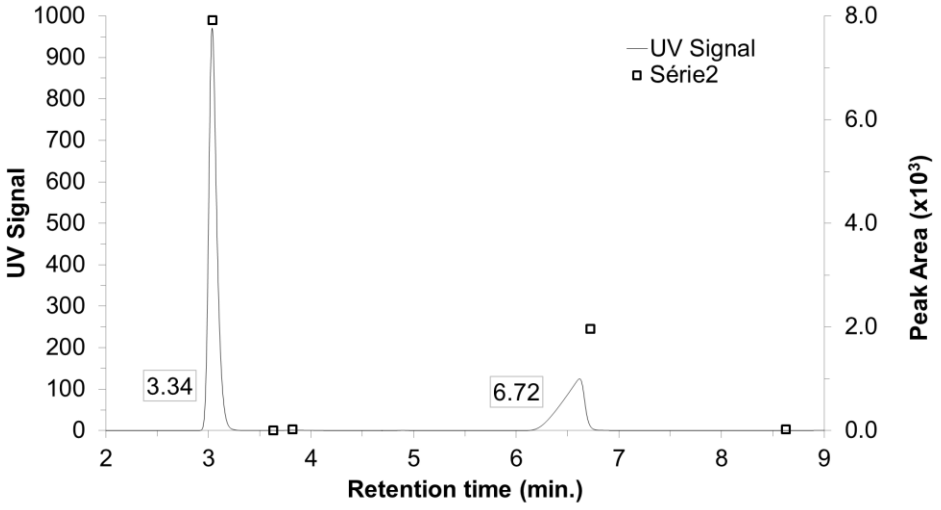

Figure IV.1 – HPLC UV signal from the aqueous mixture of amoxicillin (90.0% pure) and 4-hidroxy-L-phenylglycine (99.0% pure), each one with a concentration of 1 g.L^{-1}. The bold squares indicate the different peak areas and the label values the retention times of those peaks.